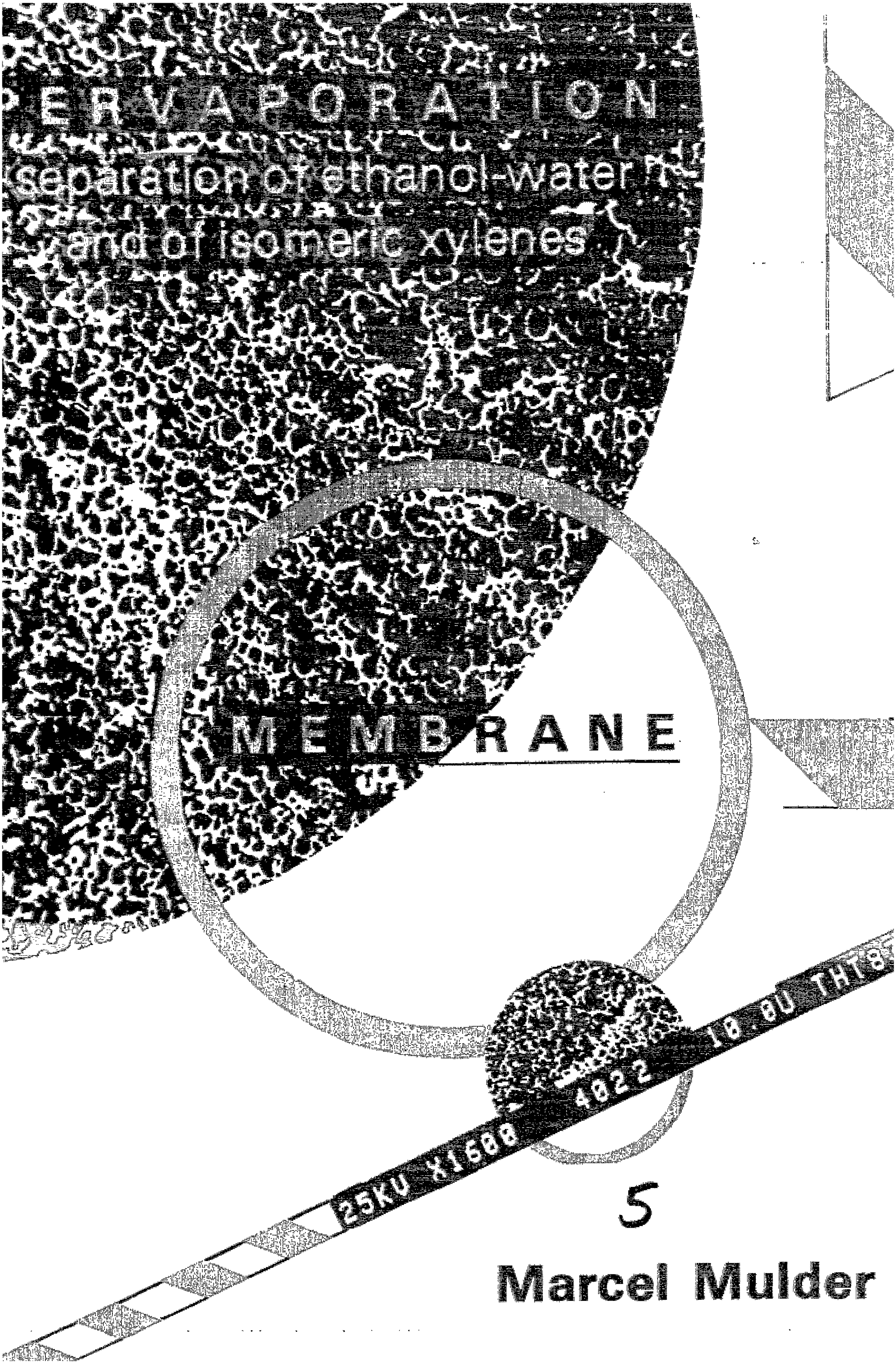

PERVAPORATION

separation of ethanol-water and of isomeric xylenes

MEMBRANE

5

Marcel Mulder

Cover design: Bert Boermans.

PERVAPORATION
separation of ethanol-water and of isomeric xylenes

PROEFSCHRIFT

ter verkrijging van de graad van doctor
in de technische wetenschappen
aan de Technische Hogeschool Twente,
op gezag van de rector magnificus,
prof. ir. W. Draijer,
volgens besluit van het College van Dekanen
in het openbaar te verdedigen op
donderdag 26 januari 1984 te 16.00 uur

door

MARCELLINUS HENDRIKUS VINCENTIUS MULDER
geboren op 6 april 1951
te Enschede

Acknowledgement:

This paper is based upon work financially supported by the Ministeries van Economische Zaken en van Onderwijs en Wetenschappen in the Netherlands.

Dit onderzoek werd uitgevoerd met geldelijke steun van de Ministeries van Economische Zaken en van Onderwijs en Wetenschappen.

Druk: Alfa, Enschede

Dit proefschrift is goedgekeurd door de promotor Prof.Dr.C.A. Smolders.
Coreferenten: Dr.P. Aptel (Université Paul Sabattier, Toulouse, France) en
Dr.D. Bargeman.

VOORWOORD

Een onderzoek kan alleen prettig verlopen en tot resultaat leiden wanneer het werkklimaat , waarin het onderzoek wordt uitgevoerd, goed is.
De sfeer in 'onze groep', de Werkgroep Membraanfiltratie, is meer dan uitstekend. In een raderwerk is een klein radertje echter even belangrijk als een groot wiel. Ook die kleine radertjes, zoals technische dienst, glasblazerij, bodediensten etc., hebben bijgedragen tot een prettig werkklimaat. Langs deze weg wil ik alle grote en kleine radertjes bedanken.

Vijf namen wil ik noemen: José, die alle membraanexperimenten heeft uitgevoerd met een bepaalde (nuchtere) volharding; Bartie, die het typewerk heeft uitgevoerd ondanks een overvol programma; Bert, voor het ontwerpen van de omslag; de 'korrigeergroep' (Johan en Hans), voor het kritisch doorlezen van de getypte versie en 'thuis' (Jos,Ivo en Joris), die er voor zorgde dat ik 's morgens weer fluitend naar het werk ging.

CONTENTS

page

CHAPTER 1 INTRODUCTION

CHAPTER 2 SEPARATION OF ISOMERIC XYLENES BY PERVAPORATION THROUGH CELLULOSE ESTER MEMBRANES

CHAPTER 3 ETHANOL/WATER SEPARATION BY PERVAPORATION

CHAPTER 4 A RATIONALE FOR THE PREPARATION OF ASYMMETRIC PERVAPORATION MEMBRANES

CHAPTER 5 ON THE MECHANISM OF SEPARATION OF ETHANOL/WATER MIXTURES BY PERVAPORATION
I. CALCULATION OF CONCENTRATION PROFILES

CHAPTER 6 ON THE MECHANISM OF SEPARATION OF ETHANOL/WATER MIXTURES BY PERVAPORATION
II. EXPERIMENTAL CONCENTRATION PROFILES

INTRODUCTION

MEMBRANE FILTRATION

Success in the development of synthetic membranes from polymeric materials is one of the main reasons for the growth of membrane technology over the past 15 years. In the USA, an intensive research and development program started in the early sixties, especially in the field of the production of fresh water from brackish and sea-water, allowed membrane technology to evolve.
Today, membrane technology has found its place in a wide range of applications such as desalination of sea-water, electrodialytical treatment of industrial effluents, dialytical detoxification of blood using an artificial kidney, controlled release of active agents in therapeutical systems, microfiltration of suspended solids and recovery of hydrogen from gas mixtures by gas separation.
Also in the Netherlands membrane separation processes have begun to emerge as technically significant and commercially relevant unit operations and some important applications are given in table 1.

The heart of every membrane process is the membrane.
A membrane can be defined as a barrier between two homogeneous phases (Fig. 1).

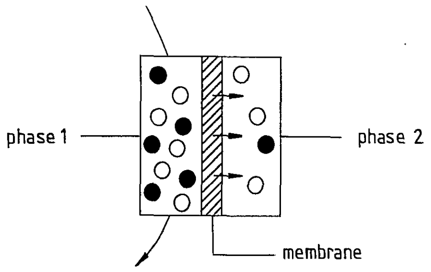

FIGURE 1. Schematic representation of a two-phase system separated by a membrane

Membrane technology in the Netherlands

Industry	process stream	membrane process	membrane configuration
AVEBE (food)	potato starch	UF [a] and HF [b]	tubular
Heineken (beverage)	potable water	HF	spiral wound
Hoogovens (metallurgic)	oil/water emulsions	UF	tubular
Nutricia (dairy)	whey	UF	plate-and-frame
Greenhouses (agriculture)	waste- or potable water	HF	spiral wound or hollow fiber or tubular

[a] UF: ultrafiltration

[b] HF: hyperfiltration

Transport through the membrane takes place when a driving force is applied to the components of phase 1 (the driving force is a potential difference across the membrane, in general a chemical potential difference). The membrane has the ability to transport one component more readily than another : it acts as a selective barrier. For different applications (i.e. different membrane processes) different membranes are needed. Most of the membranes used in the various membrane processes are asymmetric membranes. Asymmetric membranes consist of a thin dense toplayer and a porous sublayer (Fig. 2); resistance to mass transfer is determined to a large extent by the toplayer.

In the case of symmetric membranes (porous or nonporous) the resistance is determined by the total membrane thickness. Fig. 3 gives a schematical representation of different membrane pore structures. These structures can be observed in the toplayer in the case of asymmetric membranes or in the complete cross-section in the case of symmetric membranes. Figs. 3a and 3c are typical examples of structu-

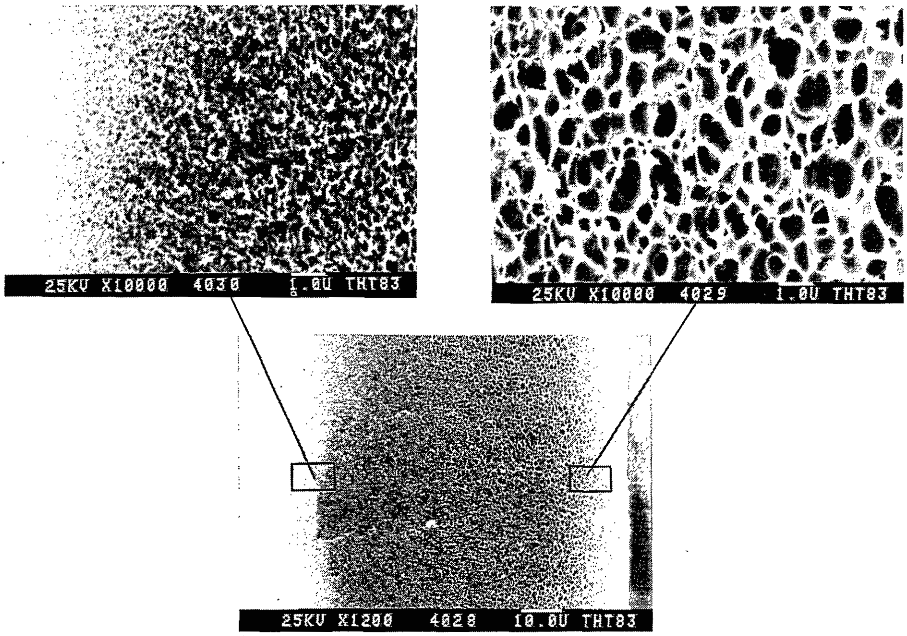

FIGURE 2. Cross-section of an asymmetric membrane.

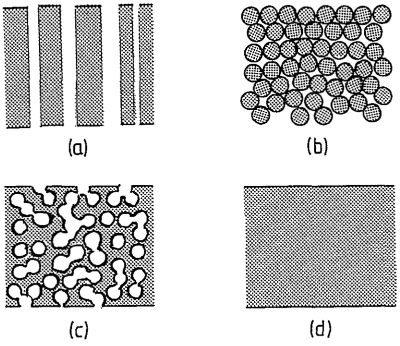

FIGURE 3. Schematic representation of different membrane structures. a) cylindrical pore structure; b) nodular structure; c) spongelike structure; d) nonporous structure.

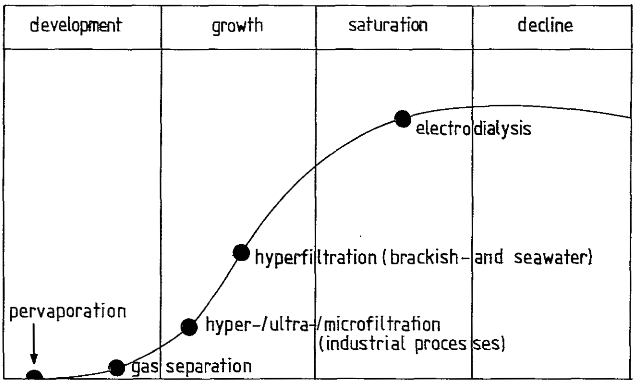

FIGURE 4. States of development of different membrane processes (ref. 3).

res found in microfiltration membranes where 3a represents a Nuclepore membrane and 3c a Millipore membrane. Fig. 3b shows a nodular structure which can be found in the toplayer of some ultrafiltration membranes, e.g. polysulfone [1] and poly(2,6-dimethylpheneleneoxide) [2]. Fig. 3d shows a homogeneous nonporous structure which can be found in the toplayer of asymmetric hyperfiltration and pervaporation membranes. No fixed pores are present and transport takes place by a solution-diffusion mechanism. The structure of these dense toplayers is difficult to characterize with direct techniques such as scanning electron microscopy (SEM). The packing density of the entangled or crosslinked chains as well as the chemical state of the polymer (glassy, rubbery, crystalline, amorphous etc.) are of utmost importance for the ultimate membrane performance.

Table 2 summarizes some important membrane processes. The commercial development of the various membrane processes did not proceed equally as can be seen from Fig. 4 [3]. Pervaporation is still in the embryonic state and

TABLE 2

Some membrane separation processes

Membrane process	phases	driving force	mechanism of separation	membrane structure	application examples
microfiltration	L/L	ΔP 10 to 100 kPa	sieving	symmetrical (coarse) porous	bacteria filter
ultrafiltration	L/L	ΔP 0.1 to 1 MPa	sieving	asymmetric	separation of macromolecules from aqueous solutions
hyperfiltration	L/L	ΔP 1 to 10 MPa	solution/ diffusion	asymmetric/ composite	separation of salts from aqueous solutions
gas separation	G/G	ΔP 0.1 to 10 MPa	diffusion	homogeneous/ asymmetric/ composite	separation of gases (N_2/O_2, CH_4/CO_2)
pervaporation	L/G	ΔC	solution/ diffusion	homogeneous/ asymmetric/ composite	separation of organic liquids
electrodialysis	L/L	ΔE	selective ion transport	symmetric	desalination of water and process streams

at the moment there is one commercial plant in Brazil for the production of ethanol from biomass [4] . Because pervaporation is the subject of this thesis, the general aspects of this process will be discussed more in detail later on in this chapter.
Gas separation is also in the phase of development and the commercial succes started quite recently, especially by the introduction of the Monsanto PRISM^{TM} system.
Microfiltration, ultrafiltration and hyperfiltration of industrial process streams are in the stage of growth.
The number of possible applications is very large.
Desalination of brackish and sea-water by hyperfiltration still has very promising growth possibilities.

PERVAPORATION

Pervaporation is a membrane process where a liquid (mixture) is in direct contact at one side of the membrane (upstream side) and where the permeated product is removed as a vapour at the other side (downstream side) by applying a very low partial pressure. This can be achieved either by creating a vacuum or by employing a carrier gas (Fig. 5). Pervaporation is the only membrane process where a phase transition occurs going from upstream side to downstream side.

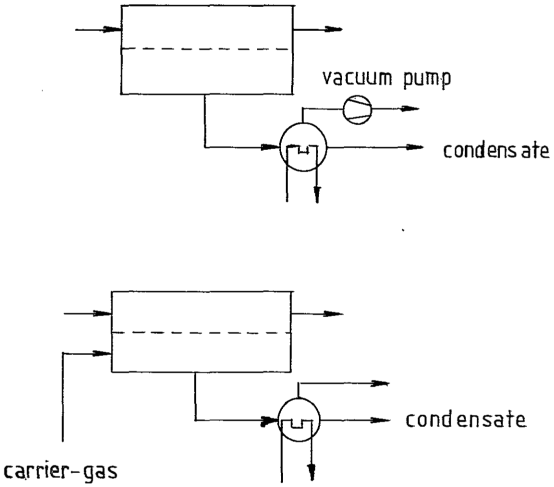

FIGURE 5. Pervaporation with downstream vacuum or carrier-gas

Already in 1906, Kahlenberg [5] reported on the permeation of hydrocarbon-alcohol mixtures through a rubber membrane. In 1917, Kober [6] introduced the term pervaporation. Around 1960, Binning and coworkers [7-10] tried to commercialize pervaporation but their attempts were not very succesful despite intensive investigations.

Today, pervaporation is still in the embryonic state (see Fig. 4), although some interesting potential applications do exist. There are three main reasons for this slow commercialization:

- The energy consumption is relatively high compared to other membrane processes such as ultrafiltration and hyperfiltration, because a phase transition occurs and the heat of vaporization has to be supplied.
- Insufficient permeation rates and/or insufficient selectivities are hard to cope with.
- Process design is difficult because of a temperature drop across the membrane and pressure losses at the downstream side.

Pervaporation can be used to separate organic liquids which are difficult to separate by distillation such as azeotropic mixtures and mixtures with close boiling points. Table 3 summarizes some applications mentioned in the literature. Most of these examples can also be found in Refs. 11 and 29.

The selectivity towards a liquid mixture is expressed by the selectivity factor α which can be defined by

$$\alpha = \frac{x_A/x_B}{y_A/y_B} \qquad (1)$$

where x_A and x_B are the concentrations of components A and B in the permeate while y_A and y_B are the concentrations in the liquid feed.

The pervaporation process essentially involves a sequence of three steps:

- Selective sorption of components of a liquid mixture into the membrane at the upstream side.
- Selective diffusion through the membrane.
- Desorption into a vapour phase at the downstream side.

Transport can be described by a solution-diffusion mechanism where selectivity towards a liquid mixture is determined by selective sorption and selective diffusion.

TABLE 3

Separation by pervaporation

Liquid mixture	membrane material	references
aqueous mixtures		
water/methanol	cellophane,PMGM	11,12
water/ethanol	CA,PVA,PAN	13,14,15
water/i,n-propanol	cellophane,CA,PVA,PTFE-PVP	11,13,14
water/sec,t-butanol	PTFE-PVP	13
water/(dimethyl)hydrazine	cellophane,CA	11
water/pyridine	cellophane,PE	11
water/acetone	PTFE-PVP,PP	13,16
water/dioxane	PTFE-PVP,PA	13,17
water/glycerol	PTFE-SO_3	26
hydrocarbons		
hexane/chloroform	PTFE-PVP	13
benzene/chloroform	PTFE-PVP	13
o-/m-/p-xylene	PE,cellulose esters	18,19
benzene/alcohol	CA,PE	11,13
benzene/(cyclo)hexane	HEMA,PP,PPO-AC,PMGM	20,24,25,27
toluene/(cyclo)hexane	PE	11,20,21
hexane/heptane	PE	22
benzene/heptane	PE,SBR,NBR	22,23
benzene/toluene	PETF	28
alcohols		
ethanol/chloroform	PTFE-PVP	13
ethanol/(cyclo)hexane	PTFE-PVP	13
ethanol/acetone	PTFE-PVP	13
i-propanol/trichloroethylene	PE	30

Solubility is a thermodynamic property and diffusivity a kinetic property and both affect selectivity. When two or more components are permeating through a membrane coupling will occur. This means that in case of a binary mixture the flux of a component in the membrane is not only determined by the presence of the other component but also by its movement. Therefore, model description is often difficult and predicting selectivity towards mixtures from permeabilities of the pure components will hardly be possible in the case of strongly interacting systems. Ethanol-water mixtures behave far from ideal. In the last decade much attention has been paid to the separation of this mixture. In fact, separation of ethanol-water became actual after the oil crisis about ten years ago because ethanol can be used as an alternative renewable fuel. Ethanol can be obtained by fermentation of cellulosic biomass. The purification of ethanol after fermentation by means of distillation into pure ethanol is one of the energy consuming steps of the total process, especially when the azeotropic composition (96 % by weight of ethanol) has to be passed. A more detailed description of ethanol-water separation by pervaporation is given in Chapter 3. In this chapter a schematic flow diagram is given for the continuous fermentation of biomass and purification of ethanol controlled by ultrafiltration and pervaporation. In this diagram pervaporation is used to separate water and ethanol over the entire composition range. At the moment a combination of distillation and pervaporation looks very attractive, using distillation for the first step (concentrating up to about 80 % by weight) and pervaporation for the final dehydration step. Fig. 6 gives a schematic flow diagram of this combined distillation/pervaporation plant which is used for the purification of bioalcohol. After distillation a purified feed stream, having an ethanol concentration of 60-96 % by weight, enters the membrane modules (so membrane fouling will be at a minimum). The inlet feed has a temperature of about 80°C (depending on the composition). Because the heat of vaporization of the permeated product has to be supplied by the feed stream, the temperature will decrease and so the temperature of the concentrate is much lower than the temperature of the inlet feed. In order to increase the temperature to 80°C again the concentrate is recirculated to the condensor of the distillation column before the next membrane unit is entered. In this way the ethanol is purified up to 99.8 % by weight. The condensed permeate is recirculated to the distillation column. An appreciable reduction in investment costs and energy consumption can be achieved by this combined distillation/pervaporation process [43,44] .

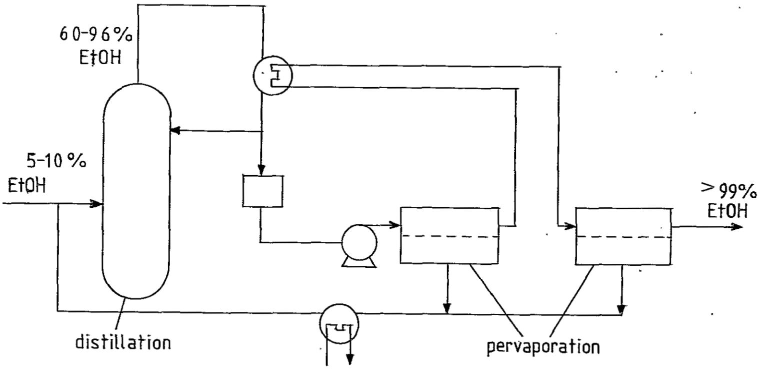

FIGURE 6. Combination of distillation and pervaporation for the purification of ethanol.

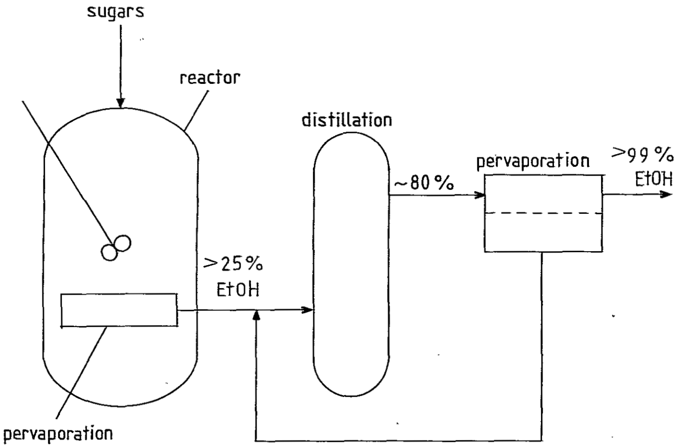

FIGURE 7. Schematic presentation of a continuous fermentation and purification process for the production of pure ethanol with a combined distillation/pervaporation process.

It is also possible to perform fermentation and purification continuously with a combined distillation/pervaporation process as shown in Fig. 7. The first pervaporation unit is put into the fermentor and this unit consists of membranes which are preferentially permeable to ethanol. This construction makes it possible to remove a certain ethanol-water mixture continuously from the fermentation broth. The permeate, containing 20 to 40 % ethanol (or even more, membranes are still in development), enters the distillation column where it is purified up to 80 % whereas the final dehydration step is performed by a second pervaporation unit containing membranes which are preferentially permeable to water. When in the near future highly selective membranes are developed the pervaporation system may even replace the distillation unit.

Although ethanol-water separations are commercially very attractive there are also other potential applications as has been summarized in table 3. From a technical point of view pervaporation can be used for the separation of every organic mixture but from a commercial point of view the number of applications is limited. Pervaporation will especially be competitive when the concentration of the component which has to be removed is low. Therefore, the major field of application will be:

- Removing of small amounts of water from organic liquids.
- Removing of organic contaminants such as aromatics and chlorinated hydrocarbons from waste water.
- Separation of isomeric liquids where just a small amount of one of the components has to be removed.
- Separation of azeotropic mixtures where the azeotropic composition is not too far from one of the pure components (examples are: water/ethanol; water/i-propanol; water/t-butanol; water/THF; water/dioxane; methanol/acetone; ethanol/hexane; propanol/cyclohexane etc.).

When highly selective membranes are available pervaporation can also be used over a wider concentration range.

For instance, when the membrane characteristics are far superior to vapour-liquid equilibria pervaporation may replace distillation over the entire composition range. Therefore, future research should be focussed on the development of highly selective membranes for each kind of separation problem, i.e. high selectivity has priority over high permeation rate.

It will be clear that the number of potential applications for pervaporation is very large. Imaging all azeotropic ethanol-water distillation units would be replaced by pervaporation units the growth of this membrane process would be explosive. Only the environmental aspects would already justify the use of pervaporation because entrainers (a.o. benzene) are not needed anymore.

At the moment pervaporation is still in the embryonic state but in the near future the number of commercial applications will grow. Pervaporation can be seen as a 'next generation membrane separation process' and the separation of ethanol-water is one of the main topics of a R&D program of the Ministry of International Trade and Industry (MITI) in Japan, clearly in expectation of the growth abilities of pervaporation.

SOME THEORETICAL CONSIDERATIONS

The kind of transport mechanism, describing selective transport through a membrane, largely depends on the kind of membrane structure. We will consider the transport through so called homogeneous membranes in which no fixed pores are present. Transport through this kind of membranes takes place by diffusion due to a chemical potential difference across the membrane. For isothermal processes the chemical potential is a function of activity and pressure. For a component i the chemical potential is given by

$$\mu_i = \mu_i^o + RT \ln a_i + \bar{V}_i \ (P_i - P_{ref}) \qquad (2)$$

PHASE 1	MEMBRANE		PHASE 2
P_1	P_1^m	P_2^m	P_2
a_1	a_1^m	a_2^m	a_2
μ_1	μ_1^m	μ_2^m	μ_2
c_1	c_1^m	c_2^m	c_2

FIGURE 8. Schematic survey of the permeation factors for transport through a membrane.

A schematic survey of the permeation factors for transport is given in Fig. 8. During pervaporation transport takes place from a liquid through the membrane into a vapour phase. If P_i^o is the vapour pressure of component i at a certain temperature and P_2 is the pressure at the downstream side then the activity of component i in the permeate, assuming ideality of the vapour, is given by

$$a_{2,i} = \frac{P_2}{P_i^o} \tag{3}$$

The vapour pressures of water and ethanol at 20°C are 2.3 and 5.8 kPa (17.5 and 43.5 mm Hg) respectively. By applying a very high vacuum ($P_i^o \gg P_2$) at the downstream side, $a_{2,i} \rightarrow 0$ and the activity gradient across the membrane will be maximal.

In the pervaporation process the pressure gradient hardly contributes to the driving force. This can be demonstrated quite easily. In pervaporation the pressure difference across the membrane is about 0.1 MPa (1 bar) and given that the molar volume of the permeant is 100 ml/mole,

the term $\overline{V}\Delta P$ is about 10 J/mole (assuming that the partial molar volume is equal to the molar volume). At room temperature RT is already 2.5 kJ/mole and therefore the pressure gradient term in eqn. (2) can be neglected. We will see later on that this has been confirmed experimentally. In general one can say that gradients in pressure and temperature are weak driving forces in respect to activity gradients (times RT). Comparing pervaporation (activity gradient) and reverse osmosis (pressure gradient) using the same (homogeneous) membrane, the same permeation rates can be obtained when infinitely high pressures are applied at the upstream side in the case of reverse osmosis and high vacuum at the downstream side in the case of pervaporation.
Assuming that the pressure inside the membrane is equal to the upstream pressure ($P_1 = P_1^m = P_2^m$) then some instructive relations can be derived with respect to the comparison of reverse osmosis and pervaporation. At the upstream/membrane and downstream/membrane interfaces we have the following equilibrium conditions.

$$\mu_{1,i} = \mu_{1,i}^m \tag{4}$$

$$\mu_{2,i} = \mu_{2,i}^m \tag{5}$$

If we have pure liquid at the upstream side and downstream side (i.e. reverse osmosis) then the following relations for the chemical potential of component i can be derived.

$$\mu_{1,i} = \mu_i^o + \overline{V}_i \ (P_1 - P_{ref}) \tag{6}$$

$$\mu_{1,i}^m = \mu_i^o + \overline{V}_i \ (P_1^m - P_{ref}) + RT \ \ln a_{1,i}^m \tag{7}$$

$$\mu_{2,i}^m = \mu_i^o + \overline{V}_i \ (P_2^m - P_{ref}) + RT \ \ln a_{2,i}^m \tag{8}$$

$$\mu_{2,i} = \mu_i^o + \overline{V}_i \ (P_2 - P_{ref}) \tag{9}$$

From eqns. (6) and (7) we can deduce that the upstream activity must be unity: $a_{1,i}^m = 1$.

From eqns. (8) and (9) we can deduce the following relation for the downstream activity in the membrane assuming $P_2^m = P_1$.

$$a_{2,i}^m = \exp\left[-\frac{\overline{V}_i}{RT}(P_1 - P_2)\right] \qquad \textit{reverse osmosis} \tag{10}$$

If we have pure liquid at the upstream side and vapour at the downstream side (i.e. pervaporation) the equations given above remain the same except for eqn. (9)

$$\mu_{2,i} = \mu_i^o + RT \ln \frac{P_2}{P_i^o} \tag{11}$$

If for convenience $P_{ref} = P_2$ then combination of eqns. (8) and (11) gives the following relation for the downstream activity in the membrane

$$a_{2_i}^m = \frac{P_2}{P_i^o} \qquad \textit{pervaporation} \tag{12}$$

The driving force for diffusion will be maximal when $a_{2,i}^m$ is as small as possible ($a_{2,i}^m \to 0$).
This is the case when $P_2 \to 0$ for pervaporation (eqn. (12)) and $P_1 - P_2 \to \infty$ for reverse osmosis (eqn. (10)). The validity of these statements have been verified experimentally by Paul [31] by comparing ceiling fluxes for hydraulic permeation and pervaporation in highly swollen rubbers. The equations derived above are rather instructive from a pedagogical point of view, demonstrating clearly the differences in driving forces for hydraulic permeation and pervaporation. They are not very useful for transport descriptions. One of the assumptions of deriving these equations is that the pressure in the polymer is uniformly equal to that in the liquid phase ($P_1 = P_1^m = P_2^m$) but in the case of little or moderately swollen glassy polymers a pressure gradient across the membrane is more likely ($P_1 \neq P_2^m$).

TRANSPORT EQUATIONS IN PERVAPORATION

Permeation of pure liquids

The transport of pure components through polymeric membranes can adequately be described by Fick's law

$$- J_i = D_i \nabla c_i \tag{13}$$

The proportionality coefficient or diffusion coefficient (D_i) is in general not a constant, especially not in polymer-permeant systems, but it is concentration dependent. In pervaporation the concentration at the upstream side of the membrane is maximal while at the downstream side the concentration will be very low. Therefore, going from upstream side to downstream side the diffusion coefficient will vary appreciably.

Empirical equations have been used to express the concentration dependency of the diffusion coefficient. Many investigators used an exponential relationship

$$D_i = D_{o,i} \exp(\gamma_i\, c_i) \tag{14}$$

where $D_{o,i}$ is the diffusion coefficient of penetrant i in the membrane at zero concentration ($c_i \rightarrow 0$) and γ_i is a plasticizing constant expressing the influence of the plasticizing action of the liquid on the segmental motions. By combining eqns. (13) and (14) and integrating across the membrane ($c_i = c^m_{1,i}$ at $x = 0$ and $c_i = c^m_{2,i}$ at $x = \ell$) eqn. (15) is obtained.

$$- J_i = \frac{D_{o,i}}{\gamma_i\, \ell} \left[\exp(\gamma_i\, c^m_{1,i}) - \exp(\gamma_i\, c^m_{2,i}) \right] \tag{15}$$

Assuming $c^m_{2,i} \rightarrow 0$ then

$$- J_i = \frac{D_{o,i}}{\gamma_i\, \ell} \left[\exp(\gamma_i\, c^m_{1,i}) - 1 \right] \tag{16}$$

Eqn. (16) describes single component transport in pervaporation quite well and many investigators [16,17,20,28,39-41] used this equation.

Permeation of liquid mixtures

In pervaporation transport takes place by a solution-diffusion mechanism. Solubility is a thermodynamic property and diffusivity is a kinetic property and both affect selectivity. During transport of a mixture through a membrane the components will interact with the membrane material and mutually. The flux of a component of a binary mixture will be modified by the presence and by the mobility of the other component. Because of these coupling phenomena, transport descriptions of binary mixtures are often difficult.

In the case of gas separation the selectivity can be predicted to a reasonable extent from the permeabilities of the individual components. However, in the case of pervaporation it would be hardly possible to predict selectivities from pure component experiments only. Table 4 gives the gas permeation (oxygen and helium) and pervaporation (water and dioxane) experiments of the pure components and of the equimolar mixtures through a Nylon-6 membrane.

TABLE 4

Gas permeation and pervaporation through a Nylon-6 membrane

gas permeation *	pervaporation †
P_{O_2}§ : 0.038	$J_{dioxane}$+ : $0.4\ 10^{-4}$
P_{He} : 0.53	J_{H_2O} : $1.2\ 10^{-4}$
P_{He}/P_{O_2} : 13.9	$J_{H_2O}/J_{dioxane}$: 3.0
α_{He/O_2} : 13.0	$\alpha_{H_2O/dioxane}$: 58.6

*Ref [42] .

†Ref [17] .

§ $10^{-10}\ \frac{cm^3(STP)\ cm}{cm^2\ sec\ cmHg}$

+cm/hr

In the case of gas separation the ratio of the pure component permeabilities (= 13.9) agrees reasonably well with the selectivity obtained for an equimolar mixture (α = 13.0). However, the pervaporation results clearly demonstrate the effect of coupling because the observed selectivity for an equimolar mixture of water and dioxane is much larger than could be expected from pure component permeability data. The permeation of liquid mixtures and the occurence of coupling is discussed further in the chapters 5, 6 and 7.

DIFFERENT FACTORS AFFECTING SELECTIVITY AND PERMEABILITY

Effect of upstream pressure

The permeation rate is almost independent of the upstream pressure, at least at moderate pressures, when high vacuum is applied downstream. In terms of the solution-diffusion model this can be explained as follows; solubility in the polymer is hardly affected by pressure while the driving force will not change too much either. Experiments performed by Greenlaw [40] on the system hexane/polyethylene showed that if low downstream pressures are applied: 200 Pa (1.5 mmHg) an increase of the upstream pressure to 2 MPa (20 bar) had no effect on the permeation rate. It is clear that selectivity will not be affected either by changing the upstream pressure as was demonstrated by several investigators [9,22,39].

Effect of downstream pressure

Downstream pressure directly affects the activity at the downstream side (see eqn. (12)) and therefore the driving force will decrease if downstream pressure increases resulting in a decreasing flux. The permeation rate will become zero if the downstream pressure reaches the saturation pressure. The influence of the downstream pressure on the permeation rate is demonstrated clearly in Fig. 9 taken from Ref.[40]. Since permeation rate is strongly affected by downstream pressure also selectivity will change because

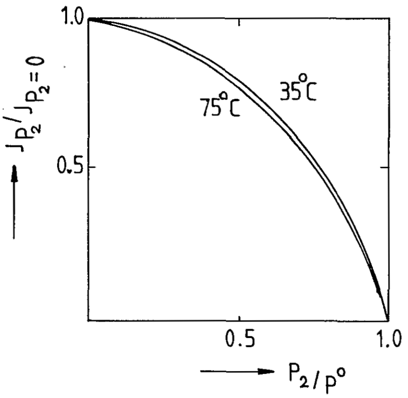

FIGURE 9. Effect of downstream pressure on the permeation rate in pervaporation for the system Nylon-6/water.

the different components to be separated have in general different vapour pressures. Hence, the influence of decreasing downstream pressure on selectivity can be positive [22] or negative [39].

Effect of film thickness

Binning [9] and Aptel [39] studied the effect of film thickness (of homogeneous membranes) on permeation rate and selectivity. From their results it was concluded that permeation rate is inversely proportional to membrane thickness. These results are in agreement with our own results on the system water/ethanol/cellulose acetate (see Fig. 10) for membrane thicknesses between 30 to 120 μm. Deviations from this reciprocal relationship were observed for smaller and larger thicknesses. Furthermore, from Fig. 10 it can be seen that film thickness has a small but significant effect on selectivity. Aptel reported also that a small but again a significant increase in selectivity could be observed when the film thickness was increased (see Ref. [40], Fig. 2), although he concluded wrongly that

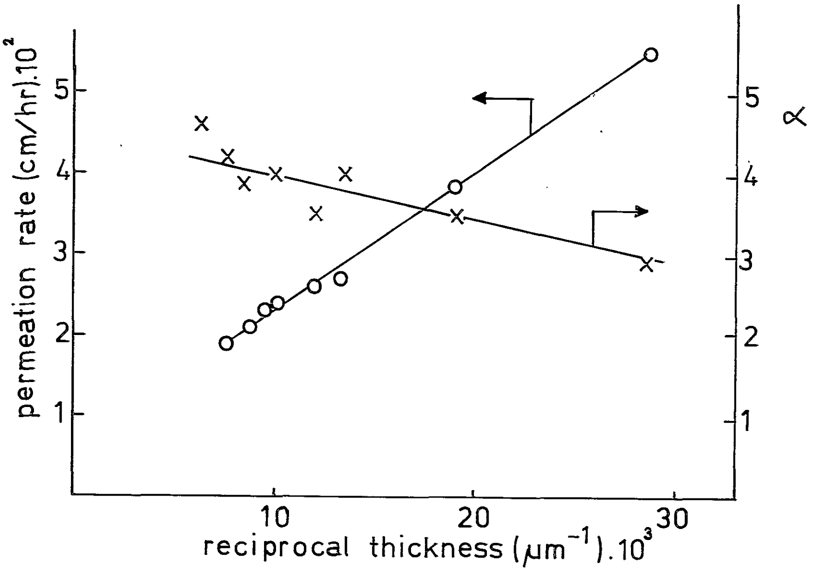

FIGURE 10. Selectivity and permeation rate as a function of the reciprocal thickness; feed: ethanol-water 50-50% by weight; temperature: 20 °C; polymer: cellulose acetate.

membrane thickness would not affect selectivity.

Effect of liquid feed composition

Selectivity and permeation rate are dependent on the composition of the liquid feed mixture. In terms of the solution-diffusion mechanism both solubility and diffusivity change when the liquid feed composition is changed. Examples of this composition dependence are given in several chapters of this thesis.

Effect of temperature

Generally, permeation rate increases and selectivity decreases (not to the same extent) as temperature increases [39]. Because the permeation rate increases exponentially (according to an Arrhenius type of relationship), while selectivity is often hardly affected, the efficiency of the pervaporation process can be improved strongly by increasing the temperature.

Effect of crystallinity

Crystallinity has a large influence on membrane performance as was demonstrated by Long [37] and Stannet [36] because solution and diffusion occur in the amorphous part and not in the crystalline regions. In our investigations primarily amorphous polymers have been considered and the influence of the crystallinity will not be discussed further.

Effect of polymeric membrane material

The most important variable determining selectivity and permeation rate is the choice of the polymer which is used as membrane material. For a given binary liquid mixture a suitable membrane material should be chosen according to the solution-diffusion mechanism. However, on forehand neither definite qualitative nor quantitative predictions can be made concerning flux and selectivity for a given mixture and membrane material. Therefore, a better understanding of preferential sorption and coupled diffusion phenomena is necessary for developing proper membranes.

Effect of membrane structure

Till now most of the pervaporation membranes used were of the homogeneous type. Because the permeation rate is roughly inversely proportional to the membrane thickness an improvement in flux can be expected when asymmetric or composite membranes are used. Systematic investigations to develop asymmetric (or composite) pervaporation membranes have not been reported yet.
The presence of a porous sublayer may have a large influence on mass transfer during pervaporation. When asymmetric membranes are used there are two possibilities of installing the membrane:

. the toplayer is facing the feed ('skin up').

. the porous sublayer is facing the feed ('skin down').

In the case of 'skin up' the resistance at the feed/membrane interface is equal to that of the homogeneous membranes but the resistance in the porous layer can be appreciable when a high vacuum is applied downstream, especially when the pore diameter is small and the permeation rate is high.

In the case of 'skin down' the porous sublayer acts as a stagnant layer and the extent of concentration polarisation will be strongly dependent on the structure of the porous sublayer and the permeation rate. Therefore, in developing asymmetric pervaporation membranes the pores in the sublayer should be as large as possible.

In all pervaporation experiments described in this thesis the toplayer is facing the feed when asymmetric (or composite) membranes have been used.

STRUCTURE OF THIS THESIS

The objective of the investigations for the thesis work can roughly be divided into two parts; development of pervaporation membranes and description of transport through membranes.

The development of the membranes is particularly described in the Chapters 2, 3 and 4 and transport description in the Chapters 5, 6 and 7. Although it seems so, it does not imply that two different subjects have been studied. During the investigations over the past four years there always was a kind of feed-back mechanism, knowledge on transport phenomena was translated to 'how to modify the membrane'. The chapters are not divided according to a time sequence but according logic in subject description.

As was already mentioned, one of the main reasons that pervaporation is still in the embryonic state is because of insufficient flux combined with insufficient selectivi-

ty. How can these properties be improved?
This thesis will try to answer this question by analyzing the roots of the problem which means investigating solubility and diffusivity. Especially the knowledge of solubility of mixtures in polymeric membranes (the occurence of preferential sorption) is far from complete. Those who are thinking that the problems will have been solved now completely must be disappointed. This thesis gives just a small contribution to the solution of the problem.

The approach followed during the investigations was to obtain a better understanding of factors which determine and influence solubility and diffusivity. In the original solution-diffusion model [45,46] the components are considered to diffuse through the membrane independently. It is very unlikely that this will occur because flows will be mutually affected, i.e. coupling occurs in the solubility part as well as in the diffusive part. Perhaps it is stated too often in this thesis but the occurence of coupling hardly permits predicting fluxes and separation factors from permeation experiments of the pure components only (see for instance Table 4 of this chapter). Therefore, in order to improve the understanding of the solution-diffusion mechanism mixtures will have to be considered rather than pure components. The number of interesting liquid mixtures to be studied is very large (see Table 3 of this chapter) and therefore one has to chose. Two kinds of mixtures have been investigated, o-xylene/p-xylene and ethanol/water. The major part of this thesis has been focussed on ethanol/water mixtures.

Ethanol/water mixtures behave far from ideal and when a polymeric membrane is involved as a third component the situation becomes even more complex. The advantage of taking this mixture is that the occurence and extent of coupled transport can be demonstrated very clearly.
The separation of isomeric xylenes has been chosen because the production of pure p-xylene is of great industrial importance. Another important aspect of this very weakly in-

teracting system is the feasibility of the pervaporation process. Because of the similarity of the two components with respect to solubility and diffusivity, small separation factors can be expected on forehand.

Chapter 2 gives a general description of the solubility parameter theory applied to o-xylene/p-xylene mixtures and cellulosic ester membranes. From the experimental data it was concluded that selectivity cannot be predicted by this solubility parameter concept. As far as single component permeation concerns this concept can be used qualitatively to select high flux membranes.

Chapter 3 gives a general picture of ethanol/water separations by pervaporation. The use of different membrane structures, i.e. homogeneous, asymmetric and composite membranes, is described. The development of asymmetric pervaporation membranes is discussed more in detail in Chapter 4. By preparing asymmetric membranes, an increase in permeation rate can be expected without loss in selectivity when a dense and compact toplayer structure is obtained. However, the gelled toplayer of an asymmetric membrane will not have in general the same structure as the homogeneous membrane.

In Chapter 5 a modified solution-diffusion model is described where second-order coupling in the solubility part as well as in the diffusive part is taken into account. In order to reduce the number of adjustable parameters, cross-term diffusion coefficients have been neglected.

In Chapter 6 experimental concentration profiles of the systems water/cellulose acetate, ethanol/cellulose acetate and water/ethanol/cellulose acetate are presented and the validity of the model described in chapter 5 is discussed.

In Chapter 7 theory and experiments on preferential sorption of ethanol/water mixtures in various polymers are described. The experimental sorption data are compared with the pervaporation data and the results are discussed in terms of the solution-diffusion mechanism.

At the very end, the work presented in this thesis is summarized.

REFERENCES

1 R.D. Sanderson and H.S. Pienaar, *Desalination*, 25 (1978) 281.

2 L.Broens, D.M. Koenhen and C.A. Smolders, *Desalination*, 22 (1977) 205.

3 Membrane Technology in Japan, Report of the 'Ministerie van Economische Zaken' in the Netherlands, October 1982.

4 H.E.A. Brüschke, W.H. Schneider and G.F. Tusel, Lecture presented at the European Workshop on Pervaporation, September 21-22, 1982, Nancy, France; *Membrane News*, No. 4, Published by the European Society of Membrane Science and Technology.

5 L. Kahlenberg, *J. Phys. Chem.*, 10 (1906) 141.

6 P.A. Kober, *J. Am. Chem. Soc.*, 39 (1917) 944.

7 R.C. Binning and F.E. James, *Petr. Refiner*, 37 (1958) 214.

8 R.C. Binning and R.J. Lee, *US Patents*; 2,953,502 (1960); 2,923,751 (1960); 2,923,749 (1960).

9 R.C. Binning, R.J. Lee, J.F. Jennings and E.C. Martin, *Ind. Eng. Chem.* 53 (1961) 45.

10 R.C. Binning, R.J. Lee, J.F. Jennings and E.C. Martin, *Am. Chem. Soc. Div. Pet. Chem. Prepr.*, 3 (1958) 131.

11 Ju.I. Dytnerski, *Membranprozesse zur Trennung flüssiger Gemische*, VEB. Deutsche Verlag für Grundstoffenindustrie, Leipzig, 1977.

12 F. Suzuki and K. Onozato, *J. Appl. Pol. Sci.*, 28 (1983) 1949.

13 P. Aptel, N. Challard, J.Cuny and J. Neel, *J. Membr. Sci.*, 1 (1976) 271.

14 R.Y.M. Huang and N.R. Jarvis, *J. Appl. Pol. Sci.*, 14 (1970) 2341

15 M.H.V. Mulder, J. Oude Hendrikman, H. Hegeman and C.A. Smolders, *J. Membr. Sci.*, 16 (1983) 269.

16 W. Featherstone and T. Cox, *Brit. Chem. Eng. Process Techn.*, 16 (1971) 817.

17 R.W.M. Tock, J.Yu. Cheung and R.L. Cook, *Sep. Sci.*, 9

(1974) 361.

18 A.S. Michaels, R.F. Baddour, H.J. Bixler and C.Y. Choo, *Ind. Eng. Chem. Process Des. Dev.*, 1 (1962) 14.

19 M.H.V. Mulder, F. Kruitz and C.A. Smolders, *J. Membr. Sci.*, 11 (1982) 349.

20 R.Y.M. Huang and V.J.C. Lin, *J. Appl. Pol. Sci.*, 12 (1968) 2615.

21 M. Fels, *AIChE Symp. Ser.*, 68 (1972) 49.

22 F.W. Greenlaw, R.A. Sheldon and E.V. Thompson, *J. Membr. Sci.*, 2 (1977) 333.

23 C. Larchet, J.P. Brun and M. Guillou, *J. Membr. Sci.*, 15 (1983) 81.

24 I. Cabasso, J. Jagur-Grodzinsky and D. Vofsi, *J. Appl. Pol. Sci.*, 18 (1974) 2117.

25 F. Suzuki and K. Onozato, *J. Appl. Pol. Sci.*, 27 (1982) 4229.

26 G. Tealdo, G. Castello, G. D'Amato and S. Munari, *J. Membr. Sci.*, 11 (1982) 3.

27 J. Terada, T. Hohjoh, S. Yoshimasu, M. Ikemi and J. Shinohara, *Polym. J.*, 14 (1982) 347.

28 F. Suzuki, K. Onozato and N. Takahashi, *J. Appl. Pol. Sci.*, 27 (1982) 2179.

29 R. Rautenbach and R. Albrecht, *J. Membr. Sci.*, 7 (1980) 203.

30 Ju.I. Dytnerski and W.N. Golowin, *Chem. Techn.*, 6 (1966) 334.

31 D.R. Paul and J.D. Paciotti, *J. Pol. Sci. A-2*, 13 (1975) 1201.

32 G.S. Park, *Trans. Far. Soc.*, 46 (1950) 684.

33 J. Crank, *Mathematics of Diffusion*, Oxford at Claredon Press, 1964.

34 D.W. Mc. Call, *J. Pol. Sci.* 26 (1957) 151.

35 P. Meares, *J. Appl. Pol. Sci.*, 9 (1965) 917.

36 C.E. Rogers, V. Stannet and M. Szwarc, *J. Pol. Sci.*, 45 (1969) 61.

37 R.B. Long, *Ind. Eng. Chem. Fundamen.*, 4 (1965) 445

38 I. Cabasso, J. Jagur-Grodzinsky and D. Vofsi, *J. Appl.*

Pol. Sci., 18 (1974) 2137.

39 P. Aptel, J. Cuny, J. Jozefowicz, G. Morel and J. Neel, *J. Appl. Pol. Sci.*, 18 (1974) 351.

40 S.N. Kim and K. Kammermeyer, *Sep. Sci.*, 5 (1970) 679.

41 J.P. Brun, G. Bulvestre, A. Kergreis and M. Guillou, *J. Appl. Pol. Sci.*, 18 (1974) 1663.

42 V.T. Stannet, *Chem Eng. Prog.*, 73 (1977) 76.

43 A.H. Ballweg, H.E.A. Brüschke, W.H. Schneider, G.F. Tusel, K.W. Böddeker and A. Wenzlaff, to be published.

44 R.J.M. Creusen, *M. Sc. Thesis*, Twente University of Technology, 1983.

45 H.K. Lonsdale, U. Merten and R.L. Riley, *J. Appl. Pol. Sci.*, 9 (1965) 1341.

46 U. Merten, *Desalination by Reverse Osmosis*, U. Merten (Ed.), M. I. T. Press, Cambridge, Mass., 1966, p. 15.

SEPARATION OF ISOMERIC XYLENES BY PERVAPORATION THROUGH CELLULOSE ESTER MEMBRANES*

M.H.V. MULDER, F. KRUITZ and C.A. SMOLDERS

SUMMARY

The interaction between the isomeric xylenes and different cellulose esters was investigated using solubility parameter considerations and through measurements of swelling values.

Hansen's three-dimensional solubility parameters δ_d, δ_p, δ_h of all the components have been calculated. These values have been used to predict the interaction between polymer and penetrant. A measure for this interaction is given by Δ, which is the distance between polymer and penetrant in the δ_d, δ_p, δ_h space. As expected, the experimental swelling values varied in inverse proportion to the calculated Δ values.

Pervaporation characteristics of different cellulose ester membranes were determined by measuring product rates and selectivity. The differences in membrane characteristics have been explained qualitatively in terms of the solubility parameter concept.

---

*Published in Journal of Membrane Science, 11 (1982) 349.

INTRODUCTION

It is well known that pervaporation can be used to separate mixtures of low molecular weight organic compounds. Contrary to other membrane processes, such as hyperfiltration, a phase transition occurs during the pervaporation process. Consequently, the energy input of the process is at least equal to the heat of vaporization of the permeating compounds. Pervaporation can be applied successfully to mixtures which are difficult to separate, such as azeotropic and isomeric mixtures.

The separation of the isomeric xylenes has been described by several authors. Michaels *et al.* [1] investigated the selective permeation of xylene isomers through commercially available polyethylene films. Sikonia [2] and Lee [3] studied the separation of isomeric xylenes by permeation through modified plastic films.

Separation can be achieved by differences in either solubility and/or diffusivity arising from a difference in size or shape. The solubility of the penetrant in the membrane, i.e. the interaction between polymer and penetrant, can be described qualitatively by means of the solubility parameter theory. It should be emphasized, however, that there are some restrictions in using the solubility parameter theory. Only energetic contributions in the mixing process are involved and entropic effects are disregarded. Moreover, solubility parameters predict the mixing of solvents and polymers from properties of the pure substances only.

Despite these shortcomings, the solubility parameter theory is convenient to use and helpful as a first estimate of interaction phenomena.

The three-dimensional solubility parameter approach, as described by Hansen [4], has been well received, and extensive tabulations are available in the literature. Such parameters may be expected to predict feasibility of membrane materials towards permeability behaviour of organic substances. However, such a treatment still remains qualitative.

It is the purpose of this study to investigate the permeation and separation characteristics of isomeric xylenes through cellulose ester membranes. The objectives of this research are: to calculate and evaluate Hansen's solubility parameters of the cellulose esters and of the isomeric xylenes; to relate the experimental swelling results to the solubility parameters and to evaluate the solubility parameter concept in order to predict the permeation behaviour of the isomeric xylenes using cellulose ester membranes.

THEORY

The basic assumption of the solubility parameter theory is that a correlation exists between the cohesive energy density of pure substances (i.e. their potential energy per unit volume) and their mutual solubility. The solubility parameter is related to the C.E.D. as given by eqn. (1)

$$\delta = (\text{C.E.D.})^{\frac{1}{2}} = \left(\frac{\Delta E}{V_m}\right)^{\frac{1}{2}} \qquad (1)$$

For miscible substances, the differences in solubility parameters are supposed to be small. Intermolecular interactions contributing to the cohesive energy of liquids can be divided into nonpolar (London dispersion forces), polar, and specific chemical forces (donor-acceptor interactions, such as hydrogen bonding).

Hansen [4] assumed that the total energy of vaporization is the sum of energies required to overcome dispersion force interactions (ΔE_d), polar interactions (ΔE_p), and to break hydrogen bonds in the liquid (ΔE_h).

$$\Delta E = \Delta E_d + \Delta E_p + \Delta E_h \tag{2}$$

Combining eqns. (1) and (2) gives:

$$\delta^2 = \delta_d^2 + \delta_p^2 + \delta_h^2 \tag{3}$$

The solubility parameter can be considered to be the resultant of three components, due to dispersion forces (δ_d), polar forces (δ_p) and hydrogen bonds (δ_h), as has been expressed in eqn. (3).

The three components lie as vectors along orthogonal axes. The end-point of the radius vector represents the solubility parameter. This means that each solvent and each polymer can be located in a three-dimensional (δ_d, δ_p, δ_h) space. The distance Δ between the end-points of the vectors representing polymer and solvent is given in [5]:

$$\Delta = [(\delta_{d,p}-\delta_{d,s})^2 + (\delta_{p,p}-\delta_{p,s})^2 + (\delta_{h,p}-\delta_{h,s})^2]^{\frac{1}{2}} \tag{4}$$

where the subscripts s and p refer to solvent and polymer respectively. A schematical representation is given in Fig. 1.

According to Froehling [5], a decrease in Δ should be proportional to an increase in swelling values. So interaction between polymer and penetrant will be higher if the value of Δ decreases.

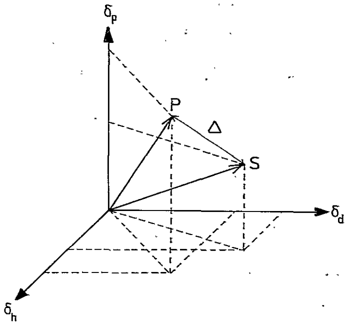

FIGURE 1. Schematic representation of polymer (P) and solvent (S) vectors in δ_p, δ_d, δ_h space; Δ is distance between end-points of vectors.

EXPERIMENTAL

Materials

Cellulose propionate was obtained from Aldrich. The other cellulose esters were obtained from Eastman Chemicals. The solvents used were of analytical grade.

Membrane preparation

Polymer solutions were prepared by dissolving the cellulose esters in a suitable solvent (usually acetone). The membranes were prepared by casting a polymer solution on a glass plate and allowing the solvent to evaporate in a nitrogen atmosphere. The membranes were completely transparent.

Pervaporation

The pervaporation experiments were carried out in the apparatus diagrammed in Fig. 2. A cross-section of the permeation cell is given in Fig. 3.

The bottom disk is fitted with porous glass (10 cm in diameter), to support the membrane.

A teflon gasket is placed on the membrane before the upper part of the cell is matched. The whole unit is tightened by means of a sovirel clamp. A heating coil is placed into the upper compartment to adjust a preselected temperature and to keep the temperature of the liquid feed constant. A thermometer is placed in the cell to determine the temperature of the liquid feed. The cell is connected to two cold traps in parallel. This makes it possible to take samples at any time without interrupting the permeation run.

Vacuum at the downstream side is maintained at a pressure of 0.1-1 mmHg (13.3-133 Pascal) by a Crompton Parkinson vacuum pump. The pressure is measured by an Edwards piranhi.

Permeation experiments were carried out for eight hours. After about three hours steady state conditions are

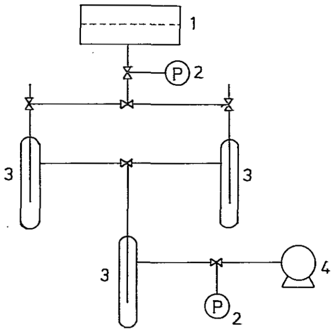

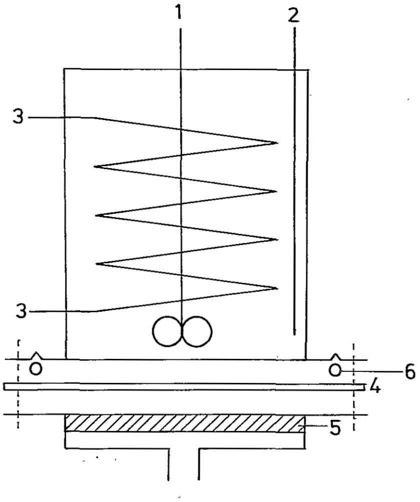

FIGURE 2. Schematic representation of the pervaporation apparatus. (1) permeation cell; (2) piranhi gauge; (3) cold traps; (4) vacuum pump.

FIGURE 3. Schematic representation of the permeation cell. (1) stirrer; (2) thermometer; (3) heating coil; (4) membrane; (5) porous glass filter; (6) teflon gasket.

reached. A product sample is taken at least every hour. Because conditioning history of the membrane is very important in diffusion experiments, the conditioning factors have been kept the same for all the experiments. The dry membrane was kept in contact with the liquid feed for 15 hours before the experiment was started.

Product analysis

Analysis of binary solutions of para- and ortho-xylene, collected in the cold traps, was conducted on a Varian model 3700 gas chromatograph.

Swelling experiments

Swelling or solubility experiments were carried out with the same membranes as used in the pervaporation experiments. Pieces of membrane were immersed in pure ortho- or para-xylene. After several periods of time, the film was taken from the liquid, carefully wiped with a tissue and weighed in a closed conical flask. This was continued until no further weight increase was observed. The solubility is expressed as a relative weight increase (g xylene/ 100 g dry polymer).

RESULTS

Determination of solubility parameters of isomeric xylenes

Although extensive tabulations of three dimensional solubility parameters are available in the literature, several substances are not found in the tables. The determination of the solubility parameters is often difficult and laborious. Koenhen [6] described the determination of solubility parameters of solvents and polymers by means of correlations with physical properties. This method offers a convenient and simple way of estimating solubility parameters.

Determination of δ_d

The relation used to estimate δ_d is a very simple one. The main idea is that the interaction energy between nonpolar molecules is dependent on the polarizability (London dispersion forces). The polarizability is related to the index of refraction by the Lorentz-Lorentz equation. The relation, given by Koenhen [6] to determine the dispersion component, δ_d, is:

$$\delta_d = 9.55\, n_D - 5.55 \qquad (5)$$

Determination of δ_p

Hansen [7] calculated the polar solubility parameter, using Böttcher's relation for estimating the contribution of permanent dipoles to the cohesive energy:

$$\delta_p^2 = \frac{12108}{V_m^2} \cdot \frac{\varepsilon-1}{2\varepsilon+n_D^2} \cdot (n_D^2 + 2)\mu^2 \qquad (6)$$

Another, and more simple, empirical relation has been given by Koenhen [6]:

$$\delta_p = 50.1 \frac{\mu}{V_m^{\frac{3}{4}}} \qquad (7)$$

Determination of δ_h

Determination of δ_h is possible if the hydrogen bond energy is known. Hydrogen bonding, however, is an interaction involving a proton donor (Lewis acid) and a proton acceptor (Lewis base).

Aromatics like benzene and xylenes are weak proton acceptors. A measure for the proton acceptor power is the extent of the shift to lower frequencies of the OD infrared absorption of deuterated methyl alcohol [8,9].

An alternative approach to determine the hydrogen bonding solubility parameter is the determination of the hydrogen bonding interaction energy of a solvent mixture. Aromatic compounds can form hydrogen bonds with chloroform. With carbon tetrachloride no hydrogen bonding occurs. The energy of mixing of aromatic solvents with chloroform and carbon tetrachloride is given in Table 1. The difference in heat of mixing of chloroform and carbon tetrachloride in the aromatic solvents (column 3 in Table 1) can be considered as the energy of that specific hydrogen bond. Because the energies of the different hydrogen bonds are known, δ_h can be calculated using eqn. (8) [4]. The values found by Hansen [4] are also given in Table 1.

$$E_h = \delta_h^2 V_m \qquad (8)$$

In our opinion the disagreement of the results given by Hansen and in this work is not very significant. We conclude here, that the method described above, using heat of mixing data, can be used to calculate δ_h values.

TABLE 1

Heat of mixing of chloroform and carbon tetrachloride with some aromatic solvents. δ_h is calculated by eqn. (8). Hansen's δ_h values are given as reference

	ΔH_m* (J/mol) in $CHCl_3$	ΔH_m† (J/mol) in CCl_4	$\Delta(\Delta H_m)$ (J/mol-H-bonding)	δ_h (eqn. (8))	δ_h § (Hansen)
Benzene	-430	115	545	1.2	1.0
Toluene	-716	- 18	698	1.3	1.1
o-xylene	-941	- 23	918	1.4	1.5
m-xylene	-894	4	898	1.3	-
p-xylene	-912	- 76	836	1.3	-

*Ref [10].
†Ref [11].
§Ref [4] .

Three-component solubility parameters

The individual solubility parameters are calculated in accordance with the procedure given above. The results are given in Table 2, together with the value by Hansen [4] for *o*-xylene. The one-component solubility parameter can

TABLE 2

Three dimensional solubility parameters of the isomeric xylenes; Hansen's *o*-xylene values are given as reference, together with the δ values calculated from Allen's CED data

	δ_d	δ_p	δ_h	δ	δ (Allen)†
o-xylene (Hansen)*	8.7	0.5	1.5	8.8	9.0
o-xylene	8.8	0.7	1.4	8.9	9.0
m-xylene	8.7	0.4	1.3	8.8	8.9
p-xylene	8.7	0	1.3	8.8	8.8

*Ref [4] .
†Ref [12].

also be calculated as the square root of the cohesive energy density (eqn. (1)). These calculated values, from experimental C.E.D. data given by Allen [12], are also given in Table 2. It can be concluded that our calculated results are in agreement with the experimentally determined C.E.D. values of Allen.

Determination of the solubility parameters of the cellulose esters

Solubility parameters of polymers are much more difficult to determine and there is no extensive compilation.

The solubility parameter of a polymer cannot be determined directly because most polymers cannot be vaporized without decomposition. A simple and convenient method of calculating solubility parameters of polymers is by means of molar attraction constants. It is necessary, therefore, to know exactly the structural formula and the density of the polymer. According to Burrel [17], the accuracy of this method is quite good to the first decimal place. This is adequate for practical purposes.

Koenhen [6] and van Krevelen [13] showed that it is possible to estimate solubility parameters of polymeric materials from molar attraction constants. There are molar attraction constants for the dispersion, polar and hydrogen bonding contributions from which the three-component solubility parameters can be calculated. The group contributions, $F_{i\mathrm{d}}$, $F_{i\mathrm{p}}$ and $E_{i\mathrm{h}}$, are given in Table 3. The values of δ_d, δ_p and δ_h for the polymers used in this work, are calculated using the following relations given by van Krevelen [13]:

$$\delta_\mathrm{d} = \frac{\Sigma F_{i\mathrm{d}}}{V_\mathrm{ms}} \tag{9}$$

$$\delta_\mathrm{p} = \frac{(\Sigma F_{i\mathrm{p}}^2)^{\frac{1}{2}}}{V_\mathrm{ms}} \tag{10}$$

TABLE 3

Solubility parameter group contributions, F_{id}, F_{ip} and E_{ih}

Structural group	F_{id}* ($cal^{1/2}\ cm^{3/2}/mol$)	F_{ip}† ($cal^{1/2}\ cm^{3/2}/mol$)	E_{ih}† (cal/mol)
$-CH_3$	201	–	–
$-CH_2-$	139	–	–
$-CH$	51	–	–
$-COO-$	193	240	1674
$-OH$	99	244	4782
$-O-$	49†	196	717
ring	93†	–	–

*Ref [6] .
†Ref [13].

$$\delta_h = \left(\frac{\Sigma E_{ih}}{V_{ms}}\right)^{1/2} \tag{11}$$

In order to calculate reliable values, one has to know the exact structure of a polymeric segment. The information necessary to calculate the solubility parameters of commercially available cellulose esters is given in Table 4.

TABLE 4

Calculation of the molar segmental volume for different cellulose esters. CA = cellulose acetate, CAB = cellulose acetate butyrate, CTP = cellulose tripropionate

No.	polymer	Content (%)		Degree of substitution		Density (g/ml)	M_s (g/mol)	V_{ms} (ml/mol)
		acetyl	alkyl	acetyl	alkyl			
1	CA 383	38.3	–	2.31	–	1.30	259.27	199.44
2	CA 398	39.8	–	2.45	–	1.30	265.16	203.97
3	CA 432	43.2	–	2.82	–	1.29	280.71	217.60
4	CAB 171	29.5	17.0	2.04	0.71	1.25	297.69	238.15
5	CAB 272	21.0	27.0	1.49	1.16	1.25	306.14	244.91
6	CTP	–	51.0*	–	2.90	1.27	324.76	255.72

*Ref [14].

The ester contents have been given by the manufacturer (Eastman Chemicals). From these data the degree of substitution and the segmental molar volume of the cellulose esters are calculated. From the data given in Table 4 it is possible to determine exactly the segmental structure of the different polymers and to estimate the solubility parameters by using Table 3. The result is given in Table 5.

A similar procedure to calculate δ_d and δ_h values of the cellulose esters has been followed by Matsuura [14], who found slightly lower values than we do.

TABLE 5

Segmental structure and solubility parameters of cellulose esters

No	Segmental structure	δ_d	δ_p	δ_h	δ
1	$(CH_2)(CH)_5(O)_2(OH)_{0.69}(OCCH_3)_{2.31}$	7.8	3.5	6.6	10.8
2	$(CH_2)(CH)_5(O)_2(OH)_{0.55}(OCCH_3)_{2.45}$	7.9	3.5	6.3	10.7
3	$(CH_2)(CH)_5(O)_2(OH)_{0.18}(OCCH_3)_{2.82}$	7.9	3.6	5.7	10.4
4	$(CH_2)(CH)_5(O)_2(OH)_{0.25}(OCCH_3)_{2.04}(OCC_3H_7)_{0.71}$	7.9	3.2	5.5	10.1
5	$(CH_2)(CH)_5(O)_2(OH)_{0.35}(OCCH_3)_{1.49}(OCC_3H_7)_{1.16}$	8.1	3.1	5.5	10.3
6	$(CH_2)(CH)_5(O)_2(OH)_{0.10}(OCC_2H_5)_{2.90}$	8.4	3.1	5.1	10.3

There is a small ring (acetylated glucose unit) contribution to δ_d which Matsuura has not taken into account.

One can compare the calculated values with experimental values. Unfortunately, not many experimental values of solubility parameters of polymers are known. For cellulose diacetate (polymer no. 1 in Table 5), an experimental value is known ($\delta = 10.9$) [18]. The agreement with the calculated value ($\delta = 10.7$) is fairly good. For the other polymers used, no experimental values have been found in the literature.

Good solvents for a polymer have solubility parameters in the range of that polymer. Therefore, one can compare these solubility parameters as a first estimate. According to Gee [19], it is not quite correct to assume that the solubility parameter of the polymer is actually the centre of the solubility range. For cellulose triacetate, the calculated value ($\delta = 10.4$) agrees well with the value of tetrachloroethane ($\delta = 10.6$). Solvents for cellulose acetate butyrates ($\delta = 10.1$-10.3) are dioxane ($\delta = 10.0$), chloroform ($\delta = 9.3$), acetone ($\delta = 9.8$), dichloroethane ($\delta = 10.2$) and tetrachloroethane ($\delta = 10.6$). (Solubility parameters of the solvents are taken from Ref. [20]).

The agreement is quite satisfactory.

Determination of Δ

Because the solubility parameters of the different cellulose esters and the isomeric xylenes have been estimated, it is possible to calculate the distance parameter Δ, according to eqn. (4).

The results are given in Table 6. The results of Table 6 are also given in Fig. 4. The differences between the isomeric xylenes is small, as could be expected. The interaction between *o*-xylene and the different polymers is always larger (Δ is smaller) than that of *p*-xylene for the same polymer. This is due to the presence of a dipole moment in *o*-xylene, whereas *p*-xylene has no dipole moment.

TABLE 6

Δ values of cellulose esters with regard to isomeric xylenes

No.	Polymer	*o*-xylene	*m*-xylene	*p*-xylene
1	CA 383	6.0	6.2	6.4
2	CA 398	5.7	5.9	6.2
3	CA 432	5.3	5.5	5.7
4	CAB 171	4.9	5.1	5.3
5	CAB 272	4.8	5.0	5.3
6	CTP	4.4	4.7	4.9

The polymer hydrophobicity increases from cellulose acetate (CA 383) to cellulose tripropionate (CTP). As can be seen from Fig. 4, an increase in hydrophobicity gives a decrease in the distance parameter Δ, therefore a higher xylene solubility can be expected going from CA 383 to CTP.

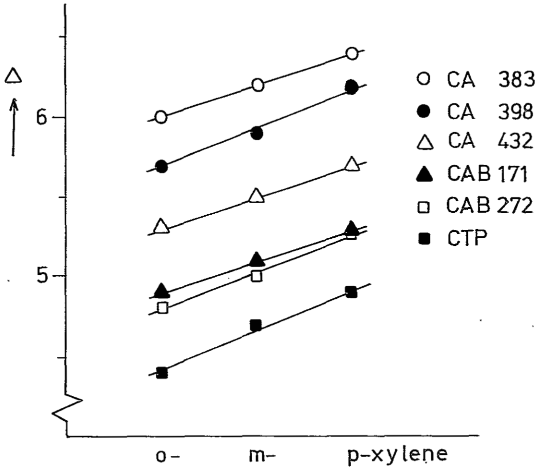

FIGURE 4. Calculated distance parameter Δ between isomeric xylenes and cellulose esters.

Swelling experiments

The results of the swelling experiments are given in Fig. 5. No liquid uptake was observed with cellulose diacetate (CA 383) and cellulose triacetate (CA 432).

From Fig. 5 it can be seen that differences in solubilities are not large, but consistently show that the solubility of *o*-xylene is larger than that of *p*-xylene.

Pervaporation experiments

The pervaporation results of the pure components and mixtures of *o*- and *p*-xylene through different cellulose esters are presented in Table 7 (temperature 20 °C) and

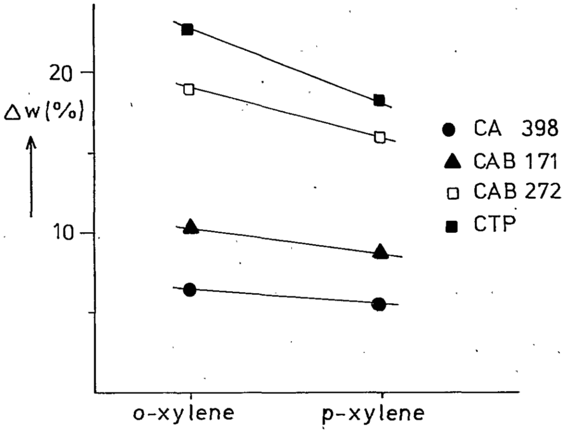

FIGURE 5. Relative weight increase (g/100 g polymer. 100%) for the cellulose esters in *o*-xylene and *p*-xylene.

TABLE 7

Pervaporation results of mixtures *o*-xylene/*p*-xylene; temperature 20 °C

Membrane	Feed* (% *p*-xylene)	Rate (cm/hr) × 10^2	Δc† (weight %)	α §
CTP	0	3.2	–	–
	25	4.0	5.5	1.29
	50	3.5	6.5	1.30
	75	4.8	4.7	1.31
	100	5.0	–	–
CAB 272	0	0.8	–	–
	25	0.6	2.8	1.16
	50	0.8	7.6	1.36
	75	1.1	4.9	1.33
	100	3.0	–	–
CAB 171	0	0.5	–	–
	25	1.6	5.6	1.36
	50	2.0	7.2	1.34
	75	2.3	5.9	1.43
	100	3.1	–	–

[*] Weight %.

[†] Concentration *p*-xylene in the permeate minus concentration *p*-xylene in the feed

[§] Separation factor; concentration ratio (weight %) y_A/y_B in the permeate divided by the concentration ratio x_A/x_B in the feed.

Table 8 (temperature 25 °C). The permeation rate through cellulose diacetate (CA 398) was extremely low ($<10^{-3}$ cm/hr) and these results have not been considered further. With cellulose diacetate (CA 383) and cellulose triacetate (CA 432) membranes no permeability at all was observed.

TABLE 8

Pervaporation results of mixtures *o*-xylene/*p*-xylene; temperature 25 °C

Membrane	Feed* (% *p*-xylene)	Rate (cm/hr) × 10^2	Δc† (weight %)	α§
CTP	0	3.3	–	–
	25	5.0	3.1	1.22
	50	6.6	4.1	1.17
	75	9.3	4.2	1.24
	100	12.9	–	–
CAB 272	0	1.5	–	–
	25	2.1	3.4	1.25
	50	2.9	5.7	1.26
	75	4.4	4.2	1.24
	100	6.1	–	–

*Weight %.

†Concentration *p*-xylene in the permeate minus concentration *p*-xylene in the feed.

§Separation factor; concentration ratio (weight %) y_A/y_B in the permeate divided by the concentration ratio x_A/x_B in the feed.

It is evident from the results that all polymers show higher permeation rates for *p*-xylene than for *o*-xylene. Furthermore, if the *p*-xylene concentration in the feed mixture increases, the permeation rate also increases. This is clearly illustrated in Figs. 6 and 7.

On the other hand, there is no relation between selectivity and the *p*-xylene concentration in the feed. In all cases studied, a maximum in selectivity (expressed as Δc: the difference between the *p*-xylene concentration in permeate and feed) is observed for equimolar mixtures. The variations of the permeability with temperature show the expected behaviour: increasing the temperature gives

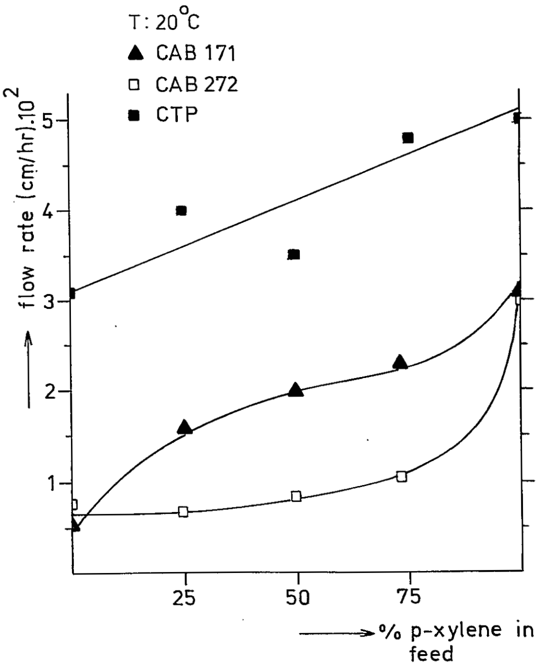

FIGURE 6. Flow rate of mixture *o*-xylene/*p*-xylene (weight %) through different cellulose esters at 20 °C.

higher permeation rates.

It is striking that results obtained with simple polymeric membranes, like the ones studied here and in the investigations of Michaels [1], are as good as the results obtained from polymers containing additives [2,3].

DISCUSSION

Solubility measurements indicate that for all membranes studied the solubility of *p*-xylene is lower than that of *o*-xylene. Differences in solubility are not large, but they are significant. Figure 4 indicates that the calculated dis-

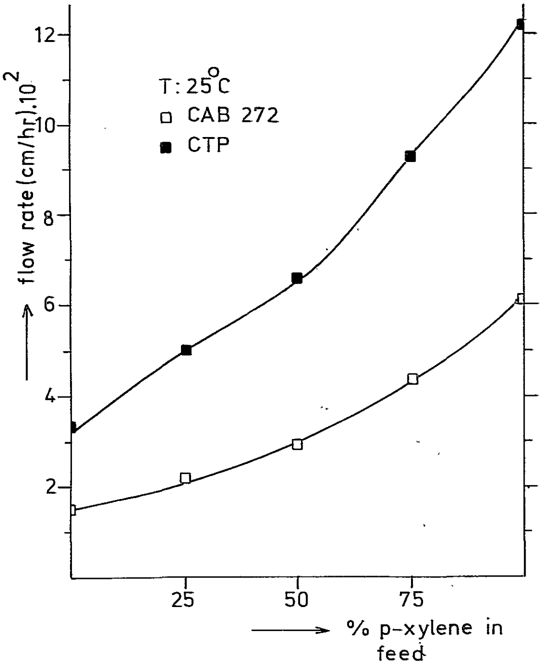

FIGURE 7. Flow rate of mixture *o*-xylene/*p*-xylene (weight %) through cellulose acetate butyrate and cellulose tripropionate at 25 °C.

tance parameter Δ between *o*-xylene and polymer is always smaller than that between *p*-xylene and polymer; thus solubility appears to be inversely proportional to Δ. This has also been found by Froehling [5] and Broens [15] using different polymers. An exception is cellulose triacetate (CA 432) with a Δ value between CA 398 and CAB 171, while for this polymer no solubility was observed.

This can be ascribed to the presence of crystalline material. Cellulose triacetate (CA 432) is more crystalline and small variations in crystallinity of the polymer can have large effects on the solubility of the penetrants in the polymer. Besides this exception, we can conclude from these results that the interaction between polymer and *o*-xylene is always larger (Δ smaller, solubility larger) than that between polymer and *p*-xylene.

The affinity of a given isomer increases from cellulose diacetate (CA 383) to cellulose tripropionate (CTP). In the same order, the polymer becomes more hydrophobic as has been clearly illustrated by the solubility parameter data (Table 5).

As to the pervaporation data of the different membranes, for a given isomer the permeability increases with increasing solubility and decreasing Δ as can be deduced from Figs. 4, 6 and 7. One is, therefore, tempted to postulate a relation between the observed permeability and the polymer-penetrant interaction. However, this relationship is not valid when data are compared for the three xylenes and each polymer. Although the affinity between *p*-xylene and a given polymer is smaller than that between *o*-xylene and polymer, the permeability is higher. These results cannot be explained in terms of molecular size, since molar volumes of the isomeric xylenes increase in the order *o*-xylene < *m*-xylene < *p*-xylene. The differences in interaction between *o*-xylene and *p*-xylene in each polymer are not large but they are significant. The stronger interaction between *o*-xylene and each polymer is due to dipole forces. Therefore we assume that these dipole-dipole interactions cause an obstruction to *o*-xylene diffusion. Since *p*-xylene has no dipole moment, the interaction of this isomer and each polymer will be less strong. As a result, the permeability of *p*-xylene is higher than that of *o*-xylene.

As has been pointed out by Binning [16], besides interaction and molecular size, there is another factor which can cause a difference in permeation rate, namely difference in shape. Michaels [1] explained the higher permeability of *p*-xylene through polyethylene by the difference between the isomers in cross-sectional area normal to the major axis. Permeability is determined by diffusivity and solubility. Despite the smaller solubility in the case of *p*-xylene the diffusivity is, when compared to *o*-xylene, so large that the permeability will be larger, too. Therefore both factors, shape and interaction, are kinetic factors which will influence the diffusivity. There is, however, no relation between the solubility parameters and the kinetic factors.

As has been stated, there is no relation between selectivity and feed composition, independent whether selectivity is expressed as the separation factor or as the difference in concentration in permeate and feed. Nor is there a relation between selectivity and permeation rate. An increase in permeation rate barely effects the selectivity.

CONCLUSIONS

We have shown that it is possible to use the solubility parameter theory in a qualitative manner to select polymers as membrane material as far as the permeability of one compound is concerned. Selectivity cannot be predicted by this δ-parameter approach.

Solubility behaviour is found to be inversely proportional to the calculated distance Δ in the δ-space. Both Δ values and solubility values are a measure for the interaction between polymer and organic solute. The results clearly indicate that, as far as one component is concerned, an increase in interaction gives an increase in permeability.

During pervaporation, a preferential selectivity for *p*-xylene has been found in every case. This is in agreement with other investigations [1-3]. Preferential selectivity for *p*-xylene in each polymer must be due to differences in molecular shape and solute-polymer interaction.

LIST OF SYMBOLS

δ	Solubility parameter (cal$^{\frac{1}{2}}$cm$^{-3/2}$)
C.E.D.	Cohesive energy density (cal cm^{-3})
ΔE	Energy of vaporization (cal mol^{-1})
V_m	Molar volume (cm^3 mol^{-1})
δ_d	Solubility parameter due to dispersion forces (cal$^{\frac{1}{2}}$cm$^{-3/2}$)
δ_p	Solubility parameter due to polar forces (cal$^{\frac{1}{2}}$cm$^{-3/2}$)
δ_h	Solubility parameter due to hydrogen bonding (cal$^{\frac{1}{2}}$cm$^{-3/2}$)
Δ	Distance between polymer and solute in δ-space (cal$^{\frac{1}{2}}$cm$^{-3/2}$)
n_D	Index of refraction
ε	Dielectric constant
μ	Dipole moment (Debye units, D)
F	Molar attraction constant (cal$^{\frac{1}{2}}$ cm$^{3/2}$ mol^{-1})
α	Separation factor
d	Density (g cm^{-3})
M	Molecular weight (g mol^{-1})

Indices

d	Dispersion
p	Polar
h	Hydrogen bonding
i	Component i
s	Segment

REFERENCES

1 A.S. Michaels, R.F. Baddour, H.J. Bixler and C.Y. Choo, *Ind. Eng. Chem. Process Des. Dev.*, 1 (1962) 14.

2 J.G. Sikonia and F.P. McCandless, *J. Membrane Sci.*, 4 (1978) 229.

3 C.H. Lee, *J. Appl. Polym. Sci.*, 26 (1981) 489.

4 C.M. Hansen and A. Beerbower, *Encyclopedia of Chemical Technology*, Supplement Volume 1971, Wiley, New York, 1971.

5 P.E. Froehling, D.M. Koenhen, A. Bantjes and C.A. Smolders, *Polymer*, 17 (1976) 835.

6 D.M. Koenhen and C.A. Smolders, *J. Appl. Polym. Sci.*, 19 (1975) 1163.

7 C.M. Hansen and K. Skaarup, *J. Paint Technol.*, 39 (1967) 511.

8 W. Gordy, *J. Phys. Chem.*, 7 (1939) 93.

9 M. Tamres, *J. Amer. Chem. Soc.*, 74 (1952) 3375.

10 E. Kauer, E. Krug and H.B. Betterich, *Chem. Techn.*, 20 (1968) 406.

11 P.J. Howell, B.J. Skillerne de Bristowe and D. Stubley, *J. Chem. Soc.*, A6 (1971) 397.

12 G. Allen, G. Gee and G.J. Wilson, *Polymer*, 1 (1960) 456.

13 D.W. van Krevelen, Properties of Polymers, Elsevier, Amsterdam, 1972.

14 T. Matsuura, P. Blais and S. Sourirajan, *J. Appl. Polym. Sci.*, 20 (1976) 1515.

15 L. Broens, D.M. Koenhen and C.A. Smolders, *Desalination*, 22 (1977) 205.

16 R.C. Binning, R.J. Jennings, R.C. Lee and E.C. Martin, *Ind. Eng. Chem.*, 53 (1961) 45.

17 H. Burrel, in: J. Brandrup and E.H. Immergut (Eds.), *Polymer Handbook*, 2nd. edn., John Wiley, New York, 1975, p. IV-337.

18 M. Magat, *J. Chim. Phys.*, 46 (1949) 344.

19 G. Gee, *Trans. Inst. Rubber Ind.*, 18 (1943) 266.

20 A.F.M. Barton, *Chem. Rev.*, 75 (1975) 731.

ETHANOL-WATER SEPARATION BY PERVAPORATION*

M.H.V. MULDER, J. OUDE HENDRIKMAN, H. HEGEMAN and
C.A. SMOLDERS

SUMMARY

The separation of ethanol-water mixtures is of great importance for the production of ethanol from biomass. Both ultrafiltration and pervaporation processes can be used for the continuous processing of fermentation and separation. The removal of ethanol from the ultrafiltration permeate can be accomplished by pervaporation. Separation of ethanol-water mixtures by the pervaporation process has been investigated. Results are presented for membranes which are preferentially permeable for ethanol and for others which are preferentially water permeable. Details on the preparation of several membrane types (homogeneous, asymmetric and composite) are given. A schematic process diagram is given in which the fermentation of sugars to ethanol is membrane-controlled.

INTRODUCTION

The application of pervaporation in biotechnology

The application of membrane separation processes in biotechnology is rapidly growing. Conventional separation

---

*Published in Journal of Membrane Science, 16 (1983) 269.

techniques such as distillation, adsorption, liquid-liquid extraction and crystallization are often inefficient and uneconomic. Contemporary membrane technology can save in process costs because energy consumption is low, raw materials and nutrients can be recovered and reused, fermentation processes can be carried out continuously and disposal problems can be reduced or eliminated.

Membrane processes can be applied to one of the oldest and most famous fermentation processes: the production of ethanol from the fermentation of biomass. In the past decade this process has become of renewed interest because of the impending petroleum shortage. One of the main advantages of this fermentation process is that fuels are produced from renewable resources.

Ethanol fermentation can be accomplished batchwise or continuously. A substantial reduction in costs can be realized by a continuous operation [1]. According to Gregor [2,3] more cost saving can be achieved by the use of various membrane processes, such as ultrafiltration, reverse osmosis and electrodialysis in combination with distillation.

In principle, a combination of ultrafiltration and pervaporation makes it possible to remove and concentrate ethanol during a continuous fermentation process. It was demonstrated by Lee [3] that an ethanol-water mixture can be removed and that the rejection of suspended solids is complete when beer from the fermentor is ultrafiltrated.

Figure 1 gives a schematic presentation of a membrane-controlled continuous fermentation of sugars to ethanol. Before the sugars enter the fermentor reverse osmosis can be applied to concentrate the feed. In the fermentor glucose is converted into ethanol. The ethanol productivity is limited by ethanol inhibition and a low cell-mass concentration. Ultrafiltration can be used as a cell recycle system, where the rejected cells are returned to the fermentor and the ethanol is removed. Thus, the rate of ethanol production remains high. The ultrafiltration permeate

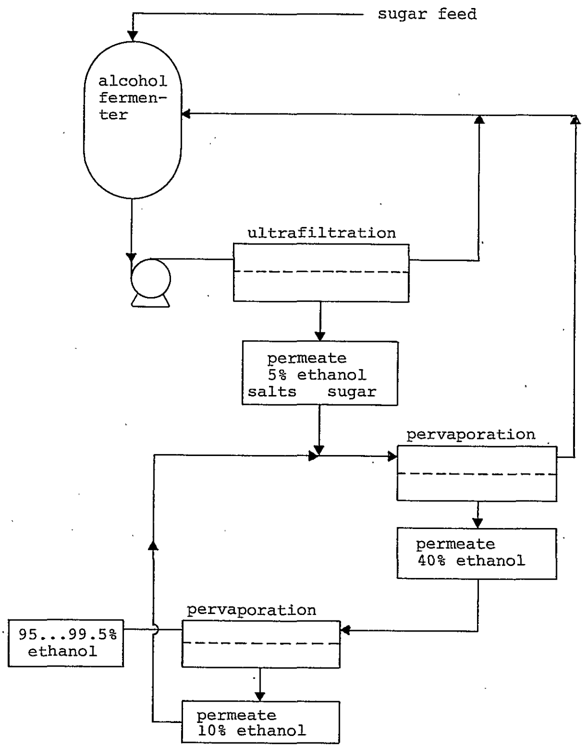

FIGURE 1. Schematic presentation of membrane-controlled continuous fermentation process for the production of pure ethanol.

contains components such as salts, glucose, ethanol and other low molecular weight substances. The ethanol concentration in the ultrafiltration permeate will be about 5 to 10% by weight. Ethanol can be purified to 99% or more by different separation techniques such as distillation, adsorption or extraction. At this moment, the most important process is distillation. The disadvantage of this process is that energy consumption is rather high, especially when the azeotropic composition is reached. Membrane processes are in general less energy consuming and a membrane process which can be used to separate ethanol-water mixtures of any composition is pervaporation.

In order to keep the energy consumption of this process as low as possible, for low ethanol concentrations in the feed pervaporation should be performed with ethanol-permeable membranes, and for high ethanol concentrations in the feed water should be preferentially removed. Therefore, Fig. 1 shows a two-stage pervaporation process with ethanol-selective membranes in the first stage and water-selective membranes in the second stage. This conceptual diagram shows a possible application of different membrane processes in biotechnology. The value of 40% for the permeate concentration in the first stage is more or less arbitrary. From a commercial point of view, the purification of ethanol from 5% to 99% by pervaporation only is not attractive, at least not at this moment.

Pervaporation in ethanol-water separation

Pervaporation involves selective sorption of a liquid mixture into the membrane, diffusion through the membrane, and desorption into a vapour phase on the permeate side. Until recently, pervaporation was not commercially available despite the prospect of interesting potential applications such as the separation of isomeric and azeotropic mixtures and the separation of aqueous organic mixtures. During the European Workshop on Pervaporation in Nancy a commercial pervaporation unit, in combination with distillation for the purification of biomass ethanol was presented [4]. A general disadvantage of the pervaporation process is the relatively high energy consumption in comparison to pressure-driven membrane processes such as reverse osmosis and ultrafiltration where no phase transition occurs. The pervaporation process consumes an amount of energy which is at least equal to the heat of vaporization of the complete pure product that has to be separated. Another disadvantage, the low permeation rate, can be compensated by membrane configurations with a large area to volume ratio such as hollow fiber systems.

Objectives of this research work

In this chapter we will describe the separation of ethanol-water mixtures by pervaporation. In the past this has been carried out primarily using dense homogeneous membranes. Table 1 gives a summary of the selectivities and permeation rates found in the literature; from this table it can be seen that the best results so far have been obtained with cellulose acetate and cellophane membranes.

TABLE 1

Separation of ethanol-water mixtures by pervaporation

Feed (% by weight)		$\alpha_{A/B}$[a]	Perm.rate (cm/hr)	Temp. (°C)	Type of membrane	Ref.
Water (A)	Ethanol (B)					
45	55	8.5	0.20	80	CA	5
4	96	2.9	0.24	25	PTFE-PVP	6
4	96	6.6	0.08	60	PTFE-PVP	7
4	96	6.2	0.01	20	cellulose	7
4	96	5.9	0.02	20	CA	7
50	50	9.0	0.13	30	cellophane	8
50	50	0.9	0.10	25	cellophane	9
50	50	2.0	0.46	45	cellophane	9
50	50	5.0	0.19	25	PTFE-PS	10
99.99	0.01	0.6^b	<0.01	25	PE	10
99.99	0.01	$<0.0006^b$	<0.01	25	PETF	11
99.99	0.01	0.4^b	0.05	25	PVA	11
99.99	0.01	7^b	<0.01	25	PDMS	11
4	96	11	0.05	60	CA	12
9.9	90.1	8	0.3	60	cellophane	12
50	50	4.6^b	0.5×10^{-3}	25	PDMS	13

[a] $\alpha_{A/B}$: Concentration A/B (weight %) in the permeate divided by the concentration A/B in the feed.

[b] $\alpha_{B/A}$.

In a search for new membranes, the type of membrane structure to be used has to be considered, because the membrane structure determines the separation mechanism. Pervaporation occurs according to a solution-diffusion mechanism [14-17], transport taking place only by diffusion and not by convective flow. This implies that very dense homogeneous membranes without fixed pores are necessary. Several types of membranes with such a dense structure can be mentioned:

- homogeneous membranes;
- asymmetric membranes;
- composite membranes.

With symmetric homogeneous membranes the whole membrane thickness contributes to the resistance to mass transfer, while for asymmetric and composite membranes the major part of the resistance is situated in the thin dense toplayer. We have developed all three types of membranes for ethanol-water separation by pervaporation.

EXPERIMENTAL

Materials

Cellulose derivatives were obtained from Eastman Chemicals except for cellulose tripropionate which was obtained from Aldrich. Polysulfone (P 3500) was obtained from Union Carbide, polyvinylidenefluoride (Solef 2008) from Solvay, polydimethylsiloxane (RTV 670) and polydimethylphenyleneoxide from General Electric, polyacrylonitrile from DuPont and polyamide (Akulon M2) from Akzo. The solvents used were of analytical grade.

Membrane preparation

Homogeneous membranes

Polymer solutions were prepared by dissolving the polymer in a suitable solvent. The membranes were prepared by casting the polymer solution on a glass plate and allowing the solvent to evaporate in a nitrogen atmosphere.

The membranes obtained were completely transparent.

Asymmetric membranes

Asymmetric membranes with a dense toplayer and a porous sublayer were prepared by phase inversion. The polymer was dissolved in a solvent to form a solution containing 10 to 30% polymer by weight. The polymer solution was cast on a glass plate and, after immersion in a nonsolvent bath, the membrane was obtained.

Composite membranes

Composite membranes were prepared by means of dip-coating. A suitable air dried support layer was immersed in a dilute polymer solution and, after evaporation of the solvent, a composite membrane was obtained with a thin homogeneous polymer toplayer on the support layer. As support layers, polyvinylidenefluoride (PVDF) and Nylon-6 membranes were used.

PVDF membranes were prepared by casting a polymer solution containing 25% PVDF, 60% dimethylacetamide and 5% dioxane by weight on a glass plate; after immersion in a water bath at 20 °C, the membrane was obtained.

Nylon-6 membranes were prepared by casting a polymer solution containing 9% Nylon-6, 18% calcium chloride and 73% methanol by weight on a glass plate; after an evaporation time of 60 seconds the film was immersed in a water bath at 0 °C.

Pervaporation

The pervaporation experiments were carried out as described in chapter 2 [18]. Vacuum at the downstream side was maintained at a pressure of 13.3 Pa (0.1 mmHg) by a Crompton Parkinson vacuum pump. The pressure was measured by an Edwards piranhi. Permeation experiments were carried out for eight hours. After about three hours steady state conditions were reached. A product sample was taken at least every hour. In most experiments a 50-50% by weight ethanol-water mixture was used as feed at a temperature of 20 °C. The asymmetric and composite membranes were installed with the toplayer facing the feed.

Product analysis

Analysis of binary ethanol-water solutions was performed on a Varian model 3700 gas chromatograph fitted with a Chromosorb 60/80 column and equipped with a thermal conductivity detector. Low ethanol concentrations (0-5%) were determined with a flame ionization detector. D-glucose was determined as D-glucose phenylosazone by spectrophotometry at 390 nm. Sodium chloride was measured by conductometry.

RESULTS AND DISCUSSION

Homogeneous membranes

Homogeneous membranes have been prepared using different polymers. These are given in the first column of Table 2; membrane thicknesses are given in the second solumn.

In pervaporation literature selectivity is usually expressed by a selectivity factor, α ($\alpha = (y_A/y_B)/(x_A/x_B)$, where y_A and y_B are concentrations of components A and B in the permeate and x_A and x_B are concentrations of components A and B in the feed). Because α may depend on the feed concentration, both selectivity factor and concentration in the permeate are given in Table 2 (third and fourth column). In the last column the permeation rates are given.

From Table 2 it can be concluded that in all cases, except that of polydimethylsiloxane (PDMS), water permeates preferentially through the membrane. Polysulfone (PSf) and polyacrylonitrile (PAN) show the best selectivities, but the permeation rates, especially for PSf, are very low. The cellulose derivatives give moderate selectivities and

TABLE 2

Pervaporation results using homogeneous membranes; feed: ethanol-water 50-50% by weight; temperature: 20 °C

Polymer	Thickness (μm)	α_{H_2O}	Weight % H_2O in permeate	Permeation rate (cm/hr) $\times 10^2$
CA 383[a]	10	2.0	66.9	11.3
CA 398	20	4.2	80.7	6.8
CTA[b]	10	2.7	73.1	8.9
CTP[c]	20	2.6	72.0	5.5
CAB 171[d]	30	4.0	80.0	4.2
CAB 272	20	4.1	80.5	3.3
CAB 381	30	3.2	76.3	2.3
PAN[e]	25	70	98.6	0.15
PVDF[f]	20	1.0	50	4.5
PSf[g]	20	332	99.7	0.04
PDMS[h]	10	0.3	21	1.7

[a] CA: cellulose acetate
[b] CTA: cellulose triacetate
[c] CTP: cellulose tripropionate
[d] CAB: cellulose acetate butyrate
[e] PAN: polyacrylonitrile
[f] PVDF: polyvinylidenefluoride
[g] PSf: polysulfone
[h] PDMS: polydimethylsiloxane

rather high permeation rates.

From reverse osmosis experiments it is known that annealing strongly affects the performance of cellulose ester membranes. Homogeneous cellulose acetate (CA 398), cellulose triacetate (CTA) and cellulose acetate butyrate (CAB 171) membranes were annealed in water at 95 °C for 10 minutes. The pervaporation results for these membranes are given in Table 3, which shows that annealing hardly affects CA 398 membranes but that the selectivity of CTA and CAB 171 membranes increases drastically in comparison with the unannealed membranes. All the experiments mentioned above were carried out with a 50-50% by weight mixture of ethanol and water.

Because selectivity may depend on liquid feed composition, the permeability and selectivity of different compositions were investigated through homogeneous CA 398 (unannealed), PAN and CTA (annealed) membranes. The results are given in Figs. 2 and 3. PSf has not been considered further because of its extremely low

TABLE 3

Pervaporation results of some homogeneous membranes with and without heat treatment; feed: ethanol-water 50-50% by weight; temperature: 20 °C; heat treatment: 10 min at 95 °C

Polymer	Without heat treatment			With heat treatment		
	α_{H_2O}	Weight % H_2O in permeate	Perm.rate (cm/hr)×10^2	α_{H_2O}	Weight % H_2O in permeate	Perm.rate (cm/hr)×10^2
CA 398	4.2	80.7	6.8	3.9	79.5	6.5
CTA	2.6	72.0	5.5	36.0	97.3	2.3
CAB 171	4.0	79.8	4.2	9.6	90.6	2.9

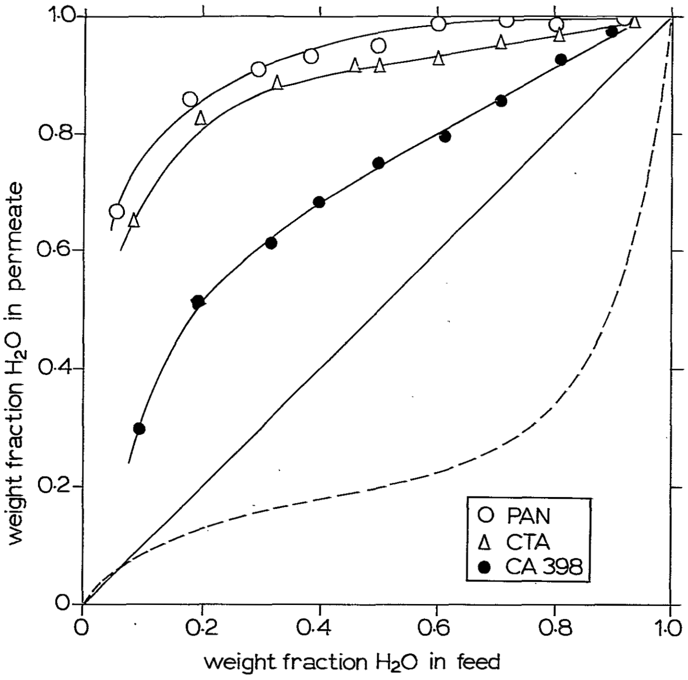

FIGURE 2. Water concentration in the permeate as a function of water concentration in the feed for different homogeneous membranes. The dashed line is the vapour-liquid equilibrium of ethanol-water at 20 °C.

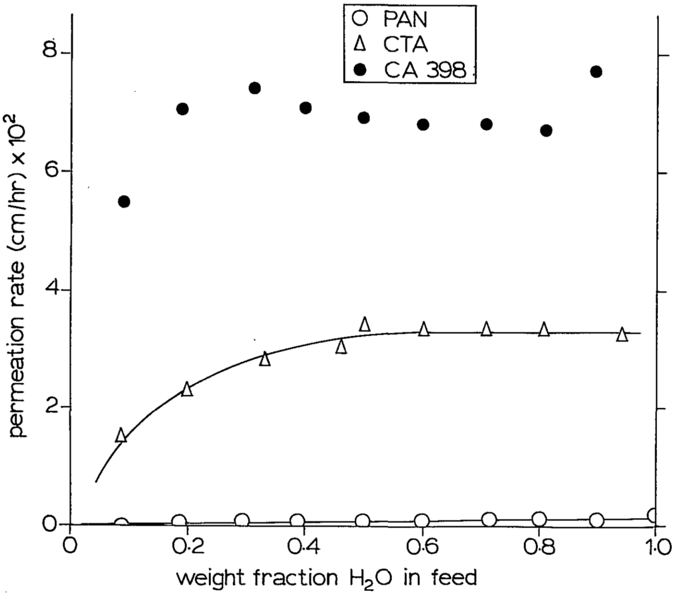

FIGURE 3. Permeation rate as a function of the concentration of water in the feed for different membranes.

permeation rate. In Fig. 2, the vapour-liquid equilibrium of ethanol-water at 20 ^{o}C and 1 bar [19] is also given (dashed curve); from this figure it can be seen that very high selectivities are achieved with simple (bulk) polymers. This result is very interesting from a commercial point of view.

Another objective of this research work was to find membranes which are preferentially permeable to ethanol in order to remove ethanol from the ultrafiltration permeate in the first step (see Fig. 1). From the results given in Table 2, it is important to note that if either a hydrophobic glassy polymer (PSf) or a more hydrophilic glassy polymer (CA) is used, water permeates preferentially in both cases. This means that for hydrophobic glassy polymers such as polysulfone (PSf) and polydimethylphenyleneoxide (PPO), which exhibit no significant water sorption, water permeates preferentially because of the presence of ethanol. With pure water, no permeability has been observed at all through PSf membranes. We conclude from these examples that it would not be possible to predict selectivity for ethanol-water mixtures from pure component permeability measurements. In a forthcoming article [17] we will discuss these phenomena in more detail.

Another interesting point to be learned from Table 2 is that when using a hydrophobic rubber instead of a hydrophobic glassy polymer, ethanol permeates preferentially. Comparing this result with the investigations of Eustache [11] on the removal by pervaporation of a large number of traces of organic contaminants from water using polyethylene (PE), polyethyleneterephtalate (PETF), polyvinyl alcohol (PVA) and polydimethylsiloxane (PDMS), the rubber membranes (PE and PDMS) show a preferential permeability to all organic solutes while the glassy polymers (PVA and PETF) show a selectivity to water. From his extended investigations the only exception found was the system polyethylene-water-ethanol. For glassy polymers diffusion through the membrane is rate determining. In the case of rubbers, where the chains between the crosslink points are much more flexible and segmental motions are less restricted than in glassy polymers, diffusion is much faster and therefore sorption on the feed/membrane interface will become important. Investigations by Hwang [29] on the permeation of oxygen through a silicone rubber membrane did show that, besides the membrane itself, interfacial resistance also contributes to the total resistance.

Because ethanol permeates preferentially through polydimethylsiloxane (PDMS) membranes, it is possible to apply pervaporation to remove ethanol from the ultrafiltration permeate. The ethanol content of the ultrafiltration permeate is low (5-10% by weight). The permeate also contains other low molecular weight substances such as salts, non-converted glucose and other organic components. To check the membrane selectivity for the various components present, we performed an experiment using a PDMS membrane and a 5% by weight solution of ethanol in water with D-glucose and sodium chloride added to the feed. Since the exact composition of the ultrafiltration permeate is difficult to establish (see Ref. [3]), we used the mixture of D-glucose, sodium chloride, ethanol and water to get an indication of the feasibility of the pervaporation process. The results are given in Table 4, from which it can be seen that the rejection of D-glucose and sodium chloride is complete. However, the selectivity is rather low for ethanol-water mixtures, lower than the vapour-liquid equilibrium.

The experiments performed with homogeneous membranes indicate that for all membranes tested, except the PDMS rubber membranes, water permeates preferentially. Very high selectivities to water can be achieved with simple homogeneous membranes but the selectivity to ethanol in the case of PDMS membranes is rather poor.

TABLE 4

Pervaporation results with a PDMS membrane and feed: a mixture of ethanol, D-glucose, sodium chloride and water; membrane thickness: 30 µm; temperature: 30 °C; permeation rate: 0.019 cm/hr

	Feed (ppm)	Permeate (ppm)
Ethanol	50,000	190,000
D-glucose	10,000	<200
NaCl	5,000	<200

Composite membranes

The results obtained with homogeneous PAN and PSf membranes are very promising as regards their selectivity, but they show low permeability. Because the permeation rate through a homogeneous membrane is roughly inversely proportional to membrane thickness, a reduction of the thickness will improve the permeability. One can achieve this by preparing asymmetric or composite membranes. These membranes consist of a thin dense toplayer and a porous sublayer with a much smaller resistance to mass transfer. In the case of composite membranes, toplayer and sublayer originate from different polymeric materials. Each of the two layers can be optimized independently for maximum performance. Different methods can be used to apply the ultrathin toplayer upon the support: dip-coating [20], interfacial polymerization [21] and plasma polymerization [22]. The most simple method is dip-coating. Hence, if it were possible to put a very thin homogeneous PAN or PSf layer, by dip-coating, upon a suitable support, we would expect an increase in permeability while the selectivity would remain the same or lessen only slightly. The choice of the support depends on the solvent used for preparing the polymer toplayer; this solvent should not attack the microporous structure of the support.

PSf is soluble in chlorinated hydrocarbons like methylene chloride, trichloroethylene and tetrachloroethylene. Polyvinylidenefluoride (PVDF), however, is able to resist these solvents. A PVDF membrane has been used as support for a composite membrane with a PSf toplayer. This PVDF membrane itself has no selectivity towards an ethanol-water mixture and the permeation rate is high (see Table 5). PAN is soluble in amides like dimethylformamide (DMF), dimethylacetamide (DMAc) and *N*-methylpyrrolidone (NMP). There are only a few polymers which are resistant to these solvents : aliphatic polyamides can be used as support materials for a PAN toplayer. For this purpose we have used a Nylon - 6 membrane which, uncoated, also shows no selectivity for ethanol-water mixtures, but still has a very high permeation rate.

The coating procedure has been described in the experimental section. The following factors have been varied:
(I) Polymer concentration in the coating solution; 0.5-8%

by weight of polymer.

(2) Coating time; generally about 2 minutes, variation from 1 to 60 minutes.

(3) Prewetting of the support.

(4) Kind of solvent used in the coating solution; dichloromethane (b.p. 40 °C) and tetrachloroethylene (b.p. 146 °C) have been used as solvents for PSf. In the case of PAN, only dimethylformamide has been used as solvent.

(5) Drying of the support; careful drying was carried out at elevated temperature (90 °C) and reduced pressure (0.6 kPa).

(6) Coating in a nitrogen atmosphere.

The best results obtained are given in Table 5. These membranes are obtained by dipping a supporting PVDF membrane in a 6% PSf/CH_2Cl_2 solution and a Nylon-6 supporting membrane in a 8% PAN/DMF solution. The permeation rates of the composite PSf and PAN membranes are one order of magnitude higher than those of the homogeneous membranes; we had anticipated a larger increase. The reason for this low permeability is the resistance which the support layer also exerts on mass transfer, and the rather thick toplayers (6 μm) which were obtained by using the high (6-8%) polymer concentration during dip-coating. When lower polymer concentrations were used, the permeability

TABLE 5

Pervaporation results of composite membranes obtained by dip-coating; feed: ethanol-water 50-50% by weight; temperature: 20 °C

Polymer (toplayer/sublayer)	α_{H_2O}	Weight % H_2O in permeate	Permeation rate (cm/hr) × 10^2
PSf/PVDF	19.0	95.0	0.5
PAN/Nylon-6	9.0	90.0	2.0
PVDF support	1.0	50.0	20
Nylon-6 support	1.0	50.0	–[a]

[a] Permeability too high

did increase but the selectivity decreased drastically. According to Cadotte [21], the possible reason for this phenomenon is that dilute low-viscous polymer solutions tend to migrate upon drying to produce defective toplayers.

One can conclude from these results that, in principle, it is possible to prepare composite membranes for ethanol-water separation by means of dip-coating. However, up to now we have not been able to prepare very thin (less than 1 µm) dense toplayers upon a support by this method without loss of selectivity. Even the best composite membranes did show a loss of selectivity compared to homogeneous membranes.

Asymmetric membranes

Another type of membrane with a very dense toplayer and a porous sublayer is formed by the asymmetric membranes. Most asymmetric membranes are prepared by phase inversion. Morphology and performance of these membranes largely depend on the choice of the ternary system polymer/solvent/nonsolvent . Two different demixing processes determine the formation of asymmetric membranes [23-27]:

(1) (Micro)crystallization or gelation for the formation of the toplayer.
(2) Liquid-liquid phase separation followed by gelation of the concentrated polymer phase for the formation of the porous sublayer.

As already mentioned, during pervaporation transport takes place by diffusion. This requires asymmetric membranes with a very dense toplayer. Different factors can favour the formation of a dense toplayer [25,27]:

- A high initial concentration of the polymer solution.
- A lower tendency of the nonsolvent to induce liquid-liquid phase separation. This means a low tendency of mixing of solvent and nonsolvent.
- A low temperature of the coagulation bath.

. An evaporation step before entering the coagulation bath.

Most of the commercially available asymmetric membranes are applied in hyperfiltration processes. The membranes generally used in the pervaporation process are of the homogeneous type. Only Aptel [7] reported on the separation of water-dioxane mixtures with asymmetric polytetrafluoroethylene membranes. In general, it can be said that asymmetric hyperfiltration membranes are not suitable for pervaporation because the toplayer is not dense enough.

Experiments performed with a Loeb-Manjikian type of CA reverse osmosis membrane [30], obtained from a polymer solution consisting of 25% cellulose acetate (E 398-3), 30% formamide and 45% acetone, did not show any selectivity towards ethanol-water mixtures. Böddeker [31] showed that reverse osmosis membranes (polybenzimidazolone (PBIL) and RC-100), which exhibit very high salt rejection ($R > 99\%$) and can be used for single-pass seawater desalination, have hardly any selectivity to ethanol-water mixtures in pervaporation processes.

With the procedure given above to obtain a more dense toplayer, we developed asymmetric pervaporation membranes for ethanol-water separation using different polymers. The results are given in Table 6.

The asymmetric CA membranes prepared from acetone-containing solutions show a better performance than the homogeneous ones: the permeability is slightly less but the selectivity is much better. The reverse is the case with PSf where the asymmetric membranes have a much higher permeability but a lower selectivity.

Polydimethylphenyleneoxide (PPO) membranes were obtained with a high selectivity but with a low permeability. CA, PSf and PPO membranes were also prepared from a more dilute polymer solution and the results are also given in Table 6. These latter membranes exhibit a much lower selectivity. It seems clear from these results that polymer concentration is a very important factor in obtaining

TABLE 6

Pervaporation results of asymmetric membranes obtained by phase inversion, feed: ethanol-water 50-50% by weight; temperature: 20 °C

Polymer	Solvent	Nonsolvent	Polym. Conc. (%)	α_{H_2O}	Weight % H_2O in permeate	Perm. rate (cm/hr)×10^2
CA	Acetone	Water	25	12.3	92.5	2.7
CA	Acetone	Water	18	5.9	85.5	4.2
CA	DMSO	Water	25	1.0	50.0	32.5
CA	DMSO	Water	18	–	–	–[b]
PSf	DMAc	Water	35	3.0	75.0	1.4
PSf	DMAc	Water	15	–	–	–[b]
PPO	TCE[a]	Methanol	20	9.3	90.3	0.2
PPO	TCE	Methanol	10	1.0	50.0	19.2

[a] TCE: trichloroethylene
[b] Permeability too high

dense-skinned asymmetric membranes suitable for pervaporation. Another important factor in obtaining dense toplayers is the solvent-nonsolvent interaction. If the solvent-nonsolvent interaction is low (i.e., a high value of the excess free energy of mixing), the binodal demixing gap for liquid-liquid phase separation in the phase diagram is shifted to higher water concentrations. This is the case for CA as polymer, acetone as solvent and water as nonsolvent. Acetone-water solutions have a very high excess free energy of mixing whereas DMSO-water solutions show a negative excess free energy of mixing which means a high mutual affinity [28]. The binodals of these systems are given in Fig. 4. For solutions of CA in DMSO, where the location of the liquid-liquid phase separation demixing gap is near the polymer-solvent axis, addition of a small amount of water is sufficient to induce liquid-liquid phase separation. As a result, membranes are obtained with a less dense toplayer [27]. Thus, membranes which were prepared from both dilute and concentrated solutions of CA in DMSO did not show any selectivity towards ethanol-water mixtures because the toplayer was not dense enough.

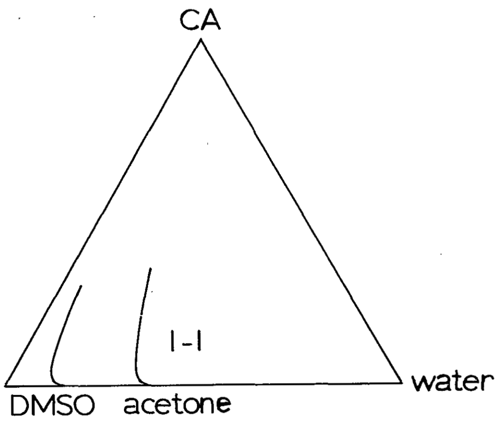

FIGURE 4 . Schematic presentation of the liquid-liquid demixing gap for CA/solvent/water systems with acetone and DMSO as solvent. (From Ref. [28].)

For solutions of CA in acetone, a relatively large amount of nonsolvent is necessary before liquid-liquid phase separation occurs. Consequently, a more dense toplayer is the result.

It is obvious that in preparing asymmetric membranes for pervaporation purposes two factors are very important: the polymer concentration in the casting solution should be high and the solvent-nonsolvent interaction should be low. Besides the thermodynamic aspects mentioned above, kinetic factors such as nonsolvent flow into the nascent membrane and solvent flow into the coagulation bath, together with the gelation/crystallization kinetics, also play an important role in membrane formation.

CONCLUSIONS

With pervaporation in combination with ultrafiltration, it is possible to remove ethanol preferentially and continuously from a fermentation reactor. The ethanol-water mixture obtained after ultrafiltration can be purified by a two-stage pervaporation process with homogeneous, composite or asymmetric membranes.

The problem with the composite membranes prepared by dip-coating is the inadequate homogeneity and/or thickness of the selective toplayer. We did not succeed in preparing very thin toplayers (less than 1 µm) by this technique without loss of selectivity.

Both homogeneous and asymmetric membranes prepared from various polymers showed very high selectivities to ethanol-water mixtures. Annealing of the homogeneous cellulose ester membranes had a positive effect on the selectivity.

REFERENCES

1 G.R. Cysewski and C.R. Wilke, *Biotechnol. Bioeng.*, 20 (1978) 1444.

2 H.P. Gregor and T.W. Jeffries, *Ann. N.Y. Acad. Sci.*, 326 (1979) 273.

3 T.S. Lee, D. Omstead, N.H. Lu and H.P. Gregor, *Ann. N.Y. Acad. Sci.*, 369 (1981) 367.

4 H.E.A. Brüschke, W.H. Schneider and G.F. Tusel, Lecture presented at the European Workshop on Pervaporation, September 21-22, 1982, Nancy, France.

5 R.C. Binning and R.J. Lee, *U.S. Patent 2,953,502* (September 20, 1960).

6 P. Aptel, N. Challard, J. Cuny and J. Neel, *J. Membrane Sci.*, 1 (1976) 271.

7 P. Aptel, J. Cuny, J. Jozefowicz, G. Morel and J. Neel, *J. Appl. Polym. Sci.*, 16 (1972) 1061.

8 R.Y.M. Huang and N.R. Jarvis, *J. Appl. Polym. Sci.*, 14 (1970) 2341.

9 E.G. Heisler, A.S. Hunter, *Science*, 124 (1956) 77.

10 G.C. Tealdo, P. Canepa and S. Munari, *J. Membrane Sci.*

9 (1981) 191.

11 H. Eustache and G. Histi, *J. Membrane Sci.*, 8 (1980) 105.

12 E. Nagy, O. Borlai and A. Ujhidy, *J. Membrane Sci.*, 7 (1980) 109.

13 K.C. Hoover and S.T. Hwang, *J. Membrane Sci.*, 10 (1982) 253.

14 R.C. Binning, R.J. Lee, J.F. Jennings and E.C. Martin, *Ind. Eng. Chem.*, 53 (1961) 45.

15 D.R. Paul and J.D. Paciotti, *J. Polym. Sci.*, A-2, 13 (1975) 1201.

16 C.H. Lee, *J. Appl. Polym. Sci.*, 19 (1975) 83.

17 M.H.V. Mulder and C.A. Smolders, *J. Membrane Sci.*, 17 (1984) 289.

18 M.H.V. Mulder, F. Kruitz and C.A. Smolders, *J. Membrane Sci.*, 11 (1982) 349; Chapter 2 of this thesis.

19 J. Gmehling and U. Onken, *Vapour-liquid Equilibrium Data Collection*, Vol. 1, Part 1, DECHEMA, Frankfurt am Main, F.R.G., 1977.

20 H.K. Lonsdale. R.L. Riley, C.R. Lyons and D.P. Carosella, Transport in composite reverse osmosis membranes, in: M. Bier (Ed.), *Membrane Processes in Industry and Biomedicine*, Plenum Press, New York, 1971, p. 101.

21 J.E. Cadotte and R.J. Petersen, Thin-film composite reverse-osmosis membranes: origin, development and recent advances, in: A.F. Turbak (Ed.), *Synthetic Membranes*, Vol. 1, ACS Symp. Ser. 153, ACS, Washington, D.C., 1981, Chap. 21.

22 H. Yasuda, Composite reverse osmosis membranes prepared by plasma polymerization, in: S. Sourirajan (Ed.), *Reverse Osmosis and Synthetic Membranes*, National Research Council Canada, Ottawa, 1977, Chap. 13.

23 D.M. Koenhen, M.H.V. Mulder and C.A. Smolders, *J. Appl. Polym. Sci.*, 21 (1977) 199.

24. L. Broens, D.M. Koenhen and C.A. Smolders, *Desalination*, 22 (1977) 205.

25 L. Broens, F.W. Altena, C.A. Smolders and D.M. Koenhen, *Desalination*, 32 (1980) 33.

26 F.W. Altena and C.A. Smolders, *J. Polym. Sci., Polym. Symp.*, 69 (1981) 1.

27 C.A. Smolders, Morphology of skinned membranes: A rationale from phase separation phenomena, in: A.R. Cooper (Ed.), *Ultrafiltration Membranes and Applications, Polym. Sci. Technol.*, 13 (1980) 57, Plenum Press, New York.

28 F.W. Altena and C.A. Smolders, *Macromolecules*, 15 (1982) 1491.

29 S.T. Hwang, T.E.S. Tang and K, Kammermeyer, *Amer. Chem. Soc. Polym. Prepr.*, 10 (1969) 978.

30 S. Manjikian, S. Loeb and J.W. McCutchan, *Proceedings of the First International Symposium of Water Desalination*, Washington, D.C., 1965, p. 159.

31 K.W. Böddeker, A. Wenzlaff and D. Cavigelli, *Report GKSS 81/E/62*, GKSS-Forschungszentrum Geesthacht GmbH, Geesthacht, F.R.G., 1982.

CHAPTER 4

A RATIONALE FOR THE PREPARATION OF ASYMMETRIC PERVAPORATION MEMBRANES

M.H.V. MULDER, J. OUDE HENDRIKMAN, J.G. WIJMANS and C.A. SMOLDERS

SUMMARY

Pervaporation is carried out primarily with homogeneous membranes. An improvement in permeation rate can be achieved using asymmetric or composite membranes. In order to maintain selectivity very dense toplayers are needed. The formation of asymmetric membranes will be discussed in terms of the model proposed by our group:

. formation of the toplayer by gelation.

. formation of the porous sublayer by liquid-liquid phase separation followed by gelation of the concentrated polymer phase.

To obtain very dense toplayers the following factors are important: the ratio of nonsolvent inflow and solvent outflow, polymer concentration, location of the liquid-liquid demixing gap and location of the gel region. Asymmetric membranes have been prepared by varying these factors and the obtained membranes have been tested on ethanol/water mixtures.

INTRODUCTION

Despite intensive investigations of Binning and coworkers [1-3] in the late fifties and early sixties, the commercial application of pervaporation as membrane separation process is still very limited. There are three main reasons for this: *i*) the energy consumption is relatively high compared to other membrane processes such as ultrafiltration and hyperfiltration because a phase transition occurs and the heat of vaporization has to be supplied, *ii*) insufficient permeation rates and/or insufficient selectivities and *iii*) process design is difficult because of a temperature drop across the membrane and pressure losses at the downstream side. Nevertheless there are several interesting potential applications such as the removal of water from organic liquids, the removal of organic contaminants (e.g. aromatics and chlorinated hydrocarbons) from waste water and the separation of some azeotropic and isomeric mixtures. In the last decade much attention has been paid to the separation of ethanol/water mixtures [4-9] and recently a commercial application was described for the production of ethanol from biomass using pervaporation for the final dehydration step [10].

The separation mechanism of pervaporation is a solution-diffusion mechanism [11-14] because very dense membranes are needed. Till now pervaporation is carried out primarily with dense homogeneous membranes. Only incidentally the use of asymmetric membranes has been reported [5,15] and no systematic investigations have been performed to obtain asymmetric pervaporation membranes.

As already mentioned above, one of the disadvantages of the pervaporation process is the low permeation rate especially with highly selective membranes. The permeation rate through a homogeneous membrane is roughly inversely proportional to membrane thickness. One way to reduce the effective membrane thickness is to prepare asymmetric membranes.

Loeb and Sourirajan [16] were the first to prepare asymmetric hyperfiltration membranes. Since their work much research has been carried out on the development of new and better asymmetric membranes, often rather empirically and sometimes by a more fundamental approach. In our laboratory much attention has been paid to the fundamental approach [17-25]. Asymmetric membranes are produced by phase inversion [26]. The concept of phase inversion covers a range of different techniques [25] and in this paper we will discuss the preparation of asymmetric membranes by immersion precipitation. Immersion precipitation is the most widely used technique for preparing asymmetric membranes: a polymer solution is cast on a suitable support and immersed in a nonsolvent coagulation bath. The asymmetric membrane is formed by exchange of solvent and nonsolvent. The ultimate membrane structure is determined by the thermodynamics and kinetics of the demixing process, i.e. by the choice of the system polymer/solvent/nonsolvent. Sometimes a curing step can improve membrane performance.

When asymmetric membranes are used in pervaporation experiments there are two possibilities of installing the membrane:

- the toplayer is facing the feed ('skin up').
- the porous sublayer is facing the feed ('skin down').

The influence of the porous sublayer on mass transfer should not be neglected. In the case of 'skin up' position the resistance at the feed/membrane interface is equal to that for the homogeneous membranes but the resistance in the porous layer can be appreciable when high vacuum is applied downstream, especially when the pore diameter is small and the permeation rate is high. In the case of 'skin down' position the porous sublayer acts as a stagnant layer and the extent of concentration polarization will strongly depend on the structure of the porous sublayer and this effect increases with increasing permeation rates. Therefore, in developing asymmetric membranes the pores in the sublayer should be as high as possible.

The objective of this chapter is to discuss the preparation of asymmetric membranes with a very dense toplayer prepared from various polymers and to discuss the different factors which govern the formation of these dense toplayers.

THEORETICAL CONSIDERATIONS

In our group the hypothesis has been adopted that two distinctly different types of phase separation processes are responsible for the formation of asymmetric membranes [17-25]

- gelation (or crystallization) for the formation of the toplayer.
- liquid-liquid phase separation followed by gelation of the concentrated polymer phase for the formation of the porous sublayer.

Koenhen [17] was the first to suggest this mechanism.
In this paper we will describe the formation of asymmetric pervaporation membranes with a very dense toplayer in terms of this mechanism.

Some polymers have no ability to crystallize; in that case the mechanism of crystallization for the formation of the toplayer can be excluded. For these amorphous polymers there is no liquid-solid transition in the thermodynamic sense and gelation generally occurs by entanglement or by physical interactions between segments. The more numerous the entanglements, the more dense the gel will be. This is also the reason why homogeneous membranes are very suitable for pervaporation. Homogeneous membranes are prepared by evaporation of the solvent from a polymer solution film. During evaporation the polymer concentration increases, the viscosity increases and the chains become more and more immobile, reaching a very high packing density when all the solvent has been evaporated. When asymmetric membranes are developed the toplayer should have at least the same dense structure as that for the homogeneous membranes obtained by complete evaporation.

Liquid-liquid phase separation

Liquid-liquid phase separation occurs if the system can lower its free enthalpy of mixing by separating into two liquid phases. Generally, membrane forming systems are ternary systems consisting of a polymer, a solvent and a nonsolvent. Figure 1 shows a schematic diagram of a ΔG_m surface for a ternary system.

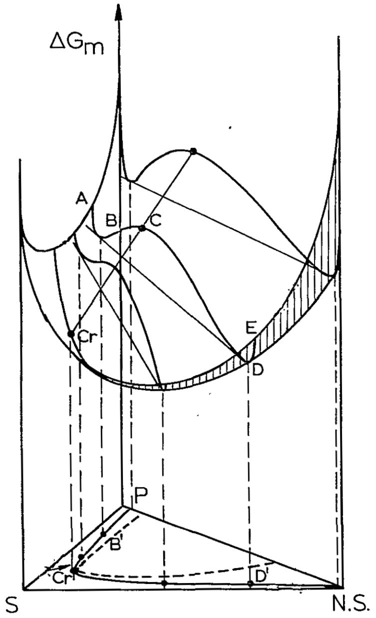

FIGURE 1. Sketch of the ΔG_m surface and miscibility gap for the system polymer (P), solvent (S) and nonsolvent (NS); Cr: Critical point.

All pairs of composition with a common tangent plane to the ΔG_m surface constitute the solid line at the bottom of the phase diagram. This line is called the binodal. The dotted line which connects the points of inflection is called the spinodal. In the critical point (C_r) the binodal and spinodal touch each other. The location of the critical point determines whether the nuclei formed at a certain point when

the binodal is crossed will have a composition high or low in polymer concentration. If the binodal is entered between point C_r' and P, demixing occurs if nuclei of the second phase (the dilute polymer phase) are generated. After nucleation, these droplets will grow further untill the surrounding polymer rich phase will have such a high polymer concentration that gelation occurs.
Figure 1 shows a liquid-liquid demixing gap only. In Figure 2 a ternary phase diagram is shown where except for the binodal demixing gap also a gel region (arbitrarily chosen) has been drawn.

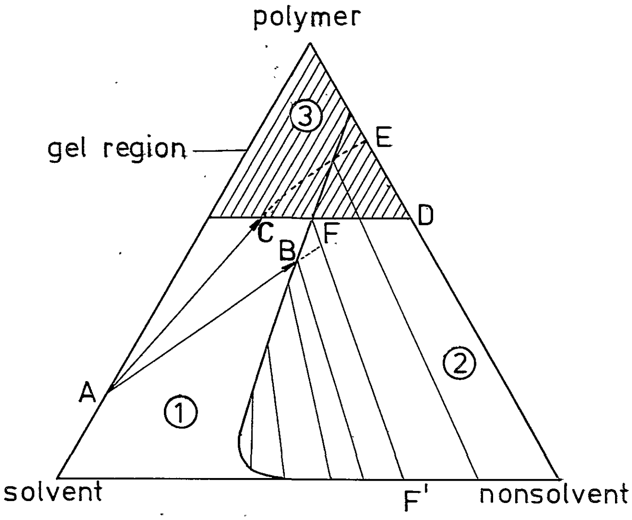

FIGURE 2. Schematic phase diagram for a ternary system with a one-phase region ① , a two-phase region ② and a gel region ③ . Further explanation of coagulation paths, see text.

The exact location of this gel region is difficult to establish. In fact, there is no fixed location because external factors such as the rate of solvent outflow and nonsolvent inflow will influence the exact location. The boundary of this gel region can be considered as a viscosity boundary and the effect of increasing viscosity on phase separation has to be taken into account.

Structure formation in asymmetric membranes reflects strongly different time regimes for composition changes at different positions in the coagulating film:

- directly below the interface coagulation bath/cast polymer solution the toplayer is being formed during rapid solvent loss.
- at greater depth below the interface the sublayer structure is being formed during a more or less gradual exchange of solvent and nonsolvent.

These different composition changes for toplayer and sublayer have earlier been described and visualized in the ternary phase diagram as 'composition path' [22,27].

For toplayer formation there are two possibilities; *i*) the coagulation path crosses the gel region before intersecting the binodal demixing gap (Figure 2, arrow AC) or *ii*) the coagulation path intersects the binodal first (Figure 2, arrow AB). In the first case the gel region is entered at point C, in a part of the phase diagram where the three components are still completely miscible with each other (one-phase region). Now suppose that upon entering the gel region the polymer chains would be immobilized completely. In that case the polymer concentration would not increase any further. However, the diffusion of solvent and nonsolvent will go on and there will be a complete exchange. In this hypothetical case the polymer-nonsolvent axis will be reached at point D. If during gelation further shrinkage of the gel volume i.e. syneresis occurs [20], it is possible that the polymer-nonsolvent axis is reached at higher polymer concentrations (point E). Syneresis will occur if the system can decrease its free enthalpy of mixing because the polymer molecules can change to a less expanded conformation involving expelling of solvent (and nonsolvent).

In the second case when the coagulation path intersects the binodal at lower polymer concentrations (Figure 2, arrow AB) one of the two demixed phases which are in equilibrium with each other (the polymer rich phase) will reach the gel region after a certain time at point F. The same will happen with this phase as mentioned above; the polymer concentration will not increase much because of the immobility of the chains and further growth of the diluted phase is impeded. Again the mechanism of syneresis should not be excluded. Research on this topic (location of the gel region and syneresis) is carried in our laboratory and the results will be published in the near future.

Membrane formation is a dynamic process, thermodynamics only cannot describe the process fully, also kinetics should be included, i.e. rates of solvent outflow and nonsolvent inflow, kinetics of gelation and kinetics of nucleation and growth during liquid-liquid demixing. Nevertheless we will demonstrate that the thermodynamic considerations provide a good indication how to obtain a more dense toplayer.

Formation of the toplayer

According to the Flory-Huggins theory [28] the free energy of mixing (ΔG_m) for a ternary system is given by

$$\frac{\Delta G_m}{RT} = n_1 \ln \phi_1 + n_2 \ln \phi_2 + n_3 \ln \phi_3 + g_{12}(u_2) n_1 \phi_2 + \chi_{13} n_1 \phi_3 + \chi_{23} n_2 \phi_3 \qquad (1)$$

The subscripts refer to nonsolvent (1), solvent (2) and polymer (3). n_i and ϕ_i are the number of moles and the volume fraction respectively. χ_{13} is the nonsolvent-polymer interaction parameter and χ_{23} the solvent-polymer interaction parameter. Both parameters are assumed to be concentration independent. g_{12} is the solvent-nonsolvent interaction parameter and this parameter is assumed to be a function of u_2, with $u_2=\phi_2/(\phi_1+\phi_2)$ in the notation of Pouchlý [29].

Different factors are very important for the formation of the toplayer:

- the ratio of nonsolvent inflow (J_1) and solvent outflow (J_2).
- polymer concentration in the casting solution.
- location of the liquid-liquid demixing gap.
- location of the gel region.

Figure 3 gives a schematic representation of the film/bath interface.

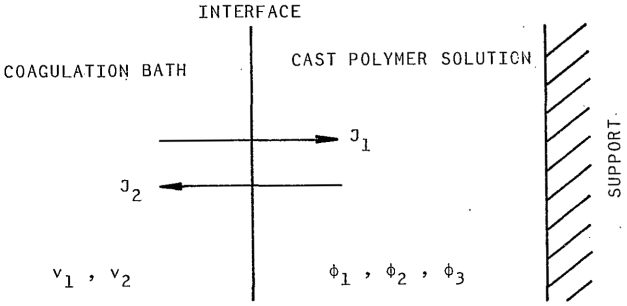

FIGURE 3. Fluxes of nonsolvent (J_1) and solvent (J_2) at the interface coagulation bath/cast polymer solution. Components: 1, nonsolvent; 2, solvent; 3, polymer.

The ratio of the solvent outflow (J_2) and nonsolvent inflow (J_1) determines the course of the coagulation path. In order to obtain a dense toplayer, the ratio J_1/J_2 should be small and the coagulation path will reach the gel region before intersecting the binodal. J_1 and J_2 can be represented by a simplified phenomenological relation

$$J_i = L_i(\phi_i, v_i)\ \Delta\mu_i \tag{2}$$

$\Delta\mu_i$, the chemical potential difference, is the driving force for mass transport of component i through the film/bath interface (see Fig. 3) and L_i is the permeability coefficient of component i which may be a function of ϕ_i and v_i.

Calculations performed by Altena [30] showed that in the early stage of membrane formation the ratio J_1/J_2 is very small and consequently a very steep coagulation path results which intersects the gel region at low nonsolvent content (see Fig. 2, arrow AC). If we disregard the influence of L_i (or assume the ratio L_1/L_2 to be 1) then the ratio J_1/J_2 is determined by the ratio of the chemical potential differences $\Delta\mu_1/\Delta\mu_2$. This latter ratio can be altered by changing the kind of solvent and nonsolvent and by modifying solvent and nonsolvent proportions in film and bath. Wijmans [25] changed the ratio of $\Delta\mu_1/\Delta\mu_2$ (and so J_1/J_2) by adding solvent to the coagulation bath. The coagulation path is then less steep and the binodal is intersected at much lower polymer concentrations (see Fig. 2, arrow AB). In this way it is even possible to obtain a microporous membrane without a dense toplayer. Contrarily, in order to obtain a dense toplayer it is necessary that the coagulation path should be as steep as possible.

Another factor which is important for the formation of a dense toplayer is the location of the binodal. Altena [23] was able to calculate numerically the location of the binodal of a ternary system using Flory-Huggins thermodynamics. He showed that the location of the binodal demixing gap primarily depends on the g_{12} and χ_{13} parameters.

For a fixed value of χ_{13} (say 1.5) an increase in g_{12} (i.e. an increase in excess free energy of mixing between solvent and nonsolvent) will cause a shift of the binodal to a higher nonsolvent content (Fig. 4a). For a fixed value of g_{12} (say 0.5) an increase in χ_{13} (i.e. decrease of polymer-nonsolvent interaction) will cause a shift of the binodal to a lower nonsolvent content (Fig. 4b). For a very high value of χ_{13} (say 4.0) the binodal is located very near to the solvent-polymer axis and an increase in g_{12} then hardly has any influence on the location of the binodal.

What is the influence of the location of the binodal on the compactness and density of the toplayer?

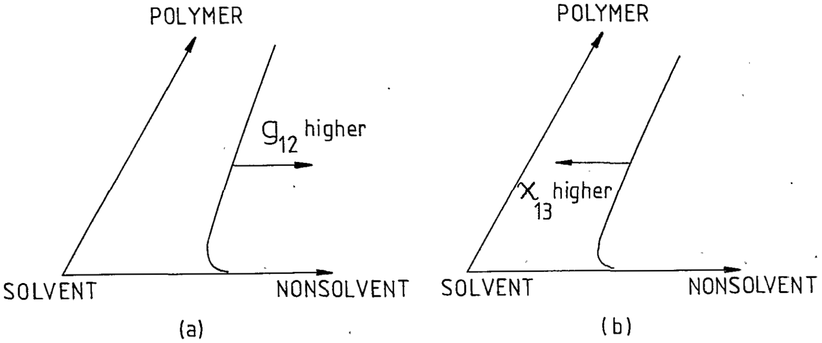

FIGURE 4. Direction of the shift of the binodal. a) increasing g_{12}; b) increasing χ_{13}.

The more the binodal has been shifted to the polymer-nonsolvent axis, the more it is likely that the gel region is reached before the binodal will be intersected. This is schematically shown in Fig. 5. In a sence this effect paral-

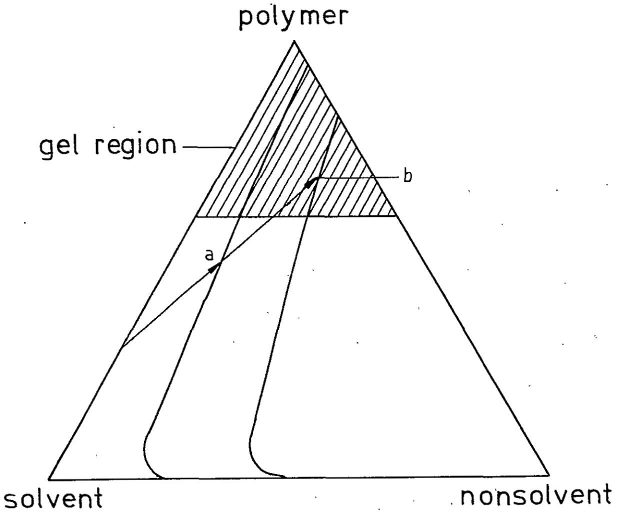

FIGURE 5. Schematic course of a coagulation path reaching first the binodal (a) or the gel region (b), depending upon the binodal curve.

lels the influence of another factor: the location of the gel region, since also when altering gelation (for instance by temperature variation) one can monitor the conditions at the intersection of the demixing gap.

In the experimental part we will focus our attention on two factors which influence the formation of a dense toplayer strongly:

- polymer concentration in the casting solution;
- location of the binodal.

The location of the gel region is still a rather unknown factor and we have not further explored it here.

EXPERIMENTAL

Materials

Cellulose acetate (E 398-3) was obtained from Eastman Chemicals, Polysulfone (P 3500) from Union Carbide, Poly-(2,6-dimethylphenyleneoxide) from General Electric and Polyacrylonitrile (T 75) from Dupont. The solvents used were of analytical grade.

Membrane preparation

Homogeneous membranes: polymer solutions were prepared by dissolving the polymer in a suitable solvent. Membranes were prepared by casting the polymer solution upon a glass plate after which the solvent was allowed to evaporate in a nitrogen atmosphere. The membranes obtained were completely transparant except for polyacrylonitrile.

Asymmetric membranes: asymmetric membranes were prepared by immersion precipitation. A polymer solution containing 10 to 30% by weight, was cast upon a glass plate and after immersion in a nonsolvent bath at room temperature the membrane was obtained.

Determination of the phase diagram

The location of the binodal in the phase diagram has been determined by titration. Solutions of solvent/nonsolvent were carefully added to polymer solutions at room temperature (20 °C) until permanent turbidity (detected visually) was obtained. This indicated the boundary between the one-phase region and the two-phase region.

Pervaporation

The pervaporation experiments were carried out as described in chapter 2 [31]. Vacuum at the downstream side was maintained at a pressure of 13.3 Pascal (0.1 mm Hg) by a Crompton Parkinson vacuum pump. The pressure was measured by an Edwards piranhi gauge. The experiments were carried out during eight hours. A product sample was taken every hour and generally steady-state conditions were reached within two or three hours. The temperature of the liquid feed mixture was 20 °C. The asymmetric membranes were installed with the toplayer facing the feed.

Product analysis

Analysis of binary ethanol-water mixtures was performed on a Varian model 3700 gaschromatograph fitted with a chromosorb 60/80 column and equipped with a thermal conductivity detector. For low ethanol concentrations (0-5%) a flame ionization detector was used.

Scanning electron microscopy

Cross-sections of the membrane were examined with a JEOL JSM 35 CF scanning electron microscope. Air dried samples were prepared by cryogenic breaking followed by coating the sample with a charge conducting layer of gold by means of a Balzer union sputter unit.

RESULTS AND DISCUSSION

In the first example to be treated here we will show the influence of the g_{12} interaction parameter on the location of the binodal and its effect on membrane performance. For this purpose we will compare the systems water/DMSO/cellulose acetate (CA) and water/acetone/cellulose acetate. The interaction parameters are taken from Altena [23] and Mulder [4]. The g_{12} parameters both for water/acetone and water/DMSO as a function of the volume fraction of water are given in Fig. 6.

If the g_{12} parameter is large (i.e. a high value for the excess free energy of mixing and a low mutual affinity), the binodal demixing gap is shifted to higher nonsolvent concentrations while for low g_{12} values (i.e. low or negative values for the free energy of mixing) the binodal is shifted to lower nonsolvent content. In Fig. 7 the binodals for the two systems, taken from Altena [23] are given. Asymmetric membranes prepared from the two systems have been tested on ethanol-water mixtures and the results are given

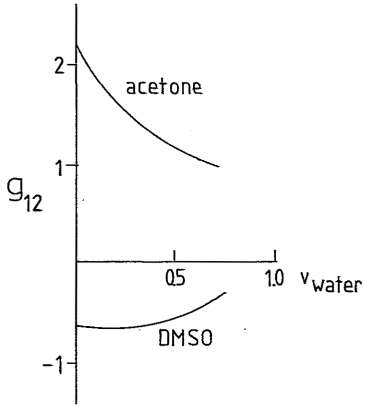

FIGURE 6. Concentration dependent g_{12} parameters for the binary systems acetone/water and DMSO/water (from ref. 23).

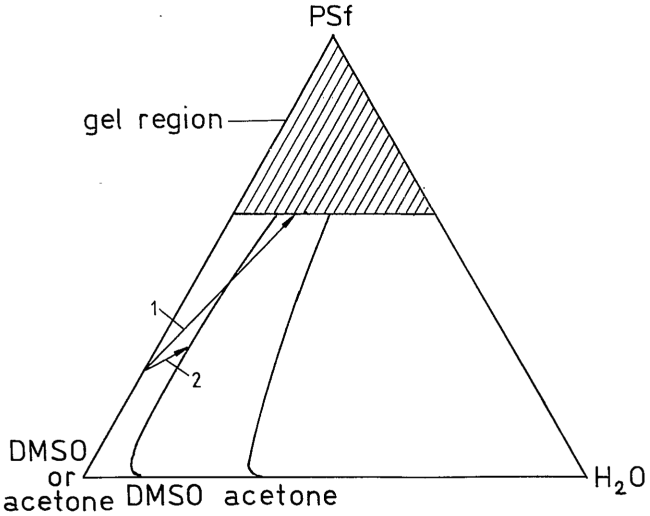

FIGURE 7. Influence of the location of the liquid-liquid demixing gap and of the direction of the coagulation path on membrane formation. The location of the binodals are taken from Altena [23]. The location of the gel region is chosen arbitrarily. 1: DMSO as solvent; 2: acetone as solvent.

TABLE 1

Pervaporation results of asymmetric cellulose acetate membranes. Feed: ethanol-water 50-50% by weight. Temperature: 20 °C

Solvent	nonsolvent	pol. conc. (%)	α	weight % H_2O in permeate	perm. rate (cm/hr).10^2
acetone	water	25	12.3	92.5	2.7
acetone	water	18	5.9	85.5	4.2
DMSO	water	25	1.0	50.0	32.5
DMSO	water	18	–	–	–[a]

[a] permeability too high

in Table 1. These results clearly show that solvent/nonsolvent interactions (i.e. location of the binodal) and polymer concentration have a large influence on membrane performance. A shift of the binodal to higher water contents (system acetone/CA) and an increase of the polymer concentration results in membranes with higher selectivities.

A second phenomenon which has to be taken into account is the direction of the coagulation path, given by the ratio J_1/J_2. In the case of acetone as solvent this ratio is much smaller in comparison with DMSO as solvent (see for instance Frommer [33]). This results in a steep coagulation path and a more dense toplayer (Fig. 7, arrow 1).

In the case of DMSO as solvent two effects cooperate to give a less dense toplayer: the binodal is located near the solvent-polymer axis and the ratio J_1/J_2 is much higher giving a less steep coagulation path. Now the coagulation path can intersect the binodal in the neighbourhood of the gel region (Fig. 7, arrow 2) giving a membrane with a less compact toplayer (Membranes prepared from a 20% solution of CA in DMSO and water as nonsolvent have ultrafiltration properties [34]).

For systems with a very high χ_{13} value such as water(1)/polysulfone(3) the location of the binodal is almost completely determined by this parameter. By changing the kind of solvent in such a way that the mutual affinity between polymer and nonsolvent increases (χ_{13} decreases), the binodal will be shifted to higher nonsolvent content. In Figure 8a the experimental and calculated binodal for the system water/DMAc/Polysulfone and the experimentally determined binodal for the system ethanol/DMAc/Polysulfone are given. The experimentally determined binodals for the system methanol (respectively ethanol,propanol)/chloroform/Polysulfone are given in Figure 8b.

From these systems asymmetric membranes have been prepared and the pervaporation results are given in Table 2. Again it is striking that selectivity increases and permeation rate decreases if the binodal has been shifted to higher nonsolvent content.

Another point to be noticed is that changing the kind of nonsolvent will also affect the location of the gel region.

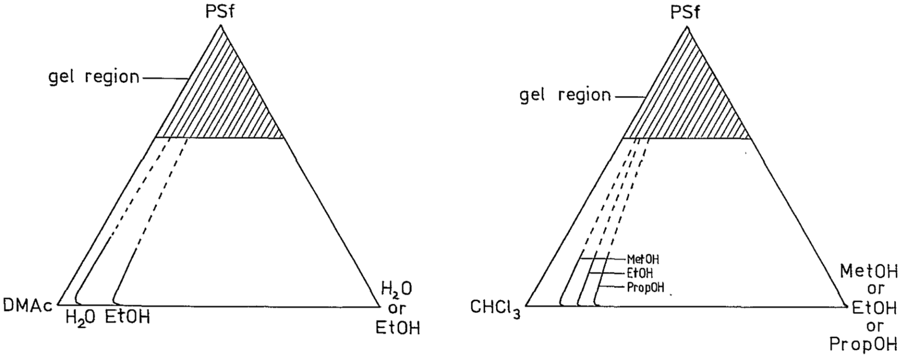

FIGURE 8. Experimentally determined binodals for water/DMAc/PSf and ethanol/DMAc/PSf (a) and for methanol(resp. ethanol, propanol/$CHCl_3$/PSf (b).

TABLE 2

Pervaporation results of asymmetric polysulfone membranes. Feed: ethanol-water 50-50% by weight. Temperature: 20 °C.

Solvent	nonsolvent	pol. conc. (%)	α	weight % H_2O in permeate	perm. rate (cm/hr).10^2
DMAc	water	15	-	-	-†
DMAc	ethanol	15	1.0	50.0	7.0
$CHCl_3$	methanol	15	8.3	89.2	0.2
$CHCl_3$	ethanol	15	58	98.3	0.1
$CHCl_3$	propanol	15	499	99.8	<0.1

† permeability too high

The last point to be considered is the influence of the polymer concentration on membrane performance. As was already demonstrated for cellulose acetate membranes, an increase in the polymer concentration of the polymer solution results in an increase in selectivity (see Table 1). For the system i-propanol/DMAc/Polysulfone we have varied the polymer concentration from 15 to 35% by weight of polymer and the results are given in table 3.

TABLE 3

Pervaporation results of asymmetric polysulfone membranes from the system i-propanol/DMAc/Polysulfone. Feed: ethanol-water 50-50% by weight. Temperature: 20°C.

Pol. conc. (%)	α	weight % H_2O in permeate	perm. rate (cm/hr).10^2
15	1.5	60.0	4.5
20	6.6	86.8	1.0
25	6.4	86.5	0.6
30	47	97.9	0.1
35	249	99.6	<0.1

From Table 3 one can see that the permeation rate decreases more than a factor 45 while the selectivity to ethanol/water mixtures increases from $\alpha = 1.5$ to $\alpha \sim 250$. Although the exact location of the binodal of this system has not been calculated (which is in fact not necessary for this qualitative explanation) the change in the coagulation path is shown schematically in Figure 9. Going from 15 to 35% the coaguation path reaches the gel region at lower nonsolvent.
Cross-sections of the asymmetric membranes from this system (i-propanol/DMAc/Polysulfone with increasing polymer concentration from 15 to 35% by weight) are given in Figures 10-14. These figures clearly show that if the polymer concentration increases also the thickness of the toplayer increases while the structure of the porous sublayer hardly changes. The increase of the toplayer thickness results in a decrease in permeation rate (see Table 3). Generally, if the thickness of a homogeneous membrane is increased, the permeation rate decreases roughly inversely proportional to membrane thickness while selectivity is hardly affected [1,36]. However,

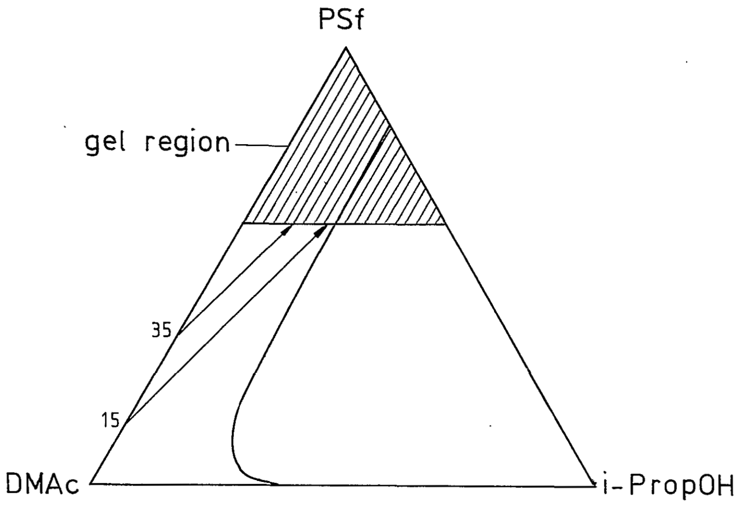

FIGURE 9. Schematic course of the coagulation paths originating from different polymer concentrations for the system i-propanol/DMAc/PSf.

if the results of Table 3 are considered, a very large increase can be observed and this cannot be explained by an increase in thickness of the toplayer. Hence, the stucture of the toplayer will change and going from 15 to 35% a more dense and compact toplayer is obtained.
The SEM photographs clearly support the hypothesis that two different types of phase separation are responsible for the formation of asymmetric membranes: gelation for the formation of the toplayer and liquid-liquid phase separation followed by gelation of the concentrated polymer phase for the formation of the porous sublayer.

Comparison of homogeneous and asymmetric membranes

The objective of our investigations was to develop asymmetric pervaporation membranes in order to improve the permeability without loss of selectivity. Therefore homogeneous membranes should be compared with the corresponding asymmetric membranes. The results are given in Table 4. One sees

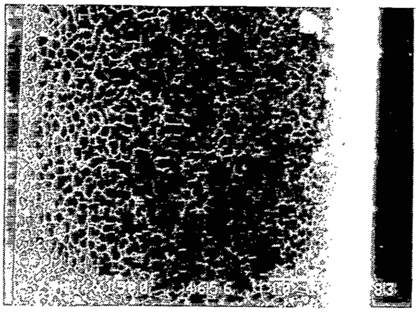

Fig. 10

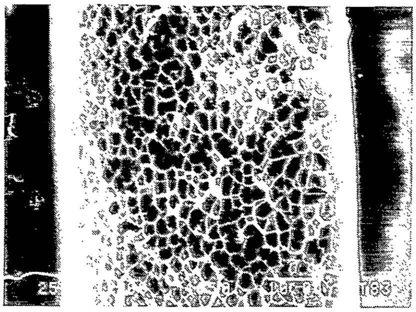

Fig. 11

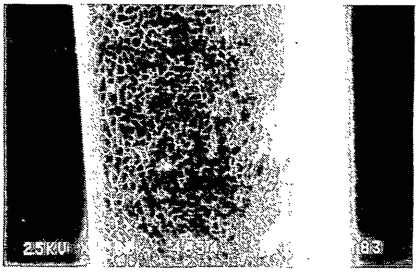

Fig. 12

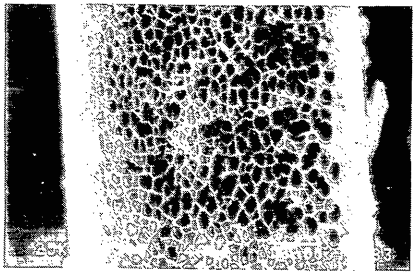

Fig. 13

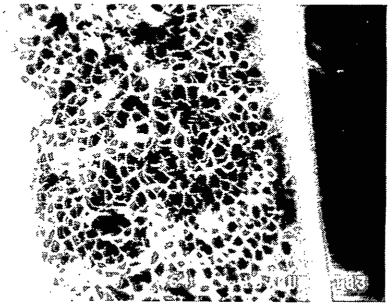

Fig. 14

FIGURES 10-14. Cross-sections of asymmetric membranes from the system i-propanol/DMAc/PSf. Fig. 10: 15% PSf; Fig. 11: 20% PSf; Fig. 12: 25% PSf; Fig. 13: 30% PSf; Fig. 14: 35% PSf.

TABLE 4

Homogeneous membranes versus asymmetric membranes. Membrane thickness (for the homogeneous membranes): 20 μm. Feed: ethanol-water 50-50% by weight. Temperature: 20°C.

	HOMOGENEOUS			ASYMMETRIC		
Polymer	weight % H_2O in permeate	α	perm. rate $(cm/hr).10^2$	weight % H_2O in permeate	α	perm. rate $(cm/hr).10^2$
CA	80.7	4.2	6.8	95.0†	19	3.3
PSf	>99.5	>200	0.04	>99.5§	>200	0.1
PPO	95.7	22	0.09	94.1*	16	0.2
PAN	>99.5	>200	0.15	97.9+	47	1.9

† system water/acetone/cellulose acetate (CA)
§ system propanol/$CHCl_3$/polysulfone (PSf)
* system ethanol/trichloroethylene/polyphenyleneoxide (PPO)
+ system i-propanol/DMAc/polyacrylonitrile (PAN)

from Table 4 that in all cases except for cellulose acetate an improvement in permeability was obtained.

The resistance to mass transfer of the asymmetric membranes is not only determined by the toplayer but also to some extent by the sublayer. If this sublayer contains very small pores then the contribution to the total resistance can be considerable and the advantage of a thin dense toplayer as sole rate limiting factor does not hold anymore. Asymmetric CA membranes obtained from the system water/acetone/CA consist of a sublayer with very small pores (< 0.1 μm) and therefore the permeation rate is not as large as expected. Moreover, the relatively low permeation rate can also be explained in part by the structure of the toplayer; it has a more dense structure in comparison with the homogeneous membranes as is indicated by the improved selectivity of the asymmetric CA membranes. The conclusion that small amounts of water increases the ordering of cellulose acetate gels resulting in a more compact structure is in agreement with differential scanning calorimetry measurements performed by Altena [35].

For the other polymers an improvement in permeation rate has been obtained, however a small loss in selectivity can be observed.

CONCLUSIONS

In order to obtain asymmetric pervaporation membranes with a dense toplayer different factors are important: the polymer concentration in the casting solution (should be high), the ratio J_1/J_2 (should be small) and the location of the binodal demixing region and the gel region.

The general mechanism of membrane formation follows the scheme:

toplayer - gelation by entanglement (in the case of amorphous polymers.

sublayer - liquid-liquid phase separation followed by gelation of the concentrated polymer phase.

The SEM photographs clearly support the hypothesis that two different types of phase separation are responsible for the formation of asymmetric membranes.

Asymmetric membranes have been prepared with high selectivities towards ethanol/water mixtures. In comparison with the homogeneous membranes the asymmetric membranes show higher permeabilities (as expected) while the selectivity remains the same or decreases slightly. Cellulose acetate is an exception because the asymmetric membranes show higher selectivities and lower permeation rates compared to the homogeneous membranes.

The highly selective asymmetric pervaporation membranes have relatively thick toplayers compared to asymmetric ultrafiltration and hyperfiltration membranes.

REFERENCES

1 R.C. Binning, R.J. Lee, J.F. Jennings and E.C. Martin, *Ind. Eng. Chem.*, 53 (1961) 45.

2 R.C. Binning and R.J. Lee, *Pet. Refiner.*, 37 (1958) 214.

3 R.C. Binning, R.J. Lee, J.F. Jennings and E.C. Martin, *Am. Chem. Soc. Div. Pet. Chem. Prepr.*, 3 (1958) 131.

4 M.H.V. Mulder, J. Oude Hendrikman, H. Hegeman and C.A. Smolders, *J. Membrane Sci.*, 16 (1983) 269.

5 P. Aptel, J. Cuny, J. Jozefowicz, G. Morel and J. Neel, *J. Appl. Pol. Sci.*, 16 (1972) 106.

6 G.C. Tealdo, P. Canepa and S. Munari, *J. Membrane Sci.*, 9 (1981) 191.

7 R.Y.M. Huang and H,R. Jarvis, *J. Appl. Pol. Sci.*, 14 (1970) 2341.

8 E. Nagy, D. Borlai and A. Ujhidy, *J. Membrane Sci.*, 7 (1980) 109.

9 K.C. Hoover and S.T. Hwang, *J. Membrane Sci.*, 10 (1982) 253.

10 H.E.A. Brüschke, W.H. Schneider and G.F. Tusel, Lecture presented at the European Workshop on Pervaporation, Sept. 21-22, 1982, Nancy, France; *Membrane News*, No. 4, 1883, published by the European Society of Membrane Science and Technology.

11 M.H.V. Mulder and C.A. Smolders, *J. Membrane Sci.*, 17 (1984) 289.

12 D.R. Paul and J.D. Paciotti, *J. Pol. Sci.*, A-2, 13 (1975) 1201.

13 C.H. Lee, *J. Appl. Pol. Sci.*, 19 (1975) 83.

14 F.W. Greenlaw, R.A. Shelden and E.V. Thompson, *J. Membrane Sci.*, 2 (1977) 333.

15 R. Rautenbach and R. Albrecht, Lecture presented at the European Workshop on Pervaporation, Sept. 21-11, 1982, Nancy, France.

16 S. Loeb and S. Sourirajan, *Advan. Chem. Ser.*, 38 (1962) 117.

17 D.M. Koenhen, M.H.V. Mulder and C.A. Smolders, *J. Appl. Pol. Sci.*, 21 (1977) 199.

18 L. Broens, D.M. Koenhen and C.A. Smolders, *Desalination*, 22 (1977) 205.

19 L. Broens, F.W. Altena, C.A. Smolders and D.M. Koenhen,

Desalination, 32 (1980) 33.

20 C.A. Smolders, in 'Ultrafiltration Membranes and Application', A.R. Cooper, ed., *Pol. Sci. Techn.*, 13 (1980) 57, Plenum Press, New York, 1980.

21 F.W. Altena and C.A. Smolders, *J. Pol. Sci. Pol. Symp.*, 69 (1981) 1.

22 H. Bokhorst, F.W. Altena and C.A. Smolders, *Desalination*, 38 (1981) 349.

23 F.W. Altena and C.A. Smolders, *Macromolecules*, 15 (1982) 1491.

24 J.G. Wijmans and C.A. Smolders, to be published in the NATO ASI Series, Reidel Publishing Company.

25 J.G. Wijmans, J.P.B. Baaij and C.A. Smolders, *J. Membrane Sci.*, 14 (1983) 263.

26 R.E. Kesting, Synthetic Polymeric Membranes, McGraw Hill, New York, 1971, Chapter 5.

27 C. Cohen, G.B. Tanny and S. Prager, *J. Pol. Sci. Polym. Phys. Ed.*, 17 (1979) 477.

28 P.J. Flory, *Principles of Polymer Chemistry* , Cornell Univ. Press, New York, 1953.

29 A. Zivný and J. Pouchlý, *J. Pol. Sci.*, A-2, 10 (1972) 1467.

30 F.W. Altena, *PhD Thesis*, Twente University of Technology, Enschede, The Netherlands, 1982, Chapter 7.

31 M.H.V. Mulder, F. Kruitz and C.A. Smolders, *J. Membrane Sci.*, 11 (1982) 349.

32 M.H.V. Mulder, T. Franken and C.A. Smolders, submitted for publication in *J. Membrane Sci.*

33 M.A. Frommer and D. Lancet, in 'Reverse Osmosis Membrane Research', H.K. Lonsdale and H.E. Podall, Eds., Plenum Press, New York, 1972.

34 R. Bloch and M.A. Frommer, *Desalination*, 7 (1970) 259.

35 F.W. Altena, J.S. Schröder, R. v.d. Hulst and C.A. Smolders, to be published in *J. Pol. Sci.*

36 P. Aptel, J. Cuny, J. Jozefowicz, G. Morel and J. Neel, *J. Appl. Pol. Sci.*, 18 (1974) 351.

CHAPTER 5

ON THE MECHANISM OF SEPARATION OF ETHANOL/WATER MIXTURES BY PERVAPORATION

I. CALCULATION OF CONCENTRATION PROFILES*

M.H.V. MULDER and C.A. SMOLDERS

SUMMARY

A solution-diffusion model for the permeation of liquid mixtures through polymeric membranes taking into account coupling of fluxes has been developed. The model is applied to the separation by pervaporation of ethanol-water mixtures through cellulose acetate. In order to determine the activities of the permeating components in the polymeric membrane, values of polymer-liquid and liquid-liquid interaction parameters are needed; polymer-liquid interaction parameters have been determined from swelling experiments and liquid-liquid interaction parameters have been calculated from excess free energy of mixing data taken from the literature.

Concentration profiles of water and ethanol in cellulose acetate membranes have been calculated using (a) apparent concentration independent diffusion coefficients, and (b) diffusion coefficients with exponential concentration dependence and two adjustable parameters. It is discussed that the transport of ethanol-water mixtures by pervaporation cannot be explained by using concentration independent diffusion coefficients.

---

*Published in Journal of Membrane Science, 17 (1984) 289.

INTRODUCTION

Transport of liquids through homogeneous polymeric membranes, as practised during pervaporation, differs from gas separation because the concentrations of the permeating components in the polymer are in general much higher. The high permeant concentrations have, in their turn, a large influence on the diffusion coefficients of the permeants. Hence transport equations derived from gas separation cannot be applied a priori to pervaporation.

For a description of a pervaporation transport model, one should distinguish single component and multicomponent permeability. Single component permeation through homogeneous polymeric membranes can be satisfactorily described by Fick's law with a concentration dependent diffusion coefficient, as has been done by several authors [1-5]. Also, the application of free volume theory to single component permeation [6] shows good agreement between theory and experiment. Paul [7] proposed a model for pressure-induced diffusion of liquids through highly swollen rubber membranes, satisfactory agreement between theory and experiment was established.

No satisfactory theory exists that described the transport of a mixture. Fels [8] tried to modify the free volume concept to include contributions from both penetrants to the total free volume. Although this approach can have a significant contribution to the study of molecular separation phenomena, the agreement between theory and experiment is still lacking.

Greenlaw [9] investigated the effect of a linear relationship between the concentrations of permeants and their diffusion coefficients. For liquid mixtures that behave almost ideally, such as the heptane-hexane mixture used by Greenlaw, this treatment may hold but it is uncertain whether this would be the case for non-ideal mixtures such as ethanol-water.

Tock [10] attempted to predict selectivities for water-dioxane mixtures from permeabilities of the pure components using Fick's law with a concentration dependent diffusion coefficient. Their results show that it would hardly be possible to predict selectivities for non-ideal mixtures from single component permeability data only.

Lee [11] used a solution-diffusion model with concentration independent diffusion coefficients and without considering a possible coupling of fluxes. As a consequence, the selectivity factor is equal to the ratio of the permeability coefficients obtained from single component permeation experiments. In the case of liquid mixtures which show hardly any mutual interaction, nor any interaction with the polymer, this treatment may hold, but with other mixtures which behave far from ideally, such as ethanol-water, this treatment is probably too simple.

When a liquid mixture permeates through a membrane there will be coupling of fluxes. The flux of a component of the binary mixture may change, not only by the presence of the other component but also by its movements. This phenomenon has been pointed out clearly by Meares [12] in a review article about transport through polymeric membranes from the liquid phase. Coupling can be divided into two parts, a thermodynamic part and a kinetic part. The thermodynamic part, the change in concentration of one component in the membrane due to the presence of another component, is caused by mutual interactions between the permeants in the membrane as well as by interactions between the individual components and the membrane material. The extent of these interactions depends on the polymer-mixed penetrant system. Kinetic coupling is due to the dependence of the concentration on the diffusion coefficients of low molecular weight components in polymers, particularly in glassy polymers. In polymers below their glass transition, such as cellulose acetate, polysulfone and polyacrylonitrile at room temperature, the thermal motions of the chain segments are very much restricted. When low molecular weight components are dissolved in such polymers, the mobility of the chains increases. In the case of a binary mixture, both components will exert a plasticizing effect on the segmental motions, and the mobilities of both permeants will be enhanced by the combined plasticizing action. Therefore, in a model description for the separation of liquid mixtures by pervaporation, coupling phenomena have to be taken into account.

The objective of this chapter is to present a modified solution-diffusion model which combines both the thermodynamic and the kinetic (diffusive) aspects of the pervaporation process. Our approach differs from the original solution-diffusion model [11,13,14] in that we now consider coupling of fluxes, whereas in the original model each component dissolved in the membrane and diffused through it independently. With the model described here it is possible to calculate concentration profiles. When data on experimental concentration profiles are available, it is possible to calculate diffusion coefficients of permeating components in polymeric membranes. In this article we will present calculated concentration profiles of ethanol and water in cellulose acetate membranes using (a) apparent concentration independent diffusion coefficients obtained from steady-state measurements, and (b) diffusion coefficients with an exponential concentration dependence with two adjustable parameters. In a forthcoming article [15] we will report on experimentally determined concentration profiles and discuss these results in terms of the proposed model.

DESCRIPTION OF THE MODEL

Although the model follows the formalism of the solution-diffusion model some assumptions have been made:

- The model applies to pervaporation processes because only boundary conditions of the pervaporation process are included. In principle the model can be modified to apply to other membrane processes.
- The model describes the flow of permeants in the mem-

brane as a one-dimensional steady-state diffusion: the permeation rate is independent of time and the chemical potential of a component in the membrane is only a function of concentration and distance and not of time. Another important point is that during steady-state the membrane undergoes no structural changes.

- The application of the model is restricted to homogeneous membranes or to very dense toplayers of asymmetric or composite membranes where transport takes place by diffusion and not by convection.
- Transport through the membrane is rate-determining. This assumption implies that surface processes such as sorption at the feed/membrane interface and desorption at the membrane/permeate interface are fast compared to diffusion processes through the membrane.
- The interfaces of the membrane are in equilibrium with the upstream and downstream phase. This means that the chemical potential of component *i* in the upstream phase is equal to the chemical potential of component *i* just inside the membrane.
- The chemical potential or activity of a component in the polymeric membrane can be described by Flory-Huggins thermodynamics [16].

Binning [1] was the first to propose that the transport of liquids through homogeneous membranes takes place by a solution-diffusion mechanism.

According to the original solution-diffusion model [13, 14], the flux of a component *i* through the membrane can be described by the product of concentration, mobility and driving force. The driving force in most membrane processes and also in pervaporation is given by the gradient in the chemical potential. For component *i* the flux can be described by

$$J_i = -c_i B_i \frac{d\mu_i}{dx} \qquad (1)$$

At constant temperature, eqn. (1) may be written as

$$J_i = -c_i B_i \left(RT \frac{\mathrm{d}\ln a_i}{\mathrm{d}x} + \overline{V}_i \frac{\mathrm{d}P}{\mathrm{d}x}\right)_T \tag{2}$$

The pressure difference between the upstream and downstream phase is about 1 bar (0.1 MPa) in pervaporation processes. Therefore, the pressure gradient can be neglected with respect to the activity gradient

$$J_i = -c_i B_i RT \frac{\mathrm{d}\ln a_i}{\mathrm{d}x} \tag{3}$$

Assuming that

$$D_i = RT\ B_i \tag{4}$$

where D_i is the diffusion coefficient of component i in the polymer-fixed frame of reference, substitution of eqn. (4) in eqn. (3) gives

$$J_i = -c_i D_i \frac{\mathrm{d}\ln a_i}{\mathrm{d}x} \tag{5}$$

The activity of a component in the membrane can be described by Flory-Huggins thermodynamics [16]. For a binary system the activities a_1 and a_2 are given by

$$\ln a_1 = \frac{\Delta\mu_1}{RT} = \ln v_1 + \left(1 - \frac{V_1}{V_2}\right) v_2 + \chi_{12} v_2^2 \tag{6}$$

$$\ln a_2 = \frac{\Delta\mu_2}{RT} = \ln v_2 + \left(1 - \frac{V_2}{V_1}\right) v_1 + \chi_{12} \frac{V_2}{V_1} v_1^2 \tag{7}$$

χ_{12} is a binary interaction parameter between components 1 and 2 called the Flory-Huggins interaction parameter. This interaction parameter is a dimensionless quantity characterizing the difference in interaction energy of a solvent molecule immersed in pure polymer compared with one in pure solvent.

In the case of a polymeric membrane and a binary liquid mixture, a ternary system, the activities a_1 and a_2 of liquid components 1 and 2 in the polymeric membrane are given by [16]

$$\ln a_1 = \ln \phi_1 + (1-\phi_1)-\phi_2 \frac{V_1}{V_2} - \phi_3 \frac{V_1}{V_3} + (\chi_{12}\phi_2+\chi_{13}\phi_3)(\phi_2+\phi_3) - \chi_{23} \frac{V_1}{V_2} \phi_2\phi_3 \tag{8}$$

$$\ln a_2 = \ln \phi_2 + (1-\phi_2)-\phi_1 \frac{V_2}{V_1} - \phi_3 \frac{V_2}{V_3} + (\chi_{12}\phi_1 \frac{V_2}{V_1} + \chi_{23}\phi_3)(\phi_1+\phi_3) - \chi_{13} \frac{V_2}{V_1} \phi_1\phi_3 \tag{9}$$

Substitution of eqns. (8) and (9) in eqn. (5) gives

$$J_1 = -\phi_1 D_1(\phi_1,\phi_2) \frac{\mathrm{d}}{\mathrm{d}x}\left[\ln \phi_1 + (1-\phi_1)-\phi_2 \frac{V_1}{V_2} - \phi_3 \frac{V_1}{V_3} + (\chi_{12}\phi_2 + \chi_{13}\phi_3)(\phi_2+\phi_3)-\chi_{23} \frac{V_1}{V_2} \phi_2\phi_3\right] \tag{10}$$

$$J_2 = -\phi_2 D_2(\phi_1,\phi_2) \frac{\mathrm{d}}{\mathrm{d}x}\left[\ln \phi_2 + (1-\phi_2)-\phi_1 \frac{V_2}{V_1} - \phi_3 \frac{V_2}{V_3} + (\chi_{12}\phi_1 \frac{V_2}{V_1} + \chi_{23}\phi_3)(\phi_1+\phi_3) - \chi_{13} \frac{V_2}{V_1} \phi_1\phi_3\right] \tag{11}$$

Equations (10) and (11) are two coupled non-linear differential equations which have to be solved numerically. One should realize that eqns. (10) and (11) are simplified phenomenological relations. Although it seems that both components will diffuse independently, this is not true. One can see from eqns. (8) and (9) (or from eqns. (10) and (11)) that the activity of component 1 is not only dependent on its concentration but also on the concentration of components 2 and 3 and on the interaction parameters of components 1 and 2 (χ_{12}), 1 and 3 (χ_{13}) and 2 and 3

(χ_{23}). Secondly, the diffusion coefficient, D_1, is concentration dependent, not only on the concentration of component 1 but also on the concentration of component 2, because in the case of a liquid mixture both components will exert a plasticizing action and the diffusion coefficients will be enhanced by the combined action. The concentrations of components 1 and 2 change continuously from upstream to downstream phase during steady-state transport. Because the diffusion coefficients are assumed to be concentration dependent they will also change accordingly across the membrane as a function of the distance.

Evaluation of the binary interaction parameter χ_{12}

Solutions involving hydrogen bonding show deviations from ideal behaviour, especially in mixtures of liquids with strong hydrogen bonding such as water and ethanol.

A measure for the deviation from ideality is given by the excess functions. In Fig. 1 the enthalpy, ΔH_m, excess entropy, ΔS^E, and excess free energy of mixing, ΔG^E, of the system ethanol-water are given [17]. One can see from Fig. 1 that the excess functions are strongly concentra-

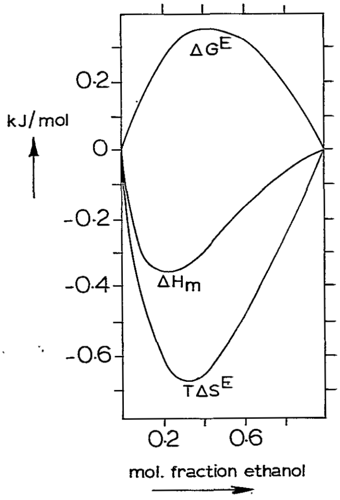

FIGURE 1. Excess functions of ethanol-water mixtures at 25 °C [17].

tion dependent. The χ_{12} parameter, which is in fact a free energy parameter, can be determined from the excess free energy of mixing, ΔG^{E}. Using Flory-Huggins thermodynamics [16], χ_{12} is given by

$$\chi_{12} = \frac{1}{m_1 v_2}\left[m_1 \ln \frac{m_1}{v_1} + m_2 \ln \frac{m_2}{v_2} + \frac{\Delta G^{E}}{RT}\right] \tag{12}$$

From eqn. (12), χ_{12} can be calculated as a function of v when data on ΔG^{E} are available. This method of calculating χ_{12} values has been used by several authors [18,19].

Dondos [20] used another equation for calculating the χ_{12} parameter:

$$\chi_{12} = \frac{\Delta G^{E}}{RT\, m_1 m_2} \tag{13}$$

Equations (12) and (13) are equal when the molar volumes of components 1 and 2 are the same. In the case of water and ethanol the ratio of the molar volumes is far from unity. The binary interaction parameter χ_{12}, calculated from eqns. (12) and (13), is given in Table 1. It is striking that χ_{12}, when calculated from eqn. (12), decreases as a function of the volume fraction of water while, when calculated from eqn. (13), χ_{12} increases.

Because eqn. (12) accounts for differences in molar volumes, we will use the χ_{12} values calculated from this equation. These values are presented in Fig. 2. From Table 1 and Fig. 2 it is clear that the χ_{12} parameter is concentration dependent; a fourth grade polynomial relation has been chosen to express the $\chi_{12}(v)$ function. The coefficients were found by using a least squares method; they are given in Table 2. In the case of a ternary system, χ_{12} is dependent of u, which is the nonsolvent part ($u_i = \frac{\phi_i}{\phi_1+\phi_2}$, $u_1+u_2=1$) in the ternary system.

TABLE 1

Binary interaction parameters for ethanol-water mixtures calculated from eqns. (12) and (13); the concentrations are given in volume fractions

Water v_1	Ethanol v_2	ΔG^E [a] (J mol^{-1})	χ_{12} eqn. (12)	 eqn. (13)
0.74	0.26	293	0.86	1.34
0.55	0.45	498	0.95	1.28
0.42	0.58	648	1.05	1.27
0.32	0.68	729	1.14	1.25
0.24	0.76	720	1.20	1.18
0.17	0.83	643	1.24	1.10
0.12	0.88	546	1.30	1.07
0.07	0.93	388	1.32	1.00
0.03	0.97	204	1.34	0.93

[a] From Ref. [21].

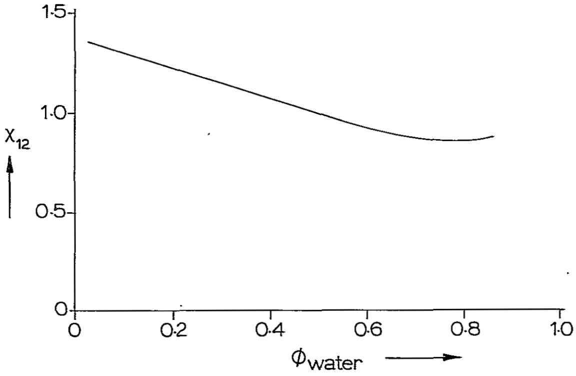

FIGURE 2. Interaction parameter, χ_{12}, for ethanol-water as a function of the volume fraction of water.

TABLE 2

Coefficients for the functions $\chi_{12}(v_2)$ or $\chi_{12}(u_2)$

$$\chi_{12} = a + b\,v_2 + c\,v_2^2 + d\,v_2^3 + e\,v_2^4$$

a	b	c	d	e
0.98	-1.35	4.15	-3.31	0.89

v_2: Volume fraction of ethanol in ethanol-water mixtures.
u_2: Volume fraction of ethanol referred to the nonsolvent part in the ternary system.

Evaluation of the binary parameters χ_{13} *and* χ_{23}

Two methods are available to determine interaction parameters of a polymer and a nonsolvent: equilibrium swelling experiments and inverse gas chromatography. The disadvantage of the latter method is that interaction parameters are obtained for infinite polymer concentration, χ^{∞}, at elevated temperatures. Because the interaction parameter is usually temperature and concentration dependent, extrapolation is often difficult. Swelling experiments are easy to perform at any temperature. The extent of swelling depends on the interaction between polymer and penetrant (in our case the nonsolvent). Polymers, applied as homogeneous or dense membranes as in pervaporation experiments, absorb only a small quantity of nonsolvent. The membrane can be considered as a swollen gel or a network with crosslinks caused by crystalline regions, chain entanglements or Van der Waals interactions. The swelling behaviour of such a network can be expressed by the Flory-Rehner theory [16]. The free energy change, ΔG, involved in the mixing of a nonsolvent and a polymer consists of two parts, the free energy of mixing, ΔG_{m}, and the elastic free energy, ΔG_{el}, [16]:

$$\Delta G = \Delta G_{\mathrm{m}} + \Delta G_{\mathrm{el}} \tag{14}$$

At swelling equilibrium, $\Delta G = 0$, eqn. (15) is obtained:

$$\ln\,(1-v_{\mathrm{p}}) + v_{\mathrm{p}} + \chi v_{\mathrm{p}}^{2} + \frac{V_{1}}{\bar{M}_{\mathrm{c}}\bar{\nu}_{\mathrm{p}}}(v_{\mathrm{p}}^{1/3} - \tfrac{1}{2}\,v_{\mathrm{p}}) = 0 \tag{15}$$

$\bar{M}_{\mathrm{c}}$ can be interpreted as the average molecular weight between two crosslinks. In polymer-nonsolvent systems with small amounts of nonsolvent in the polymer, the last term in eqn. (15) can be neglected. In the case of cellulose acetate the values of χ will not differ by more than 0.05, even for very unrealistic values of $\bar{M}_{\mathrm{c}}$ ($\bar{M}_{\mathrm{c}} = 265$, the molecular weight of one segment). This is within the accuracy of the values determined experimentally. Equation (15) has thus been reduced to a very simple form:

$$\chi = - \frac{[\ln(1-v_p) + v_p]}{v_p^2} \tag{16}$$

The results of the swelling experiments are given in Table 3. The solubility of water in cellulose acetate is in close agreement with values obtained by other investigators [13,22]. For the calculations of the profiles, the χ_{13} and χ_{23} parameters have been considered as constant.

TABLE 3

Sorption values and binary interaction parameters of cellulose acetate/water and cellulose acetate/ethanol

	Solubility (g penetrant/ 100 g dry polymer)	Weight fraction penetrant	Volume fraction penetrant	χ
CA/water	14.3	0.125	0.157	1.4
CA/ethanol	21.5	0.177	0.262	1.1

Calculation of concentration profiles

In order to calculate concentration profiles the following approach has been followed. A homogeneous membrane is divided into a number of infinitesimally thin layers [23-25]. The fluxes, J_1 and J_2, across every layer are the same because of the steady-state condition. Since the concentration difference over a thin layer is small, linear relations can be written between fluxes and forces. The intensive variables (i.e., chemical potentials) change continuously from the feed across the membrane to the permeate side. Equilibrium exists at the hypothetical interfaces of the thin layers; therefore, the chemical potential of a component at the outstream side of the nth layer is equal to that at the instream side of the (n+1)th layer.

In cases where the concentration profiles in the membrane are far from linear one can question if it is permissible to use linear relation because a small number of layers is responsible for the major part of the concentration difference. In such a case the membrane has to be divided into a large number of layers to keep the concentration difference over every single layer small. By using a large number of layers ($n > 100$) of equal thickness, results of the calculation procedure become independent of this number, which is an indication that the procedure followed is correct.

An alternative procedure, as suggested by McCallum [25] is to divide the membrane into a number of layers of equal concentration difference but of unequal thickness. With this procedure it is also possible to treat non-linear behaviour, but the computation is more complex than the procedure we applied. By taking each layer to be infinitesimally thin, it is assumed that the concentration gradient across a layer is equal to the concentration difference across the layer divided by its thickness:

$$\frac{d\phi}{dx} \equiv \frac{\phi_{x+\Delta x} - \phi_x}{\Delta x} \tag{17}$$

The transport equations (10) and (11) can be applied to each of the layers. When eqn. (17) is substituted into eqns. (10) and (11), two coupled non-linear differential equations have been transformed into two non-linear equations with two variables ϕ_1 and ϕ_2. It is also possible to transform these non-linear equations into linear equations, by expressing ln a_1 and ln a_2 as total differentials of ϕ_1 and ϕ_2. After substitution, eqn. (5) becomes

$$J_1 = -\phi_1 D_1 \frac{d \ln a_1}{dx} = -\phi_1 D_1 \left[\frac{\partial \ln a_1}{\partial \phi_1} \frac{d\phi_1}{dx} + \frac{\partial \ln a_1}{\partial \phi_2} \frac{d\phi_2}{dx} \right] \tag{18}$$

$$J_2 = -\phi_2 D_2 \frac{d \ln a_2}{dx} = -\phi_2 D_2 \left[\frac{\partial \ln a_2}{\partial \phi_1} \frac{d\phi_1}{dx} + \frac{\partial \ln a_2}{\partial \phi_2} \frac{d\phi_2}{dx} \right] \quad (19)$$

The partial derivatives $\partial \ln a_1/\partial\phi_1$, $\partial \ln a_1/\partial\phi_2$, $\partial \ln a_2/\partial\phi_1$ and $\partial \ln a_2/\partial\phi_2$ can be obtained by differentiating eqns. (8) and (9) to ϕ_1 and ϕ_2 respectively (see Appendix). Two linear equations for J_1 and J_2 with two variables ϕ_1 and ϕ_2 are the result:

$$J_1 = -\frac{\phi_1(n-1) D_1(\phi_1,\phi_2)}{\Delta x} \{g_{11}[\phi_1(n)-\phi_1(n-1)] + g_{12}[\phi_2(n)-\phi_2(n-1)]\} \quad (20)$$

$$J_2 = -\frac{\phi_2(n-1) D_2(\phi_1,\phi_2)}{\Delta x} \{g_{21}[\phi_1(n)-\phi_1(n-1)] + g_{22}[\phi_2(n)-\phi_2(n-1)]\} \quad (21)$$

The coefficients g_{11}, g_{12}, g_{21} and g_{22} are defined in the Appendix. From eqns. (20) and (21) the concentration profiles can be calculated as follows.

When the interaction parameters χ_{12}, χ_{13} and χ_{23}, the permeation rates J_1 and J_2, the diffusion coefficients D_1 and D_2, the molar volumes V_1, V_2 and V_3 and the initial concentrations $\phi_1(n=1)$, $\phi_2(n=1)$ and $\phi_3(n=1)$ are known, the two variables $\phi_1(n=2)$ and $\phi_2(n=2)$ can be calculated. These concentrations are the starting values for the next layer. In this way we are able to calculate the concentrations ϕ_1, ϕ_2 and ϕ_3 ($\Sigma\phi_i=1$) as a function of the penetration distance.

EXPERIMENTAL

Materials

Cellulose acetate (E 398-3) was obtained from Eastman

Chemicals. Acetone (reagent grade) was used without further purification.

Membrane preparation

Homogeneous cellulose acetate membranes were prepared by casting a solution of cellulose acetate in acetone upon a glass plate after which the acetone was allowed to evaporate in a nitrogen atmosphere. The membranes were completely transparent.

Swelling measurements

Dried strips of cellulose acetate membrane (about 0.3 g) were immersed in conical flasks containing water or ethanol. The flasks were placed in a thermostated bath at 20 °C. After 24 hours the strips were removed, pressed between tissue paper and weighed in a closed flask. This procedure was continued until no further weight increase was observed. The solubility can be expressed as a relative weight increase (g penetrant/100 g dry polymer).

Pervaporation

The pervaporation experiments were carried out as described in chapter 2 [26]. Vacuum at the downstream side was maintained at a pressure of 13.3 Pa (0.1 mmHg) by a Crompton Parkinson vacuum pump. The pressure was measured by an Edwards piranhi. The experiments were carried out for eight hours. Samples were taken every hour and steady-state conditions were usually reached after about three hours. The thickness of the homogeneous membrane was about 20 μm. The temperature of the liquid feed mixture was about 20 °C.

Product analysis

Analysis of binary ethanol-water mixtures was performed on a Varian model 3700 gas chromatograph fitted with a chromosorb 60/80 column and equipped with a thermal conductivity detector.

RESULTS AND DISCUSSION

Concentration profiles of ethanol and water in cellulose acetate membranes have been calculated using (a) apparent concentration independent diffusion coefficients calculated from steady-state pervaporation experiments, and (b) diffusion coefficients with an exponential concentration dependence.

Concentration independent diffusion coefficients

The diffusion coefficients given in the first example have been calculated from a steady-state pervaporation experiment and are in fact mean or apparent diffusion coefficients (see eqn. (22)):

$$\bar{D}_i = \frac{J_i . l}{\phi_i} \tag{22}$$

These calculated values are given in Table 4, together with the permeation rates, membrane thickness and volume fractions just inside the membrane at the feed/membrane boundary. These volume fractions are obtained numerically from eqns. (6)-(9). From an equilibrium sorption experiment, performed under the same conditions as the pervaporation experiment, an overall sorption value of 0.34 (= volume fraction) has been obtained. This result agrees reasonably well with the calculated values of ϕ_1 and ϕ_2 given in Table 4. The binary interaction parameters, determined as described earlier, are also given in Table 4, together with the ratios of the molar volumes which have been taken from the literature [19, 27].

TABLE 4

Parameters obtained from pervaporation experiments; feed: ethanol-water 73-27% by weight; temperature; 20 °C

Pervaporation parameters	Other parameters
$J_1 = 0.033$ cm hr^{-1}	$V_1/V_2 = 0.309$
$J_2 = 0.042$ cm hr^{-1}	$V_1/V_3 = 0.002$
$l = 20$ µm	$V_2/V_3 = 0.0065$
$\phi_1 = 0.133$	$\chi_{13} = 1.4$
$\phi_2 = 0.230$	$\chi_{23} = 1.1$
$\phi_3 = 0.637$	
$\bar{D}_1 = 13.8 \times 10^{-8}$ cm^2 sec^{-1}	
$\bar{D}_2 = 10.1 \times 10^{-8}$ cm^2 sec^{-1}	

The concentration profiles of water and ethanol in cellulose acetate have been calculated from eqns. (20) and (21), using the parameters given in Table 4. These profiles are given in Fig. 3. One can see from Fig. 3 that

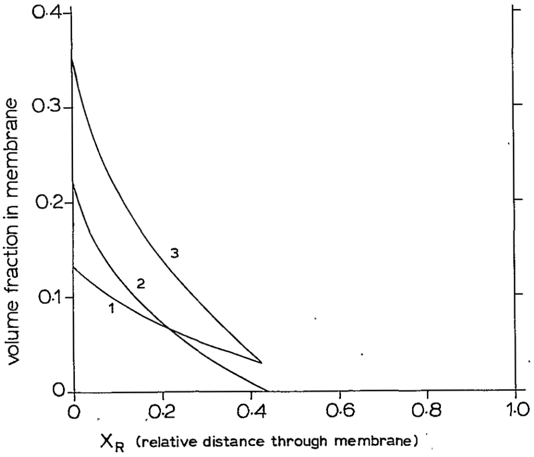

FIGURE 3. Calculated concentration profiles with concentration independent diffusion coefficients obtained from steady-state pervaporation experiments. 1, water; 2, ethanol; and 3, mixture; $\bar{D}_1 = 13.8 \times 10^{-8}$ cm^2/sec; $\bar{D}_2 = 10.1 \times 10^{-8}$ cm^2/sec.

somewhere in the membrane the concentration of ethanol becomes zero, which is not possible. Hence, it is not correct to use transport equations for liquid mixtures such as ethanol/water assuming concentration independent diffusion coefficients and uncoupled flow. This conclusion was already stated clearly by Meares [12]. In a forthcoming article [15] we will give experimental evidence for this statement. As a consequence, the model description of Lee [11] cannot be applied to this kind of liquid mixture or to any liquid mixture where the liquids exert a plasticizing action on the polymer.

The ethanol and water profiles given in Fig. 3 can be changed by increasing the diffusion coefficients. This can be carried out quite easily numerically. If the diffusion coefficients of ethanol and water increase by a factor two, while the other parameters are kept constant, profiles are obtained as given in Fig. 4. The profiles shown in Figs. 3 and 4 do not deviate much from linearity. This can be explained by the fact that concentration independent diffusion coefficients have been used.

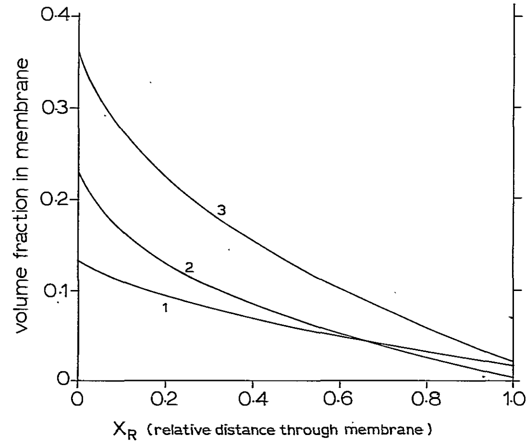

FIGURE 4. Calculated concentration profiles with concentration independent diffusion coefficients. 1, water; 2, ethanol; and 3, mixture; $\bar{D}_1 = 27 \times 10^{-8}$ cm^2/sec; $\bar{D}_2 = 25 \times 10^{-8}$ cm^2/sec.

Concentration dependent diffusion coefficients

We will now consider the case of concentration dependent diffusion coefficients. Different relationships can be used to express the relation between diffusion coefficient and concentration. Most authors have used a linear [9,28] or an exponential [2-5,10,29,30] relationship. An exponential relationship holds for the case where the diffusion coefficient is more strongly concentration dependent:

$$D_i = D_{0i}\exp(\gamma_i \phi_i) \tag{23}$$

In the case of a binary mixture, the diffusion coefficients of components 1 and 2 are given by

$$D_1 = D_{01}\ \exp(\gamma_1\phi_1 + \gamma_2\phi_2) \tag{24}$$

$$D_2 = D_{02}\ \exp(\gamma_1\phi_1 + \gamma_2\phi_2) \tag{25}$$

Except for the concentration itself, two other factors determine the values of the diffusion coefficients: D_0, which is the diffusion coefficient at zero concentration of penetrant and the exponential factor, γ, which is a plasticizing constant, showing the effect of the penetrant concentration on the mobility of the penetrant in the membrane. In the case of liquid mixtures, there will be a combined plasticizing action (see eqns. (24) and (25)). In our model calculations the same values for the other parameters have been used as given in Table 4.

The influence of the proportionality factor, D_0, and the exponential factor, γ, on the concentration profiles are given in Figs. 5 and 6. In Fig. 5 the proportionality factor, D_0 has been given a higher value and in Fig 6 a higher value is given to the exponential factor, γ. Both figures show a typical exponential behaviour. However, the curvature strongly depends on the exponential factor, γ. In Figs. 5 and 6 the exponential factor γ has the same value for both components. The actual values of γ_1 and γ_2 will

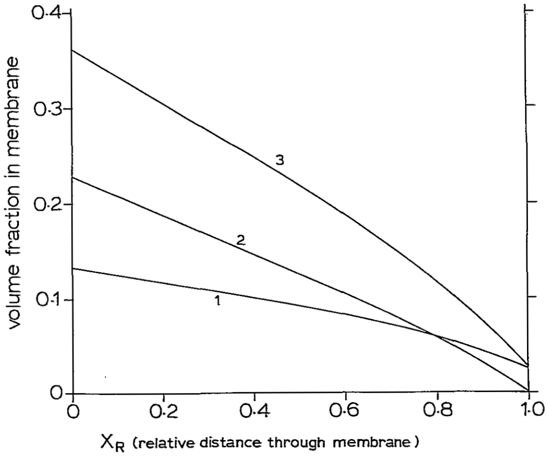

FIGURE 5. Calculated concentration profiles with concentration dependent diffusion coefficients. D_{01} = 8.8×10^{-8} cm^2/sec; D_{02} = 6.0×10^{-8} cm^2/sec; $\gamma_1 = \gamma_2 = 7.3$; 1, water; 2, ethanol; and 3, mixture.

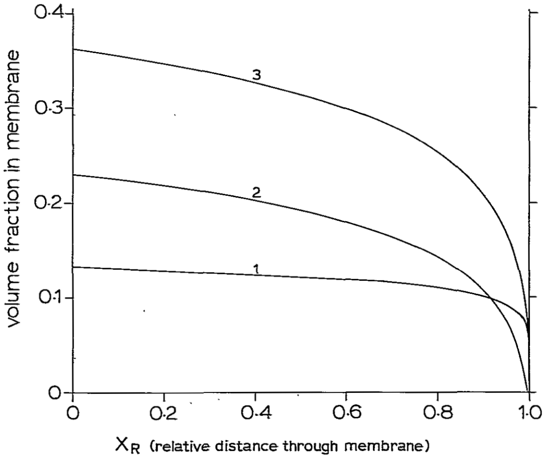

FIGURE 6. Calculated concentration profiles with concentration dependent diffusion coefficients. D_{01} = 7.0×10^{-9} cm^2/sec; $D_{02} = 1.1 \times 10^{-9}$ cm^2/sec; $\gamma_1 = \gamma_2 = 20.78$; 1, water; 2, ethanol; and 3, mixture.

not be identical because both components will not exert the same plasticizing action.

The differences between Figs. 5 and 6 are evident. If γ increases (Fig. 6), the concentration profiles become more concave. This can be expected since the exponential factor has a more important contribution than the proportionality factor, D_0. The exponential factor γ is undoubtedly related to the Flory-Huggins interaction parameter, so for the system water/ethanol/cellulose acetate, γ_2 (ethanol) will have a higher value than γ_1 (water).

At this stage a more precise study of the influence of the different factors (D_0, γ) on the concentration profile did not seem relevant to us without detailed information about experimental concentration profiles. In a forthcoming article [15] we will report on experimental concentration profiles of different binary mixtures in polymeric membranes. Diffusion coefficients will be calculated according to the model described in this article.

CONCLUSIONS

- A modified solution-diffusion model has been developed which describes the transport of liquid mixtures through homogeneous membranes. In the present study, transport of ethanol-water through cellulose acetate membranes has been investigated.
- The model takes into account coupling in the thermodynamic part as well as in the diffusive part of the transport equations.
- Transport of aqueous mixtures cannot be described with a concentration independent diffusion coefficient.

LIST OF SYMBOLS

a	Activity
B	Mobility (mmol $\mathrm{sec}^{-1}\cdot \mathrm{N}^{-1}$)
D	Diffusion coefficient ($\mathrm{cm}^2\cdot \mathrm{sec}^{-1}$)
$\bar{D}$	Mean or apparent diffusion coefficient ($\mathrm{cm}^2\ \mathrm{sec}^{-1}$)
D_0	Diffusion coefficient at zero concentration ($\mathrm{cm}^2\ \mathrm{sec}^{-1}$)
ΔG_m	Free energy of mixing (J mol^{-1})
ΔG^E	Excess free energy of mixing (J mol^{-1})
J	Permeation rate ($\mathrm{cm}\cdot \mathrm{hr}^{-1}$)
l	Membrane thickness (μm)
m	Mole fraction
n	Number of layers
P	Pressure (Pa)
R	Gas constant (J $\mathrm{mol}^{-1}\ \mathrm{K}^{-1}$)
T	Temperature (K)
u	Volume fraction referred to the nonsolvent part in the ternary system
v	Volume fraction in the binary system
V	Molar volume ($\mathrm{cm}^3\ \mathrm{mol}^{-1}$)
Δx	Thickness of one layer (μm)

γ	Exponential factor
χ	Flory-Huggins interaction parameter
ϕ	Volume fraction in the ternary system
μ	Chemical potential (J mol^{-1})
$\bar{\nu}$	Specific volume ($\mathrm{cm}^3\cdot \mathrm{g}^{-1}$)
ρ	Density (g cm^{-3})

Indices

1	Water
2	Ethanol
3	Cellulose acetate
i	Component i
p	Polymer

REFERENCES

1 R.C. Binning, R.J. Lee, J.F. Jennings and E.C. Martin, *Ind. Eng. Chem.*, 53 (1961) 45.

2 S.N. Kim and K. Kammermeyer, *Sep. Sci.*, 5 (1970) 679.

3 R.Y.M. Huang and V.J.C. Lin, *J. Appl. Polym. Sci.*, 12 (1968) 2615.

4 R.B. Long, *Ind. Eng. Chem. Fundam.*, 4 (1965) 445.

5 P. Aptel, J. Cuny, J. Jozefowicz, G. Morel and J. Neel, *J. Appl. Polym. Sci.*, 18 (1974) 351.

6 M. Fels and R.Y.M. Huang, *J. Appl. Polym. Sci.*, 14 (1970) 537.

7 D.R. Paul and O.M. Ebra-Lima, *J. Appl. Polym. Sci.*, 15 (1971) 2199.

8 M. Fels, *AIChE Symp. Ser.*, 68 (1972) 49.

9 F.W. Greenlaw, R.A. Shelden and E.V. Thompson, *J. Membrane Sci.*, 2 (1977) 333.

10 R.W.M. Tock, J. Yu. Cheung and R.L. Cook, *Sep. Sci.*, 9 (1974) 361.

11 C.H. Lee, *J. Appl. Polym. Sci.*, 19 (1975) 83.

12 P. Meares, *Ber. Bunsenges. Phys. Chem.*, 83 (1979) 342.

13 H.K. Lonsdale, U. Merten and R.L. Riley, *J. Appl. Polym. Sci.*, 9 (1965) 1341.

14 U. Merten, Transport properties of osmotic membranes, in: U. Merten (Ed.), *Desalination by Reverse Osmosis*, The M.I.T. Press, Cambridge, Mass., 1966, p. 15.

15 M.H.V. Mulder, T. Franken and C.A. Smolders, *J. Membrane Sci.*, submitted.

16 P. Flory, *Principles of Polymer Chemistry*, Cornell University Press, Ithaca, New York, 1953.

17 A.G. Mitchell and W.F.K. Wynne-Jones, *Disc. Faraday Soc.*, 15 (1953) 161.

18 T.M. Aminabhavi and P. Munk, *Macromolecules*, 12 (1979) 607.

19 F.W. Altena and C.A. Smolders, *Macromolecules*, 15 (1982) 1491.

20 A. Dondos, P. Rempp and H. Benoit, *J. Polym. Sci.*,

Part C, 30 (1970) 9.

21 S. Westmeier, *Chem. Techn.*, 28 (1976) 350.

22 M.A. Frommer, M. Shporer and R.M. Messalem, *J. Appl. Polym. Sci.*, 17 (1973) 2263.

23 O. Kedem, Water and salt transport in hyperfiltration, in: H.K. Lonsdale and H.E. Podall (Eds.), *Reverse Osmosis Membrane Research*, Plenum Press, New York, 1972, p. 17.

24 K.S. Spiegler and O. Kedem, *Desalination*, 1 (1966) 311.

25 C. McCallum and P. Meares, *J. Membrane Sci.*, 1 (1976) 65.

26 M.H.V. Mulder, F. Kruitz and C.A. Smolders, *J. Membrane Sci.*, 11 (1982) 349; chapter 2 of this thesis.

27 R.C. Weast, *Handbook of Chemistry and Physics*, 54th Edition, CRC Press, Cleveland, Ohio, 1973-1974.

28 R. Rautenbach and R. Albrecht, *J. Membrane Sci.*, 7 (1980) 203.

29 H.W. Chandler and E.J. Henley, *AIChE J.*, 7 (1961) 295.

30 D.W. McCall, *J. Polym. Sci.*, 26 (1957) 151.

APPENDIX

It is assumed that the binary interaction parameter, χ_{12}, is concentration dependent while the polymer-nonsolvent parameters χ_{13} and χ_{23} are considered as constants. In the case of a ternary system, χ_{12} depends only on the composition of the nonsolvent mixture in the polymer ($\chi_{12} = \chi_{12}(u_2)$).

$$u_2 = \frac{\phi_2}{\phi_1 + \phi_2} = \frac{\phi_2}{1 - \phi_3} \tag{A1}$$

For the $\chi_{12}(u_2)$ function, a fourth grade polynomial relation has been chosen:

$$\chi_{12} = a + b\,u_2 + c\,u_2^2 + d\,u_2^3 + e\,u_2^4 \tag{A2}$$

The coefficients are given in Table 2. By differentiation of eqns. (8) and (9) with respect to ϕ_1 and ϕ_2, the partial derivatives $\partial \ln a_1/\partial\phi_1$, $\partial \ln a_1/\partial\phi_2$, $\partial \ln a_2/\partial\phi_1$ and $\partial \ln a_2/\partial\phi_2$ are obtained.

$$\ln a_1 = \ln \phi_1 + (1-\phi_1) - \phi_2\left(\frac{V_1}{V_2}\right) - \phi_3\left(\frac{V_1}{V_3}\right) + (\chi_{12}(u_2)\phi_2 + \chi_{13}\phi_3)$$

$$(\phi_2+\phi_3) - \chi_{23}\left(\frac{V_1}{V_2}\right)\phi_2\phi_3 - u_1 u_2 \phi_2 \frac{\partial\chi_{12}}{\partial u_2} \tag{8}$$

$$\ln a_2 = \ln \phi_2 + (1-\phi_2) - \phi_1\left(\frac{V_2}{V_1}\right) - \phi_3\left(\frac{V_2}{V_3}\right) + (\chi_{12}(u_2)\phi_1 \frac{V_2}{V_1} + \chi_{23}\phi_3)$$

$$(\phi_1+\phi_3) - \chi_{13}\left(\frac{V_2}{V_1}\right)\phi_1\phi_3 + \left(\frac{V_2}{V_1}\right) u_1^2 \phi_2 \frac{\partial\chi_{12}}{\partial u_2} \tag{9}$$

From eqns. (8) and (9) it is derived that:

$$\begin{aligned}\frac{\partial \ln a_1}{\partial \phi_1} = g_{11} &= \frac{1}{\phi_1} - 1 + \frac{V_1}{V_3} - \chi_{12}\phi_2 + \chi_{23}\phi_2 \frac{V_1}{V_2} \\ &\quad -\chi_{13}(2-2\phi_1-\phi_2)+\phi_2(1-\phi_1)\frac{\partial \chi_{12}}{\partial \phi_1} \\ &\quad + u_1 u_2^3 \frac{\partial^2 \chi_{12}}{\partial u_2^2} + u_2^2(1-2u_2)\frac{\partial \chi_{12}}{\partial u_2}\end{aligned} \tag{A3}$$

$$\begin{aligned}\frac{\partial \ln a_1}{\partial \phi_2} = g_{12} &= -\frac{V_1}{V_2} + \frac{V_1}{V_3} + \chi_{12}(1-\phi_1)+\chi_{13}(\phi_1-1) \\ &\quad + \chi_{23}\frac{V_1}{V_2}(2\phi_2+\phi_1-1)+\phi_2(1-\phi_1)\frac{\partial \chi_{12}}{\partial \phi_2} \\ &\quad - u_1^2 u_2^2 \frac{\partial^2 \chi_{12}}{\partial u_2^2} - 2u_1^2 u_2 \frac{\partial \chi_{12}}{\partial u_2}\end{aligned} \tag{A4}$$

$$\begin{aligned}\frac{\partial \ln a_2}{\partial \phi_1} = g_{21} &= -\frac{V_2}{V_1} + \frac{V_2}{V_3} + \chi_{12}\frac{V_2}{V_1}(1-\phi_2)+\chi_{13}\frac{V_2}{V_1}(2\phi_1+\phi_2-1) \\ &\quad -\chi_{23}(1-\phi_2) + \frac{V_2}{V_1}\phi_1(1-\phi_2)\frac{\partial \chi_{12}}{\partial \phi_1} \\ &\quad - \frac{V_2}{V_1} u_1^2 u_2^2 \frac{\partial^2 \chi_{12}}{\partial u_2^2} + 2\frac{V_2}{V_1} u_1 u_2^2 \frac{\partial \chi_{12}}{\partial u_2}\end{aligned} \tag{A5}$$

$$\begin{aligned}\frac{\partial \ln a_2}{\partial \phi_2} = g_{22} &= \frac{1}{\phi_2} - 1 + \frac{V_2}{V_3} - \chi_{12}\frac{V_2}{V_1}\phi_1 + \chi_{13}\frac{V_2}{V_1}\phi_1 \\ &\quad +\chi_{23}(2\phi_2+\phi_1-2) + \frac{V_2}{V_1}\phi_1(1-\phi_2)\frac{\partial \chi_{12}}{\partial \phi_2} \\ &\quad + \frac{V_2}{V_1} u_1^2(1-2u_2)\frac{\partial \chi_{12}}{\partial u_2} + \frac{V_2}{V_1} u_1^3 u_2 \frac{\partial^2 \chi_{12}}{\partial u_2^2}\end{aligned} \tag{A6}$$

$\partial\chi_{12}/\partial\phi_1$ and $\partial\chi_{12}/\partial\phi_2$ can be obtained by differentiating eqn . (A2) to ϕ_1 and ϕ_2, respectively, bearing in mind that u_2 is a function of ϕ_1 and ϕ_2. The coefficients g_{11}, g_{12}, g_{21} and g_{22} have been substituted into eqns. (20) and (21).

CHAPTER 6

ON THE MECHANISM OF SEPARATION OF ETHANOL/WATER MIXTURES BY PERVAPORATION. II. EXPERIMENTAL CONCENTRATION PROFILES

M.H.V. MULDER, T. FRANKEN and C.A. SMOLDERS

SUMMARY

Experimental concentration profiles have been determined for the system water-ethanol-cellulose acetate. Knowledge of these profiles permits the investigator to extract more appropriate diffusion data for the pervaporation process.

The concentration profiles have been determined by a film-stack method, using three to six individual layers. First a transport model will be discussed where cross-term diffusion coefficients have been neglected. Then cross-term diffusion coefficients will be considered too. In order to measure ternary effects (the extent of coupling) it is assumed that the main-term diffusion coefficients are equal to the binary diffusion coefficients.

Furthermore, from the experimental concentration profiles the occurence of sorption resistances can be demonstrated.

INTRODUCTION

Separation of mixtures by pervaporation takes place by a solution-diffusion mechanism. In most cases coupled transport will occur which means that the flux of a component of a mixture may change not only by the presence of the other component but also by its movement. This phenomenon has been pointed out clearly by Meares [1,2]. Because of the occurence of coupling it would be hardly possible to predict selectivities from parameters obtained from single component permeation experiments as was demonstrated by Tock [3] for the separation of water-dioxane mixtures through a Nylon-6 membrane.

In chapter 5 a solution-diffusion model had been described taking into account coupling, both in the solubility part as well as in the kinetic part. The basic feature of the model is that each component in a binary mixture will not permeate independently but in a coupled way according to $J_i = S_i(c_1,c_2)\ D_i(c_1,c_2)$ where S is the solubility and D the diffusivity of component i. Many investigators made use of concentration dependent diffusion coefficients but generally coupling in the solubility part was neglected. In most cases ideal sorption was assumed [5-7], i.e. a linear relationship should exist between the concentration of a component of a binary mixture inside the membrane and the concentration of that component in the liquid feed mixture. In chapter 7 it is shown that the assumption of ideal sorption cannot be used for ethanol-water mixtures or in general for mixtures where preferential sorption occurs [8]. Therefore, coupling in the solubility part should be taken into account too.

The objective of this chapter is to present experimental concentration profiles for the system water(1)-ethanol(2)-cellulose acetate(3). Knowledge of these profiles permits the investigator to extract more appropriate data about diffusion coefficients in pervaporation. The concentration profiles have been determined by a so called film-stack method. This method has already been used by a number of investigators [3,9-11].

In the model described in chapter 5 second-order coupling effects are considered but cross-terms in the flux equations are neglected. The results presented here permit to verify this assumption.

THEORY

Experimental concentration profiles of single components and of binary mixtures have been determined and therefore single component permeation and the permeation of mixtures will be considered.

Single component permeation

If we assume that linear relations exist between fluxes and forces where forces are written in terms of chemical potential gradients then we can write for a diffusing component i through a membrane

$$-J_i = L_i \nabla \mu_i \tag{1}$$

For single component permeation the generalized Fick's law can be derived from eqn. (1). Writing activities instead of chemical potentials eqn. (1) becomes

$$-J_i = L_i RT \frac{\partial \ln a_i}{\partial c_i} \nabla c_i \tag{2}$$

The activity a_i of a component in a polymeric membrane can be described by Flory-Huggins thermodynamics [12]. For the binary case the activity of a component (index i) in the polymer (index j) is given by

$$\ln a_i = \ln v_i + (1 - \frac{V_i}{V_j}) v_j + \chi_{ij} v_j^2 \tag{3}$$

where v_i is the volume fraction of penetrant, v_j the volume fraction of polymer and χ_{ij} the Flory-Huggins interaction parameter (for this case χ_{ij} is assumed to be concentration independent). If we define a diffusion coefficient D_i as

$$D_i(c_i) = L_i \; RT \, \frac{\partial \ln a_i}{\partial c_i} \tag{4}$$

which for an ideal system ($V_i = V_j$ and $\chi_{ij} = 0$) reduces to

$$L_i = \frac{D_i(c)\, c_i}{RT} \tag{5}$$

A combination of eqns. (2) and (4) gives

$$-J_i = D_i(c) \; \nabla c_i \tag{6}$$

D_i is the diffusion coefficient of component i in the polymer-fixed frame of reference. Diffusion coefficients of permeating components in polymers are in general strongly dependent on the state of swelling of the polymer because of the plasticizing action of the liquid on the segmental motions.

In the case of pervaporation anisotropic swelling in the membrane from upstream side to downstream side occurs. At the upstream side the concentration is maximal while it is almost zero at the downstream side. Therefore, diffusion coefficients will vary considerably across the membrane.

Different expressions can be used to quantify the relation between diffusion coefficient and concentration. Most authors have suggested an exponential relationship [3,9,10, 13-16].

$$D = D_0 \; \exp(\gamma c) \tag{7}$$

where D_0 is the diffusion coefficient at zero concentration of penetrant and γ is a plasticizing constant showing the effect of the penetrant concentration on the mobility of the penetrant in the membrane.

When combining eqns. (6) and (7) and integrating across the membrane using the following boundary conditions: $c_i = c_{0_i}$ at $x = 0$ and $c_i = 0$ at $x = \ell$, eqn. (8) is obtained

$$J_i = \frac{D_{0_i}}{\gamma_i \ell} \left[\exp(\gamma_i c_{0_i}) - 1\right] \tag{8}$$

Defining a relative distance in the membrane ($x_R = \frac{x}{\ell}$), then a substitution of this quantity in eqns. (6) and (7) gives

$$-J_i = \frac{D_{0_i}}{\ell} \exp(\gamma_i c_i) \frac{\partial c_i}{\partial x_R} \tag{9}$$

and integrating eqn. (9) gives, assuming steady-state

$$c_i = \frac{1}{\gamma_i} \ln \left[x_R(1 - \exp(\gamma_i c_{0_i})) + \exp(\gamma_i c_{0_i})\right] \tag{10}$$

Note that the concentration profile (eqn. (10)) does not contain diffusivity terms anymore. When experimental concentration profiles are determined, γ_i and c_{0_i} can be obtained from eqn. (10). D_{0_i} can then be obtained from steady-state permeation experiments with the help of eqn. (8).

Permeation of liquid mixtures

In the case of liquid mixtures coupling phenomena should be taken into account. In chapter 5 eqn. (11) was used to describe the transport of binary liquid mixtures through polymeric membranes. In fact, eqn. (11) can be obtained by combining eqns. (1) and (5)

$$-J_i = \frac{c_i D_i(c)}{RT} \nabla\mu_i \tag{11}$$

Using eqn. (11) second-order effects are taken into account because the chemical potential of component i (μ_i) depends on the concentration of component j and on the different interaction parameters used in the Flory-Huggins expression for a ternary system. Furthermore, the diffusion coefficient D_i is assumed to be dependent on the concentration of component i and j. In this approach cross-term diffusion coefficients are assumed te be zero (or $\frac{D_{ii}}{D_{ij},i \neq j} >> 1$) and in a following section we will discuss if it is allowed to make use of this assumption. If the concentration is expressed as volume fraction (ϕ) and if activities are used instead of chemical potentials, eqn. (11) becomes

$$-J_1 = \phi_1 D_1(\phi_1,\phi_2) \left[\left(\frac{\partial \ln a_1}{\partial \phi_1}\right) \nabla\phi_1 + \left(\frac{\partial \ln a_1}{\partial \phi_2}\right) \nabla\phi_2 \right] \tag{12}$$

$$-J_2 = \phi_2 D_2(\phi_1,\phi_2) \left[\left(\frac{\partial \ln a_2}{\partial \phi_1}\right) \nabla\phi_1 + \left(\frac{\partial \ln a_2}{\partial \phi_2}\right) \nabla\phi_2 \right] \tag{13}$$

Eqns. (12) and (13) are equal to eqns. (8) and (9) of

The partial derivatives $\frac{\partial \ln a_1}{\partial \phi_1}$, $\frac{\partial \ln a_1}{\partial \phi_2}$, $\frac{\partial \ln a_2}{\partial \phi_1}$ and $\frac{\partial \ln a_2}{\partial \phi_2}$ can be obtained from the Flory-Huggins equations for ternary systems (see Appendix of Chapter 5). When data on experimental concentration profiles are available values for the diffusion coefficients ($D_1(\phi_1,\phi_2)$ and $D_2(\phi_1,\phi_2)$) can be obtained from eqns. (12) and (13).

EXPERIMENTAL

Materials

Cellulose acetate (E 398-3) was obtained from Eastman Chemicals. The solvents used were of analytical grade.

Membrane preparation

Polymer solutions were prepared by dissolving the polymer in a suitable solvent (acetone or dioxane). The membranes were prepared by casting the polymer solution upon a glass plate and the solvent was allowed to evaporate in a nitrogen atmosphere. The membranes obtained were completely transparant.

Pervaporation

The pervaporation experiments were carried out in the apparatus shown in Fig. 1. A cross-section of the permeation cell is given in Fig. 2. This cell, which is different from that described in Chapter 2 [14]has been developed in order to remove the membrane as quickly as possible.

Vacuum at downstream side was maintained at a pressure of 13.3 Pascal (0.1 mm Hg) by a Crompton Parkinson vacuum pump.

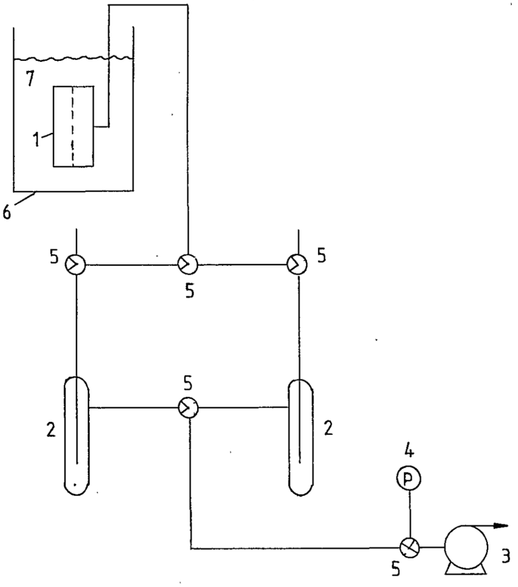

FIGURE 1. Schematic presentation of the pervaporation apparatus: 1, permeation cell; 2, cold traps; 3, vacuum pump; 4, piranhi gauge; 5, two-way cocks; 6, jar; 7, liquid feed.

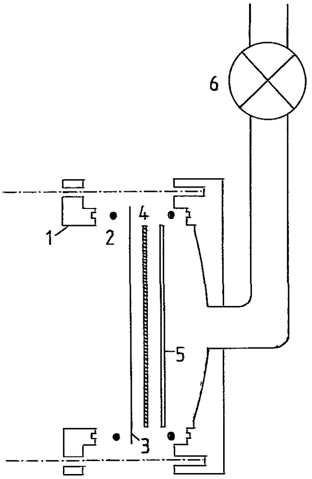

FIGURE 2. Schematic presentation of the permeation cell: 1, metal ring; 2, gaskets; 3, membrane; 4, porous metal fileter; 5, support disc; 6, cock; 7, screws.

The pressure was measured by an Edwards piranhi gauge. The concentration profiles were determined when steady-state conditions were reached. Product samples were taken at least every hour.

Product analysis

Analysis of binary ethanol-water mixtures was performed on a Varian model 3700 gaschromatograph fitted with a chromosorb 60/80 column and equipped with a thermal conductivity detector. For low ethanol concentrations (0-5%) a flame ionization detector was used.

Determination of the concentration profiles

The multilayer membrane was prepared as follows: 3 to 6 individual layers, each of them with a thickness of at least 100 μm, were swollen in the liquid feed mixture. After equilibrium the layers were stacked one by one and the multilayer membrane was installed in the permeation cell. By preparing the multilayer membranes in this way it turned out that the resistance at the interface of the different layers was negligible. This was controlled by comparing permeation experiments with a multilayer membrane and with an unilayer membrane of the same thickness. In both cases the same permeation rates were obtained. When steady-state conditions were reached, the permeation cell was removed from the jar, the surface was wiped quickly with tissue paper and the multilayer membrane was cut from the cell with a sharp knife. The individual layers were peeled off and immediately put in weighing tubes. The liquid present in each layer was removed from the membrane using a distillation technique as will be described in Chapter 7.

The amount of liquid was determined by weighing and the composition was determined by gaschromatography. The largest error is made by determining the concentration in the first layer because the time in between removing the permeation cell from the liquid feed and putting the first layer in a weighing tube is about 1 minute. During this time desorption from the membrane occurs i.e. the actual concentration will differ from the measured concentration. In order to correct for these errors, control experiments have been carried out in which the weight decrease was measured as a function of time. The measured concentrations have been corrected for these weight losses due to desorption. The second and subsequent layers have been put in a weighing tube 5 to 10 seconds after each other and it was not necessary to correct the obtained results. The error in the mass balance was less than 5%.

RESULTS AND DISCUSSION

Table 1 summarized the results of the permeation experiments for the system water-cellulose acetate. The experimental concentration profile for this system is given in Fig. 3. The obtained profile is in agreement with the observations of Kim [10] on the same system. Another interesting

TABLE 1

Permeation characteristics for the binary system water-cellulose acetate

Temperature	17 °C
c_{eq}, equilibrium sorption	0.125 g/g
c_o^m	0.125 g/g
J, permeation rate	1.1 10^{-3} cm/hr
ℓ, membrane thickness	500 µm
Number of layers	3 - 5
D_0	5.5 10^{-9} cm^2/sec

point from Fig. 3 is that the equilibrium sorption value (arrow in Fig. 3) and the concentration just inside the membrane during steady-state pervaporation are quite close, indicating that the sorption resistance at the liquid/polymer interface is negligible and hence diffusion through the mem-

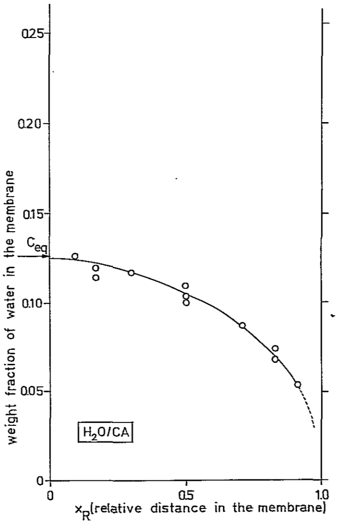

FIGURE 3. Concentration profile of water in cellulose acetate during steady-state pervaporation. c_{eq} (arrow) indicates the equilibrium sorption value.

brane is rate-determining.

Table 2 and Fig. 4 give the results obtained for the binary system ethanol-cellulose acetate. Comparing the results of the systems water-cellulose acetate and ethanol-cellulose

TABLE 2

Permeation characteristics for the binary system ethanol-cellulose acetate

Temperature	20 °C
c_{eq}, equilibrium	0.177 g/g
c_o^m	0.109 g/g
J, permeation rate	7.8 10^{-4} cm/hr
ℓ, membrane thickness	500 µm
Number of layers	3
D_o	1.1 10^{-10} cm^2/sec

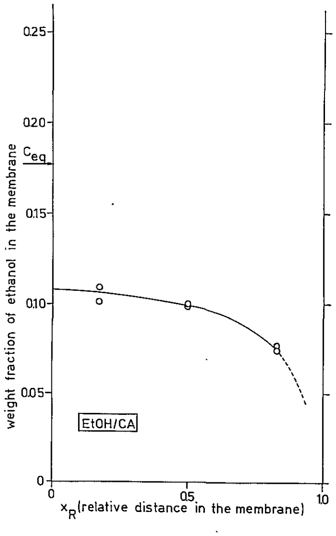

FIGURE 4. Concentration profile of ethanol in cellulose acetate during steady-state pervaporation. c_{eq} (arrow) indicates the equilibrium sorption value.

one does observe a number of differences:

- the permeation rate of water through cellulose acetate is much larger;
- the concentration profile of ethanol in cellulose acetate is much more concave, especially on the downstream half of the membrane;
- the difference between the equilibrium sorption value and the concentration just inside the membrane at the liquid/polymer interface is considerable for the system ethanol-cellulose acetate;
- the D_o value for ethanol is 50 times smaller than that for water.

Also for other systems (polyethylene-benzene and polyethylenedioxane) considerable differences have been found between equilibrium sorption values and concentrations just inside the membrane [10].

The results for the ternary system water-ethanol-cellulose acetate are given in Table 3 and Figs. 5, 6 and 7. Again the difference between equilibrium sorption value and concentration just inside the membrane is considerable. When the in-

TABLE 3

Permeation characteristics for the ternary system water-ethanol-cellulose acetate

Temperature	17 °C
Concentration of water in the feed	35 % by weight
c_{eq}, equilibrium sorption	0.253 g/g
c_o^m (overall)	0.169 g/g
J, permeation rate	$1.6\ 10^{-3}$ cm/hr
ℓ, membrane thickness	500 µm
Number of layers	4 - 6
c_o^m (water)	0.100 g/g
c_{eq} (water)	0.147 g/g
c_o^m (ethanol)	0.069 g/g
c_{eq} (ethanol)	0.106 g/g
α, separation factor	9.8

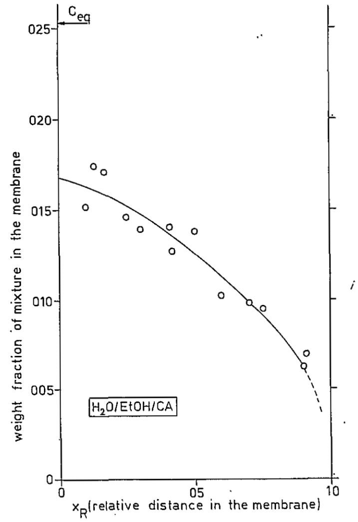

FIGURE 5. Concentration profile of an ethanol-water mixture in cellulose acetate during steady-state pervaporation. Concentration in the feed: 35% by weight of water; overall profile.

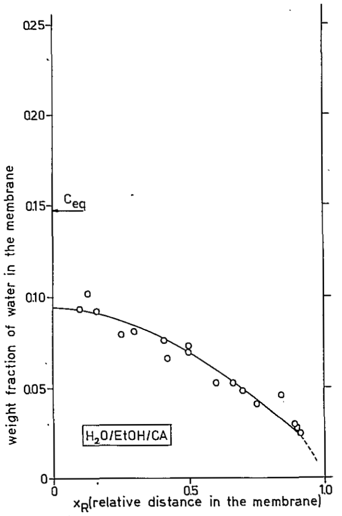

FIGURE 6. Concentration profile of an ethanol-water mixture in cellulose acetate during steady-state pervaporation. Concentration in the feed: 35% by weight of water; water profile.

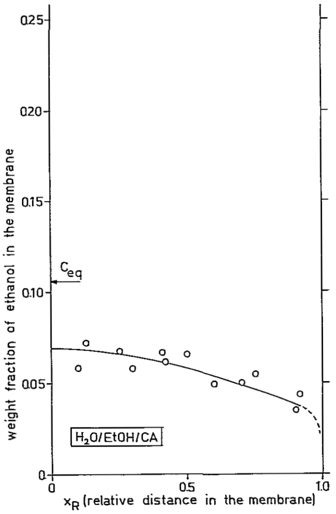

FIGURE 7. Concentration profile of an ethanol-water mixture in cellulose acetate during steady-state pervaporation. Concentration in the feed: 35% by weight of water; ethanol profile.

dividual profiles are considered one can observe that both ethanol and water show a concentration drop at the liquid/ membrane boundary. This observation is important because it demonstrates clearly the occurence of a coupled sorption process. Furthermore, the ethanol and water profiles are rather similar in respect to the profiles of the pure components. Because the concentration profiles are known the values for the diffusion coefficients of water and ethanol in cellulose acetate for the ternary system can be calculated from eqns. (12) and (13).

However, problems appear in applying our simple approach of neglecting cross-term diffusion coefficients because negative values for the diffusion coefficient of ethanol are obtained. The reason for this negative D_2 values will be discussed now. Therefore, we have to recall eqns (12) and (13).

The term between the square brackets should have a negative value. Across the membrane from $x = 0$ to $x = \ell$ the values of $\frac{d\phi_1}{dx}$ and $\frac{d\phi_2}{dx}$ are negative, as are also the partial derivatives $\frac{\partial \ln a_1}{\partial \phi_2}$ and $\frac{\partial \ln a_2}{\partial \phi_1}$. The partial derivatives $\frac{\partial \ln a_1}{\partial \phi_1}$ and $\frac{\partial \ln a_2}{\partial \phi_2}$ are positive. Further $\left|\frac{\partial \ln a_i}{\partial \phi_i}\right| > \left|\frac{\partial \ln a_i}{\partial \phi_j}\right|_{i \neq j}$. In case of water (component 1) there are no problems because $\left|\frac{\partial \ln a_1}{\partial \phi_1} \quad \frac{d\phi_1}{dx}\right| > \left|\frac{\partial \ln a_1}{\partial \phi_2} \quad \frac{d\phi_2}{dx}\right|$. Problems arise in the case of ethanol because for low penetration distances $\left|\frac{d\phi_2}{dx}\right|$ is very small (Fig. 7) and since $\left|\frac{d\phi_1}{dx}\right| > \left|\frac{d\phi_2}{dx}\right|$ while $\left|\frac{\partial \ln a_2}{\partial \phi_2}\right| \simeq \left|\frac{\partial \ln a_2}{\partial \phi_1}\right|$ the terms of eqn. (13) between square brackets will have a positive value resulting in negative value for the diffusion coefficient (D_2). Therefore, the simple phenomenological eqn. (1) should be replaced by an equation where cross-term diffusion coefficients are taken into account.

Cussler [17] gave some empirical rules for deciding when multicomponent diffusion effects will be large. Two of these rules can be applied to the system water-ethanol-cellulose acetate: *i)* the components show strong thermodynamic interactions and *ii)* the concentration gradient of water in cellulose acetate is much different from that of ethanol in cellulose acetate. The equations used so far (eqns. (12) and (13)) hold for the case where main-term diffusion coefficients are much larger than the cross term diffusion coefficients ($D_{ii} \gg D_{ij}, i \neq j$). In a forthcoming article [8] we will report on experimental concentration profiles of o-xylene and p-xylene in cellulose acetate and discuss the results of this weakly-interacting system using main-term diffusion coefficients only.

Taking cross-terms into account eqn. (1) becomes

$$- J_j = \sum_{j=1}^{n} \frac{D_{ij} c_j}{RT} \nabla \mu_j \tag{14}$$

For steady-state transport of water and ethanol through a cellulose acetate membrane we now have

$$-J_1 = \frac{D_{11}c_1}{RT} \nabla\mu_1 + \frac{D_{12}c_2}{RT} \nabla\mu_2 \tag{15}$$

$$-J_2 = \frac{D_{21}c_1}{RT} \nabla\mu_1 + \frac{D_{22}c_2}{RT} \nabla\mu_2 \tag{16}$$

The first term on the right-hand side of eqn. (15) describes the flux of component 1 due to its own gradient and the second term of this equation describes the flux of component 1 due to the gradient of component 2. This second term represents the coupling effect. In the system water-ethanol-cellulose acetate the cross-term diffusion coefficient ($D_{ij}, i \neq j$) will be a significant fraction of the main-term diffusion coefficient especially in the case of component 2 (ethanol) where it will dominate the effect of the main coefficient. This implies that the flux of ethanol due to the gradient of water should have a larger value than the flux of ethanol caused by its own gradient.

In general, the cross-term diffusion coefficients are not symmetric, i.e. $D_{12} \neq D_{21}$.

By expressing the concentration as volume fraction and using activities instead of chemical potentials eqns. (15) and (16) become

$$\begin{aligned} -J_1 = {} & \frac{D_{11}\phi_1}{\Delta x} \left[\frac{\partial \ln a_1}{\partial \phi_1} \Delta\phi_1 + \frac{\partial \ln a_1}{\partial \phi_2} \Delta\phi_2 \right] + \\ & \frac{D_{12}\phi_2}{\Delta x} \left[\frac{\partial \ln a_2}{\partial \phi_1} \Delta\phi_1 + \frac{\partial \ln a_2}{\partial \phi_2} \Delta\phi_2 \right] \end{aligned} \tag{17}$$

$$\begin{aligned} -J_2 = {} & \frac{D_{21}\phi_1}{\Delta x} \left[\frac{\partial \ln a_1}{\partial \phi_1} \Delta\phi_1 + \frac{\partial \ln a_1}{\partial \phi_2} \Delta\phi_2 \right] + \\ & \frac{D_{22}\phi_2}{\Delta x} \left[\frac{\partial \ln a_2}{\partial \phi_1} \Delta\phi_1 + \frac{\partial \ln a_2}{\partial \phi_2} \Delta\phi_2 \right] \end{aligned} \tag{18}$$

Cussler [17] summarized different theories to quantify the cross-term diffusion coefficients. A general approach is to assume that the main-term diffusion coefficients (D_{ii} i=1,2) are closely related to the binary diffusion coefficients. These binary diffusion coefficients can be obtained from single component permeation experiments, as given in Tables 1 and 2. The cross-diffusion coefficient can now be calculated from eqns. (17) and (18).

The ratios $\left|\frac{D_{12}}{D_{11}}\right|$ and $\left|\frac{D_{21}}{D_{22}}\right|$, or better $\left|\frac{D_{12}}{D_{11}}\frac{\nabla\mu_2}{\nabla\mu_1}\right|$ and $\left|\frac{D_{21}}{D_{22}}\frac{\nabla\mu_1}{\nabla\mu_2}\right|$ respectively, are a measure for the ternary effects and each of them is given in Figs. 8 and 9 as a func-

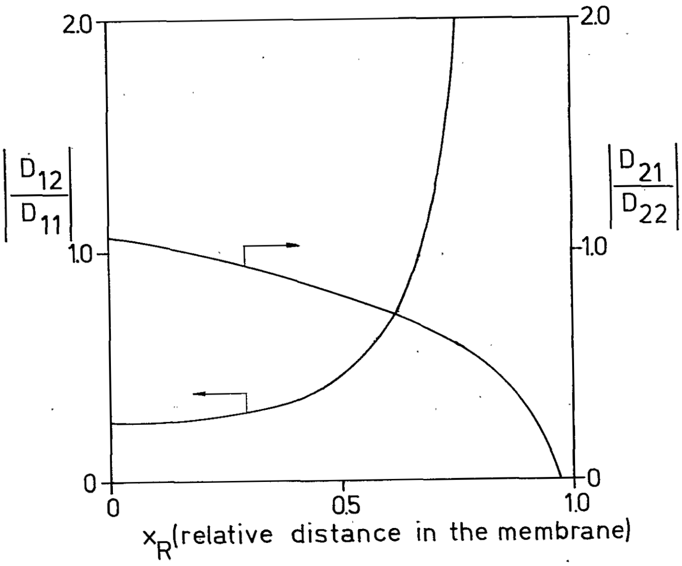

FIGURE 8. Ratio of cross-term diffusion coefficients and main-term diffusion coefficients as a function of the relative distance in the membrane.

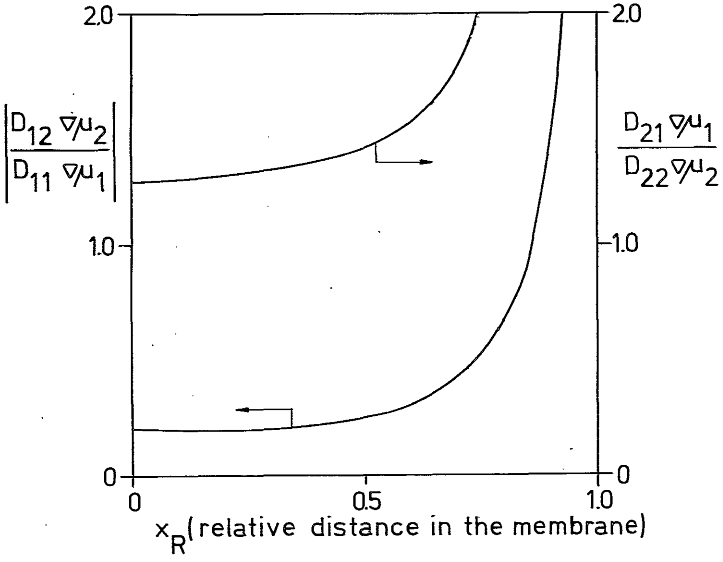

FIGURE 9. Ratio of cross-term diffusion coefficient times gradient and main-term diffusion coefficient times gradient as function of the relative distance in the membrane.

tion of the relative distance through the membrane (x_R). Comparing Figs. 8 and 9 one can see that the value of $\left|\frac{D_{21}}{D_{22}}\right|$ decreases when x_R increases while the term $\left|\frac{D_{21}}{D_{22}}\frac{\nabla\mu_2}{\nabla\mu_2}\right|$ increases in value. In fact, $\left|\frac{D_{21}}{D_{22}}\frac{\nabla\mu_1}{\nabla\mu_2}\right|$ is a better measure for multicomponent diffusion effects than $\left|\frac{D_{21}}{D_{22}}\right|$ because also the effects of the gradients are involved.

From Fig. 8 one can see that $\left|\frac{D_{21}}{D_{22}}\frac{\nabla\mu_1}{\nabla\mu_2}\right| > 1$ implying that the flux of component 2 (ethanol) due to the gradient of component 1 (water) has a larger value than the flux of component 2 caused by its own gradient. This is in agreement with the negative values for the diffusion coefficient D_2 obtained from eqn. (13) implying that the assumption of using binary diffusion coefficients is not so bad after all. The flux of water is hardly affected by the gradient of ethanol, at least at small penetration distances ($x_R < 0.5$). At high penetration distance coupling effects become more and more important.

The results presented here demonstrate beyond any doubt the occurence of coupling. Because it has been assumed that the main-term diffusion coefficient is simply equal to the binary diffusion coefficient it is hardly possible to draw quantitative conclusions about the magnitude of the coupling effect.

Boundary resistance

Boundary resistances exist in every permeation experiment (this means that the chemical potential of a component *i* in the feed is not equal to the chemical potential of component *i* just inside the membrane). Hwang [19] showed that the boundary resistance contributed to a large extent to the total resistance during the permeation of dissolved oxygen in water through a silicone rubber membrane.

By investigating the concentration profiles of the system water-ethanol-cellulose acetate (pure components and mix-

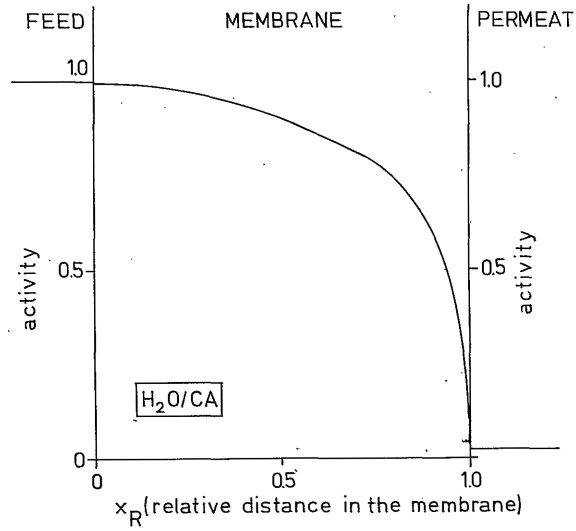

FIGURE 10. Activity profile for the binary system water-cellulose acetate.

ture) the occurence of boundary resistances could be demonstrated (see Figs. 4-7). Because of the non-ideality of the various systems activity profiles are preferred over concentration profiles. In Figs. 10 and 11 the activity profiles for the systems water-cellulose acetate and ethanol-cellulose acetate are given. These activity profiles have been calculated from the experimental concentration profiles using Flory-Huggins thermodynamics (eqn. (3)). In the case of water no resistance at the liquid/membrane interface can be observed (Fig. 10) while in the case of ethanol there is an appreciable resistance. Comparing Fig. 4 with Fig. 11 one can see that the activity drop is much smaller than the concentration drop.

CONCLUSIONS

The transport of ethanol-water mixtures through cellulose acetate membranes cannot be described with a simple phenome-

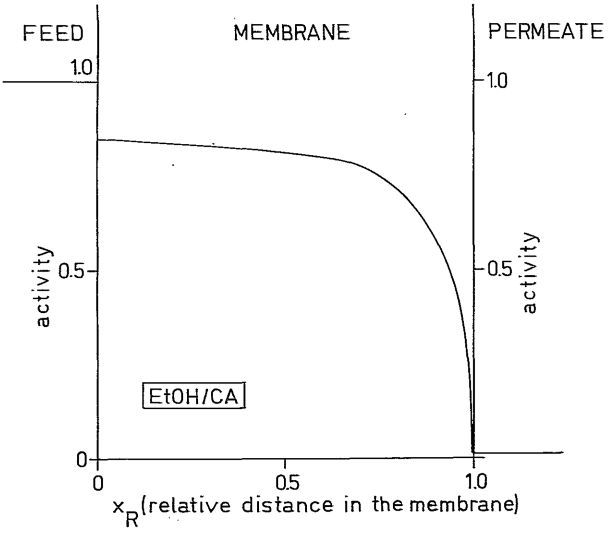

FIGURE 11. Activity profile for the binary system ethanol-cellulose acetate.

nological model where cross-term diffusion coefficients are neglected. Therefore, multicomponent effects should be considered. Cross-term diffusion coefficients appear to be a significant fraction of the main-term diffusion coefficients and in the case of ethanol, diffusing through cellulose acetate in the presence of water, the cross-term effect even dominates the main-term effect.

Boundary resistances found in pervaporation are caused by sorption phenomena and in the case of permeation of liquid mixtures, these sorption resistances are coupled too.

LIST OF SYMBOLS

a	activity
D	diffusion coefficient ($cm^2\ sec^{-1}$)
D_0	diffusion coefficient at zero concentration ($cm^2\ sec^{-1}$)
D_{ii}	main-term diffusion coefficient ($cm^2\ sec^{-1}$)
$D_{ij,i \neq j}$	cross-term diffusion coefficient ($cm^2\ sec^{-1}$)
J	permeation rate ($cm\ hr^{-1}$)
c_{eq}	equilibrium sorption value (g/g dry polymer)
c_0^m	concentration inside the membrane at $x = 0$ (g/g dry polymer)
ℓ	membrane thickness (cm)
L	phenomenological coefficient ($cm\ mol\ sec^{-1}\ N^{-1}$)
R	gas constant ($J\ mol^{-1}\ K^{-1}$)
T	temperature (K)
v	volume fraction in the binary system
V	molar volume ($cm^3\ mol^{-1}$)
x_R	relative thickness in the membrane
Δx	thickness of an infinitesimal thin layer (cm)
α	separation factor
γ	exponential factor
χ	Flory-Huggins interaction parameter
ϕ	volume fraction in the ternary system
μ	chemical potential ($J\ mol^{-1}$)

Indices

1	water
2	ethanol
3	cellulose acetate
i	component *i*
j	component *j*

REFERENCES

1 P. Meares, *The physical chemistry of transport and separation by membranes*, in P. Meares (Ed.), Membrane Separation Processes, Elsevier, Amsterdam 1976, Chapter 1.
2 P. Meares, *Ber. Bunsenges. Phys. Chem.*, 83 (1979) 342.
3 R.W.M. Tock, J. Yu. Cheung and R.L. Cook, *Sep. Sci.*, 9 (1974 361.
4. M.H.V. Mulder, T. Franken and C.A. Smolders, *J. Membrane Sci.*, 17 (1984) 289.
5 A.B. Krewinghaus, *PhD Thesis*, Massachusetts Institute of Technology, April 1966.
6 F.W. Greenlaw, R.A. Shelden and E.V. Thompson, *J. Membrane Sci.*, 2 (1977) 333.
7 R. Rautenbach and R. Albrecht, *J. Membrane Sci.*, 7 (1980) 203.
8 M.H.V. Mulder, T. Franken and C.A. Smolders, submitted to *J. Membrane Sci.*
9 P. Aptel, J. Cuny, J. Jozefowicz, G. Morel and J. Neel, *J. Appl. Pol. Sci.*, 18 (1974) 351.
10 S.N. Kim and K. Kammermeyer, *Sep. Sci.*, 5 (1970) 679.
11 S. Rosenbaum and O. Cotton, *J. Pol. Sci.*, A-1 7 (1969) 101.
12 P.J. Flory, *Principles of Polymer Chemistry*, Cornell University Press, Ithaca, New York, 1953.
13 R.Y. Huang and V.J.C. Lin, *J. Appl. Pol. Sci.*, 12 (1968) 2615.

14 R.B. Long, *Ind. Eng. Chem. Fundam.*, 4 (1965) 445.

15 H.W. Chandler and E.J. Henley, *AIChEJ*, 7 (1961) 295.

16 D.W. McCall, *J. Pol. Sci.*, 16 (1957) 151.

17 E.L. Cussler, *Multicomponent diffusion*, Elsevier, Amsterdam, 1976.

18 M.H.V. Mulder, T. Franken and C.A. Smolders, submitted to *J. Membrane Sci.*

19 S.T. Hwang, T.E.S. Tang and K. Kammermeyer, *Am. Chem. Soc. Polym. Prepr.*, 10 (1969) 978.

CHAPTER 7

PREFERENTIAL SORPTION VERSUS PREFERENTIAL PERMEABILITY IN PERVAPORATION

M.H.V. MULDER, T. FRANKEN and C.A. SMOLDERS

SUMMARY

Transport of liquids by pervaporation takes place by a solution-diffusion mechanism. In order to investigate the 'solution-part' of this transport model , preferential sorption has been compared with preferential permeability. Sorption equilibria and pervaporation performance for the systems water-ethanol-cellulose acetate, water-ethanol-polyacrylonitrile and water-ethanol-polysulfone have been investigated. Theoretical values of preferential sorption have been derived from Flory-Huggins thermodynamics, extended with concentration dependent interaction parameters. These calculated sorption values show a reasonable agreement with experimental values. The large difference in molar volumes between water and ethanol determines the preferential sorption of water in these systems to a great extent and this effect increases with decreasing swelling value.

Comparison of preferential sorption experiments with pervaporation experiments indicates, that apart from the effect of differences in diffusivity for the permeating components, preferential sorption contributes to a major extent to selective transport.

INTRODUCTION

In most membrane processes transport of molecules takes place in the direction of decreasing chemical potential. In pervaporation, the driving force for transport is the concentration difference across the membrane. The transport process can be divided into three steps, *i)* sorption into the membrane at the upstream side, *ii)* diffusion through the membrane and *iii)* desorption into a vapour phase at the downstream side. The separation mechanism of pervaporation is a solution diffusion-mechanism [1-4], i.e. the permeation rate is a function of solubility and diffusivity. Solubility is a thermodynamic property and diffusivity is a kinetic property and both affect selectivity. In case of a liquid mixture separation is obtained because the membrane has the ability to transport one component more readily than the other even if the driving forces are equal. Hence, prediction of selectivity is often difficult because in general there will be coupling of fluxes, i.e. the permeation rate of one component can be changed by the presence and movement of the other component. In a previous chapter [4] a solution-diffusion model has been developed for the permeation of a liquid mixture through a polymeric membrane taking into account coupling of fluxes.

The objective of this chapter is to investigate the thermodynamic aspects of the membrane separation process by comparing preferential sorption of a water-ethanol mixture by a polymeric membrane with preferential permeability through that membrane.

Aptel [5] showed that for systems with polyvinylpyrrolidone-polytetrafluoroethylene as membrane material and various binary liquid mixtures, the component that was sorbed preferentially was also transported preferentially. Even the occurence of selectivity inversion was in agreement with their sorption experiments.

Our investigation can be divided into two parts:

a) thermodynamics of preferential sorption;

b) comparison of preferential sorption versus preferential permeability.

Preferential or selective sorption is given by the difference in composition of a binary liquid mixture inside the polymeric membrane and outside in the liquid feed mixture. Theoretical values on preferential sorption have been derived from Flory-Huggins thermodynamics [6] using concentration dependent interaction parameters. To improve the agreement between experimental and theoretical data on preferential sorption Pouchly [7,8] introduced a second order interaction parameter, the ternary parameter g_T. Another way of describing second order effects is by taking the interaction parameters concentration dependent. In this paper we will follow the latter approach.

Experimental data on preferential sorption have been obtained by separating the sorbed liquid quantitatively from the membrane phase by a distillation technique. These experimental data will be compared with the theoretical values. The following polymers have been studied: cellulose acetate (CA), polyacrylonitrile (PAN) and polysulfone (PSf), while water/ethanol was used as the liquid mixture. Except for equilibrium sorption measurements pervaporation experiments have also been performed. The selectivity in pervaporation will be compared with the preferential sorption data and the results will be discussed in terms of the solution-diffusion mechanism.

THEORY

The equilibrium between a polymeric membrane (index 3) and a binary mixture of nonsolvents (indices 1 and 2) can be considered as an osmotic equilibrium. Preferential sorption occurs when the compositions of the binary liquid mixture inside the polymer and in the liquid feed mixture are different. The index 1 is given to the component that is sorbed preferentially by the polymer. If we denote the concentration of a component of the binary liquid mixture in the polymeric phase by

$$u_i = \frac{\phi_i}{\phi_1+\phi_2} = \frac{\phi_i}{1-\phi_3} \qquad i = 1,2 \tag{1}$$

and the concentration (volume fraction) in the liquid phase by v_i then the preferential sorption ε is given by [7]

$$\varepsilon = u_1 - v_1 = v_2 - u_2 \tag{2}$$

The condition for equilibrium between the two phases, the binary liquid phase and the ternary polymer phase, is expressed by equality of the chemical potentials in the two phases. The polymer free phase is denoted with the superscript ^{o} and the ternary (membrane) phase with the superscript ^{m}. At equilibrium

$$\Delta\mu_1^o = \Delta\mu_1^m + \Pi V_1 \tag{3}$$

$$\Delta\mu_2^o = \Delta\mu_2^m + \Pi V_2 \tag{4}$$

The chemical potentials can be obtained from Flory-Huggins thermodynamics [6]. The Gibbs free energy of mixing for a ternary system is given by

$$\frac{\Delta G_{mix}}{RT} = n_1 \ln \phi_1 + n_2 \ln \phi_2 + n_3 \ln \phi_3 + g_{12}(u_2)n_1\phi_2 + g_{13}(u_2,\phi_3)n_1\phi_3 + g_{23}(u_1,\phi_3)n_2\phi_3 \tag{5}$$

Again the indices 1 and 2 refer to the nonsolvents and index 3 to the polymer. n_i and ϕ_i are the mole fraction and volume fraction of component i respectively. The binary interaction parameters g_{12}, g_{13} and g_{23} are assumed to be concentration dependent. When these parameters are taken concentration independent they reduce to the well-known χ parameters (in the original Flory-Huggins theory χ parameters are concentration independent [6]). Differentiation of eqn. (5) to n_1 and n_2 respectively, yields the following equations for the chemical potentials of components 1 and 2 in the polymer phase.

$$\frac{\Delta\mu_1^m}{RT} = \ln \phi_1 + \phi_2(1 - \frac{V_1}{V_2}) + \phi_3(1 - \frac{V_1}{V_3}) + (g_{12}\phi_2 + g_{13}\phi_3)(\phi_2 + \phi_3)$$
$$- u_1 u_2 \phi_2 \frac{\partial g_{12}}{\partial u_2} - g_{23}\frac{V_1}{V_2}\phi_2\phi_3 - u_1 u_2 \phi_3 \frac{\partial g_{13}}{\partial u_2} - \phi_1\phi_3^2 \frac{\partial g_{13}}{\partial \phi_3}$$
$$+ \frac{V_1}{V_2} u_2^2 \phi_3 \frac{\partial g_{23}}{\partial u_1} - \frac{V_1}{V_2}\phi_2\phi_3^2 \frac{\partial g_{23}}{\partial \phi_3} \qquad (6)$$

$$\frac{\Delta\mu_2^m}{RT} = \ln \phi_2 + \phi_1(1 - \frac{V_2}{V_1}) + \phi_3(1 - \frac{V_2}{V_3}) + (g_{12}\frac{V_2}{V_1}\phi_1 + g_{23}\phi_3)(\phi_1+\phi_3)$$
$$- \frac{V_2}{V_1} u_1^2 \phi_2 \frac{\partial g_{12}}{\partial u_2} - g_{13}\frac{V_2}{V_1}\phi_1\phi_3 + \frac{V_2}{V_1} u_1^2 \phi_3 \frac{\partial g_{13}}{\partial u_2}$$
$$- \frac{V_2}{V_1}\phi_1\phi_3^2 \frac{\partial g_{13}}{\partial \phi_3} - u_1 u_2 \phi_3 \frac{\partial g_{23}}{\partial u_1} - \phi_2\phi_3^2 \frac{\partial g_{23}}{\partial \phi_3} \qquad (7)$$

According to the Flory-Huggins thermodynamics, the Gibbs free energy of mixing for the binary phase is given by eqn. (8) where x_i is the mole fraction of component i in the binary liquid

$$\frac{\Delta G_m}{RT} = x_1 \ln v_1 + x_2 \ln v_2 + g_{12}(v_2)x_1 v_2 \qquad (8)$$

Differentiation with respect to x_1 and x_2 yields eqns. (9) and (10)

$$\frac{\Delta\mu_1^{o}}{RT} = \ln v_1 + (1-\frac{V_1}{V_2})v_2 + g_{12}\, v_2^2 - v_1 v_2^2 \frac{\partial g_{12}}{\partial v_2} \tag{9}$$

$$\frac{\Delta\mu_2^{o}}{RT} = \ln v_2 + (1-\frac{V_2}{V_1})v_1 + \frac{V_2}{V_1}\, g_{12} v_1^2 + \frac{V_2}{V_1}\, v_2 v_1^2 \frac{\partial g_{12}}{\partial v_2} \tag{10}$$

Assuming $\frac{V_1}{V_3} \approx \frac{V_2}{V_3} \approx 0$ and $\frac{V_1}{V_2} = \ell$, substitution of eqns. (6), (7), (9) and (10) in eqns. (3) and (4) and elimination of Π gives

$$\begin{aligned} \ln(\frac{\phi_1}{\phi_2}) - \ln(\frac{v_1}{v_2}) = {} & (\ell-1)\ln\frac{\phi_2}{v_2} - g_{12}(u_2)[\phi_2-\phi_1] - g_{12}(v_2)[v_1-v_2] \\ & -\phi_3(g_{13}-\ell g_{23}) + u_1\phi_2 \frac{\partial g_{12}}{\partial u_2} - v_1 v_2 \frac{\partial g_{12}}{\partial v_2} \\ & +\phi_3 u_1 \frac{\partial g_{13}}{\partial u_2} - \frac{V_1}{V_2}\, u_2\phi_3 \frac{\partial g_{23}}{\partial u_1} \end{aligned} \tag{11}$$

Krigbaum [9] used a different coefficient for expressing the preferential sorption, namely the composition ratio CR ($CR \equiv \frac{\phi_1/\phi_2}{v_1/v_2} \rightarrow \ln CR = \ln(\frac{\phi_1}{\phi_2}) - \ln(\frac{v_1}{v_2})$). The preferential sorption coefficient ε and the composition ratio CR are directly related to each other,

$$\varepsilon = \frac{(CR-1)v_1 v_2}{[1+(CR-1)v_1]} \tag{12}$$

The left hand side of eqn. (11) is equal to the logarithm of the composition ratio. One can see that the expression for the preferential sorption (eqn. (11)) does not contain derivatives of g_{13} and g_{23} with respect to ϕ_3 anymore while in equations for the osmotic pressure these derivatives are present. If the interaction parameters are assumed to be concentration independent, eqn. (11) reduces to the same equations as have been derived by Scott [10] for systems with $\ell=1$ and by Krigbaum [9] for systems with $\ell \neq 1$.

From eqn. (11) the preferential sorption can be calculated numerically if the interaction parameters and their partial derivatives, the ratio of the molar volumes ℓ and the volume fraction of polymer ϕ_3 (or the overall sorption) are known.

Evaluation of the binary interaction parameter g_{12}

In Chapter 5 it was shown that if data on excess free energy of mixing are available, $g_{12}(v_2)$ (or $g_{12}(u_2)$) can be calculated according to eqn. (13) [11,12].

$$g_{12} = \frac{1}{x_1 v_2}\left[x_1 \ln \frac{x_1}{v_1} + x_2 \ln \frac{x_2}{v_2} + \frac{\Delta G^E}{RT}\right] \tag{13}$$

Data on ΔG^E were taken from literature [13].

$$g_{12}(v_2) = 0.9820 - 1.3483\, v_2 + 4.15\, v_2^2 - 3.3116\, v_2^3 + 0.8897\, v_2^4 \tag{14}$$

For the liquid mixture in the polymer, v_2 has to be replaced by u_2.

Evaluation of the binary parameters g_{13} and g_{23}

Interaction parameters between a polymer and a nonsolvent can be determined experimentally by equilibrium swelling measurements as has been described in Chapter 5. For the system studied the swelling measurements and interaction parameters are given in Table 1.

The parameters given in the last column of Table 1 are binary parameters. In order to consider second order or ternary effects the g_{13} and g_{23} parameters are assumed to be concentration dependent, i.e. g_{13} and g_{23} are functions of u_i (i=1,2) and ϕ_3. We will use such a mathematical ex-

TABLE 1

Solubility and interaction parameters of water (component 1) and ethanol (component 2) in the polymers (3) cellulose acetate (CA), polyacrylonitrile (PAN) and polysulfone (PSf)

polymer	penetrant	solubility g penetrant per 100 g dry polymer	volume fraction of polymer [a]	χ [b]
CA	water	14.3	0.84	1.4
PAN	water	8.9	0.91	1.8
PSf	water	0.1	0.999	5.9
CA	ethanol	21.5	0.74	1.1
PAN	ethanol	0.4	0.994	4.2
PSf	ethanol	2.3	0.96	2.5

[a] indicated as $\underset{u_2\to 0}{\phi_3}$ and $\underset{u_1\to 0}{\phi_3}$ in eqns. (15) and (16) respectively.

[b] indicated as $\underset{u_2\to 0}{g_{13}}$ and $\underset{u_1\to 0}{g_{23}}$ in eqns. (15) and (16) respectively.

pression for these parameters that if the concentration u_2 in the polymer increases, g_{13} will increase and if u_1 increases, g_{23} will increase. Furthermore, if the polymer concentration increases both g_{13} and g_{23} will increase.

$$g_{13} = \underset{u_2\to 0}{g_{13}} + au_2 + b(\phi_3 - \underset{u_2\to 0}{\phi_3}) \tag{15}$$

$$g_{23} = \underset{u_1\to 0}{g_{23}} + cu_1 + d(\phi_3 - \underset{u_1\to 0}{\phi_3}) \tag{16}$$

For the limiting cases $u_2\to 0$ and $u_1\to 0$ and (16) reduce to $g_{13} = \underset{u_2\to 0}{g_{13}} = \chi_{13}$ and $g_{23} = \underset{u_1\to 0}{g_{23}} = \chi_{23}$. The values of the constants $\underset{u_2\to 0}{g_{13}}$, $\underset{u_1\to 0}{g_{23}}$, $\underset{u_2\to 0}{\phi_3}$ and $\underset{u_1\to 0}{\phi_3}$ have been given in Table 1. The molecular interpretation of the constants *a*, *b*, *c* and *d* is left for future study. These coefficients can be chosen in such a way as to improve the agreement between theory and experiment, as we will see later on.

EXPERIMENTAL

Materials

Cellulose acetate (E 398-3) was obtained from Eastman Chemicals, polysulfone (P 3500) from Union Carbide and polyacrylonitrile (T 75) from Dupont. The solvents used were of analytical grade.

Membrane preparation

Polymer solutions were prepared by dissolving the polymer in a suitable solvent. The membranes were prepared by casting the polymer solution upon a glass plate and the solvent was allowed to evaporate in a nitrogen atmosphere. The membranes used were completely transparent except for polyacrylonitrile.

Swelling measurements

Dried strips of polymeric membrane (about 0.3 g) were immersed in different conical flasks containing water/ethanol mixtures of different compositions. The flasks were placed in a thermostated bath at 20 °C. After 24 hours the strips were removed, pressed between tissue paper and weighed in a closed flask. This procedure was continued until no further weight increase was observed. The solubility has been expressed as a relative weight increase (g penetrant/100 g dry polymer).

Pervaporation

The pervaporation experiments were carried out as described in Chapter 2. Vacuum at the downstream side was maintained at a pressure of 13.3 Pascal (0.1 mm Hg) by a Crompton Parkinson vacuum pump. The pressure was measured by an Edwards piranhi gauge. The experiments were carried out for eight hours. A product sample was taken every hour and generally steady-state conditions were reached in about three hours. The thickness of the homogeneous membranes was about 20 µm. The temperature of the liquid feed mixture was 20 °C.

Product analysis

Analysis of binary ethanol-water mixtures was performed on a Varian model 3700 gaschromatograph fitted with a chromosorb 60/80 column and equipped with a thermal conductivity detector. For low ethanol concentrations (0-5%) a flame ionization detector was used.

Analysis of the binary liquid mixtures inside the polymeric membrane

The composition of the liquid mixture in the polymeric membrane was determined by a distillation technique as described by Patat [15]. The experiments were carried out with the apparatus shown in Fig. 1. The apparatus was flushed thoroughly with nitrogen before the experiments were started. The polymeric membrane was immersed in a conical flask containing the binary ethanol-water mixture. After sorption equilibrium, which can be verified by repeated weighing, the membrane sample was pressed between tissue paper and put immediately in tube 1. The closed tube 1 was cooled with liquid nitrogen and installed in the apparatus. The system was brought to a pressure of about 1.3 Pascal (0.01 mm Hg) while tube 1 was still cooled. After about 5-10 minutes valve 5 was closed, tube 2 was cooled with liquid nitrogen (the level up to which cooling is performed is indicated by the dashed line) and tube 1 was heated with boiling water. Within 10 to 30 sec-

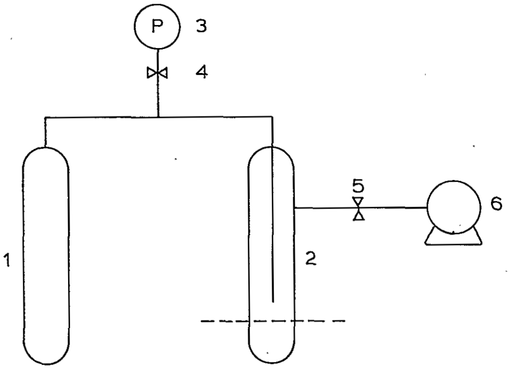

FIGURE 1. Apparatus to determine the composition of the liquid mixture inside the polymer. 1,2: collecting tubes; 3: piranhi gauge; 4,5: valves; 6: vacuum pump.

onds, the liquid inside the membrane started to boil and the vapour was condensed in tube 2. After about 10-15 minutes the experiment was stopped because no more liquid could be removed from the membrane. This was verified in two ways: by following the pressure during the experiment and by performing experiments for longer periods of time. The amount of liquid isolated from the membrane could be determined by gaschromatography.

The experimental error depends on the amount of liquid sorbed by the membrane. The maximum amount of liquid sorbed in a PSf membrane is about 3% while for CA membranes up to 25% was sorbed. The mass balance error is about 5% for polysulfone systems.

RESULTS AND DISCUSSION

The experimental total sorption values of ethanol-water mixtures in cellulose acetate, polysulfone and polyacrylonitrile are given in Fig. 2. Fig. 2 clearly demonstrates the difference in thermodynamic behaviour between the different polymers and ethanol-water mixtures; low swelling values in PSf and PAN and much higher values in CA. PSf and PAN show opposite behaviour, hardly any water sorption in PSf while PAN shows hardly any ethanol sorption. The solubility of ethanol/water mixtures in CA passes through a maximum at about 65% ethanol in the feed.

Values for the preferential sorption have been determined experimentally and theoretically. The theoretical values can be calculated from eqn. (11), which shows that preferential sorption depends on the differences in molar volumes of the two penetrants, the affinity of both components towards the polymer and the mutual interaction between the two penetrants.

The effect of the difference in molar volume has its origin in the combinatorial entropy . This effect upon the preferential sorption increases if the difference in

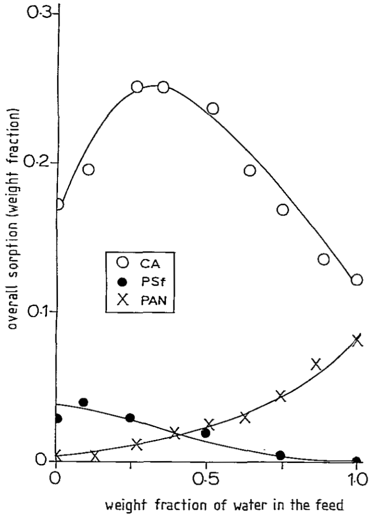

FIGURE 2. Total sorption as a function of the water content of the water/ethanol liquid feed mixture for different polymers.

molar volume increases and if the polymer concentration increases. The component with the smaller molar volume will be sorbed preferentially. For water-ethanol the ratio of the molar volumes $\ell(=\frac{V_1}{V_2})$ is 0.31 which means that water will be sorbed preferentially.

Positive values of the term containing the interaction parameters with respect to the polymer $(\ell.g_{23}-g_{13})$ will favour the preferential sorption of component 1 and this effect also depends on the polymer concentration. For the systems studied this value is negative. Hence, this term contributes to selectivity towards component 2 (ethanol).

The influence of g_{12} on the preferential sorption depends on the concentration in the binary liquid phase and on the sign of the g_{12} interaction parameter. In the case of water-ethanol the interaction parameter g_{12} has a positive value over the entire composition range. This implies that the term $g_{12}(v_2-v_1)$ has a positive effect on the preferential sorption of water for high ethanol feed concentrations $(v_2>v_1)$ while it has a negative effect for high water feed concentrations $(v_1>v_2)$. The same accounts for $g_{12}(\phi_1-\phi_2)$, but the effect of this term is much smaller because ϕ_1 and ϕ_2 are smaller for the systems studied compared to v_1 and v_2.

The influence of the derivatives of g_{13} and g_{23} with respect to u_2 and u_1 respectively depends on the magnitudes of the variables a and c (see eqns. (15) and (16)). The term containing the derivative $\frac{\partial g_{12}}{\partial v_2}$ has a positive effect on the preferential sorption of water while the term with $\frac{\partial g_{12}}{\partial u_2}$ has a negative effect, the latter being smaller than the former.

When neglecting the concentration dependency of the interaction parameters it can be deduced from eqn. (11) that for the limiting case $\phi_3 \rightarrow 1$, the liquid mixture inside the polymer consists almost exclusively of the component with the smaller molar volume.

Some numerical examples will demonstrate the influence of the different factors (difference in molar volume, difference in affinity towards the polymer and the mutual interaction between ethanol and water) on the preferential sorption applied to ethanol-water mixtures. Fig. 3 gives the preferential sorption of ethanol-water for different polymer concentrations assuming equal and constant polymer-nonsolvent parameters ($\chi_{13} = \chi_{23} = 1.0$). For g_{12} (water-ethanol) eqn. (14) has been used. It is obvious that the effect of the difference in molar volume on the preferential sorption of water becomes stronger if the polymer concentration increases.

Fig. 4 is an example of an opposite effect. The smaller molar volume of water, which favours the preferential sorption of water, is opposed by the small mutual affinity of water and polymer. When the χ_{13} parameter increases, keeping χ_{23} constant, the preferential sorption of water decreases and even an inversion in preferential sorption can be observed. Furthermore, the lower curve of Fig. 4 (χ_{13} = 2.0) clearly demonstrates the influence of the g_{12} parameter on the preferential sorption: g_{12} is positive over the en-

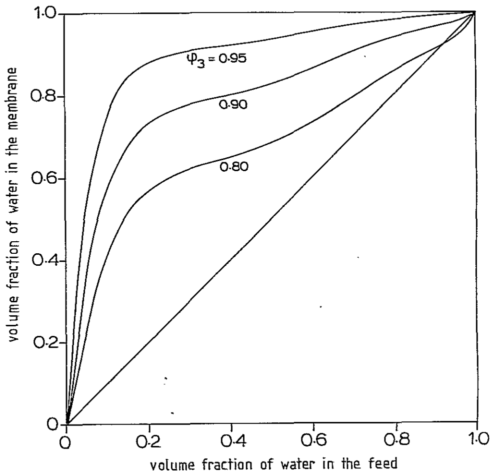

FIGURE 3. Preferential sorption in a ternary system water-ethanol-polymer for different polymer concentrations (ϕ_3 = 0.95; ϕ_3 = 0.9; ϕ_3 = 0.8). Other parameters: $\chi_{13} = \chi_{23} = 1.0$; $g_{12} = g_{12}(u_2)$ (see eqn. (14)); ℓ = 0.31.

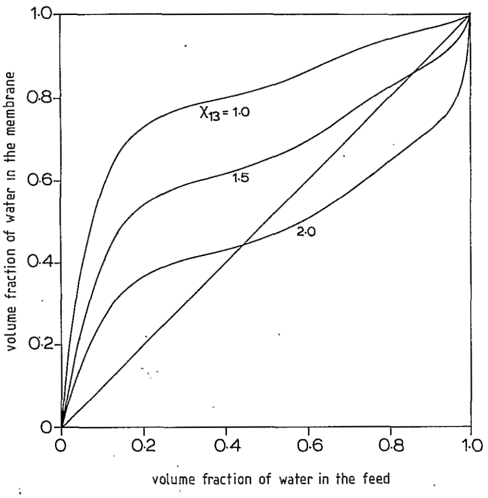

FIGURE 4. Preferential sorption in a ternary system water-ethanol-polymer for different values of χ_{13} (χ_{13} = 1.0; χ_{13} = 1.5; χ_{13} = 2.0).. Other parameters: χ_{23} = 1.0: $g_{12} = g_{12}(u_2)$ (see eq. (14); ℓ = 0.31: ϕ_3 = 0.90.

tire composition range (see eqn. (14)) and the contribution to the preferential sorption is positive for low water concentration in the feed while it has a negative effect for high water concentrations in the feed.

In the case of polysulfone and polyacrylonitrile as membrane materials, the polymer concentration (ϕ_3) is quite high (see Fig. 2). For the system water-ethanol-polyacrylonitrile we expect a large preferential sorption for water because the component with the smaller molar volume (water) has also a larger affinity towards the polymer (see Table 1 and Fig. 2). For the system water-ethanol-polysulfone the preferential sorption for water due to the effect of the smaller molar volume is counteracted by the very small affinity of water to polysulfone. In the next section we will see whether the experimental and theoretical data agree.

The system water-ethanol-cellulose acetate (sorption results)

In Fig. 5 the theoretical values for the preferential sorption calculated according to eqn. (11) with constant interaction parameters ($g_{ij} = \chi_{ij}$) and with concentration dependent interaction parameters, together with the experimental values are given as a function of the water concentration in the feed. The experimental values show that water is sorbed preferentially over the entire composition range. The preferential sorption increases with decreasing water concentration in the feed mixture.

From the calculated values using constant polymer-nonsolvent interaction parameters an inversion of the preferential sorption can be observed which is not in agreement with the experimental observations. To improve the agreement between experimental and theoretical values, concentration dependent g_{13} and g_{23} parameters have been used. By investigating the effect of the variables a, b, c and d (see eqns. (15) and (16)) on the preferential sorption, it

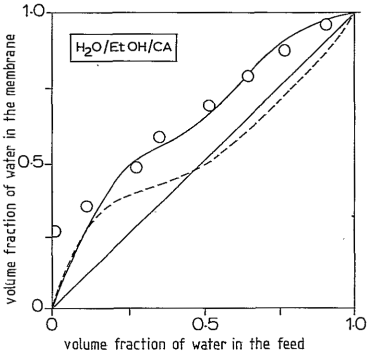

FIGURE 5. Experimental values (o) for the preferential sorption (expressed as volume fraction of water inside the polymer) and calculated values using concentration dependent (full curve) and constant (dotted curve) interaction parameters as a function of the volume fraction of water in the liquid feed, for the system water-ethanol-cellulose acetate.

became clear that a reasonable agreement between theory and experiment was obtained when the coefficient a has a higher value than c. The concentration dependence of g_{13} and g_{23} is given in Fig. 6.

The influence of the g_{13} and g_{23} parameters on the preferential sorption is caused to a large extent by their derivatives and the choice of the coefficients a and c. Hence a>c results in $\frac{\partial g_{13}}{\partial u_2} > \frac{\partial g_{23}}{\partial u_1}$ which has a positive effect on the preferential sorption of water (see eqn. (11)).

The system water-ethanol-polyacrylonitrile (sorption results)

The experimental and theoretical values for the preferential sorption are given in Fig. 7. The theoretical values have been calculated according to eqn. (11) using constant interaction parameters given in Table 1 ($g_{13} = \chi_{13} =$ 1.8 and $g_{23} = \chi_{23} = 4.2$).

For low water concentrations in the feed no experimental values could be obtained because the amount of sorbed liq-

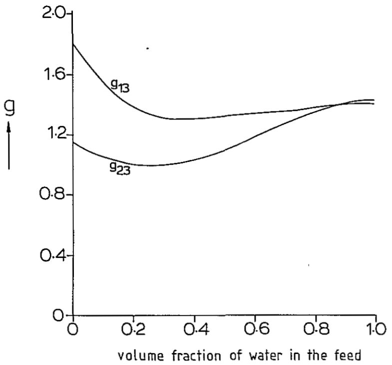

FIGURE 6. Interaction parameters g_{13} and g_{23} in the system water/ethanol/cellulose acetate as a function of the water concentration in the feed. Parameters used in eqns. (15) and (16) are: $a = 0.6$; $b = 2.2$; $c = 0.1$; $d = 2.2$.

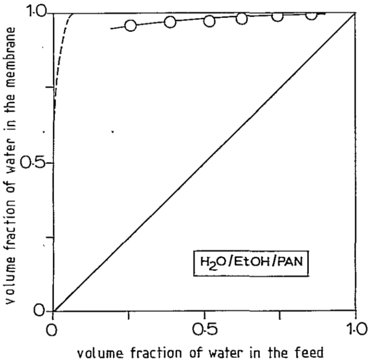

FIGURE 7. Experimental (o) and theoretical (---) values for the preferential sorption in the system water-ethanol-polyacrylonitrile as a function of the volume fraction of water in the liquid feed.

uid was too small (see Fig. 2). From Fig. 7 very high values for the preferential sorption of water can be observed. This behaviour could already be expected because of the smaller molar volume of water and the much higher affinity between water and polyacrylonitrile in comparison with ethanol and polyacrylonitrile. The theoretical values hardly change when concentration dependent g_{13} and g_{23} parameters are used. Because of the very high fractional water content inside the membrane, the value of g_{13} will not change very much ($u_2 \rightarrow 0$, see eqn. (15)) while a higher value of g_{23} has no influence on the preferential sorption.

The system water-ethanol-polysulfone (sorption results)

This system is a very interesting one because the effect of the difference in molar volume, contributing to a large extent to the preferential sorption of water in the two other systems studied, is opposed here by the very small mutual affinity between water and polysulfone.

Because a very small amount of liquid is sorbed by polysulfone, especially at high water concentrations in the feed, only one experimental value has been obtained at a high ethanol feed concentration. The theoretical and experimental results are given in Table 2.

TABLE 2

Theoretical and experimental value of preferential sorption in the system water-ethanol-polysulfone

	water in feed (v_1) (weight fraction)	water in membrane (u_1) (weight fraction)
Experimental	0.11	0.23
Theoretical	0.11	0.28

Parameters used in eqns. (15) and (16) are: a = 0.2; b = 65.0; c = 1.2; d = 65.0.

Using concentration independent interaction parameters, the term $\ell\chi_{23}-\chi_{13}$(= −5.1) which is very large, dominates completely and predicts a preferential sorption of component 2 (ethanol). By taking the interaction parameters concentration dependent, preferential sorption of water can be calculated. However, the coefficients a, b, c and d (see eqs. (15) and (16)) have completely different values as in the case of cellulose acetate. Although a reasonable agreement can be obtained between theory and experiment, the physical interpretation of the values for the coefficients a, b, c and d is still unexplained.

Nevertheless, it is striking that even in hydrophobic polymers such as polysulfone, water is sorbed preferentially.

Preferential sorption versus preferential permeation

The main objective of this work was to investigate preferential sorption in relation to selective transport in pervaporation. Successively we will discuss the systems water-ethanol-cellulose acetate, water-ethanol-polyacrylonitrile and water-ethanol-polysulfone.

The system water-ethanol-cellulose acetate (sorption vs. permeability)

In Fig. 8 the experimental sorption values and pervaporation results are given as a function of the weight fraction of water in the feed mixture. It is obvious that both curves show practically the same behaviour. If these results are considered in terms of the solution-diffusion model, in which the flux of a component through the membrane is a function of solubility (S) and diffusivity (D), it can be shown that solubility contributes to a major extent to selective transport

$$\frac{J_1}{J_2} = \frac{S_1(C_1,C_2)}{S_2(C_1,C_2)} \cdot \frac{D_1(C_1,C_2)}{D_2(C_1,C_2)} \qquad (17)$$

In the case of water and ethanol, permeating through cellulose acetate, both the ratios S_1/S_2 and D_1/D_2 are lar-

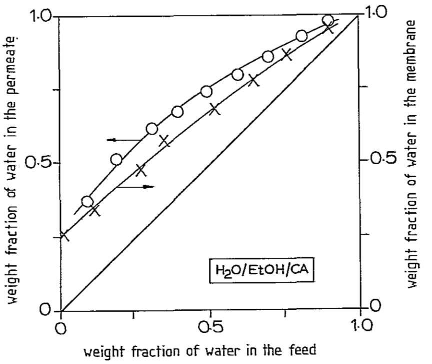

FIGURE 8. Experimental values for preferential sorption (expressed as weight fraction of water inside the polymer) and for pervaporation (expressed as weight fraction of water in the permeate) for the system water-ethanol-cellulose acetate as a function of the weight fraction of water in the feed.

ger than one. For water and ethanol the ratio D_1/D_2 is larger than one because of the difference in size of the molecules (see for instance Behrens [16]). So in order to obtain very high selectivities the ratios S_1/S_2 and/or D_1/D_2 should be very large. For the system water-ethanol-cellulose acetate the ratio S_1/S_2 is rather low and moderate selectivities are obtained implying that the ratio D_1/D_2 will not be very large either.

The system water-ethanol-polyacrylonitrile (sorption vs. permeability)

For this system the experimental preferential sorption values and the pervaporation results as a function of the weight fraction of water in the feed are given in Fig. 9. Again, both curves show the same behaviour.

Because the ratio S_1/S_2 is much larger here compared to that for cellulose acetate, very high selectivities could be expected and are achieved indeed. Also for this system the contribution of the preferential sorption to the selectivity in permeation turns out to be the leading factor.

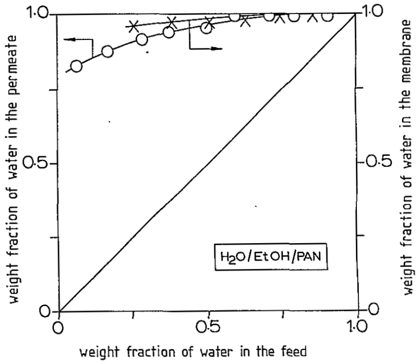

FIGURE 9. Experimental values for preferential sorption and pervaporation for the system water-ethanol-polyacrylonitrile as a function of the weight fraction of water in the feed.

The system water-ethanol-polysulfone (sorption vs. permeability)

In a previous section it was shown that water is sorbed preferentially in the strongly hydrophobic polymer polysulfone from an ethanol-water mixture. Analogous to the other systems studied a preferential permeability for water should be expected. In Fig. 10 the one experimental sorption value and a curve for pervaporation results are given as a function of the weight fraction of water in the liquid feed. As was found for the other two systems, preferential sorption and preferential permeation show parallel behaviour but in contrast to the other two systems, the sorption selectivity is much lower than the selectivities found in the pervaporation process. We think that in this system the mobility of the ethanol molecules has been decreased because of the hydrophobic interactions between ethanol and polysulfone. As a consequence the ratio D_1/D_2 should be very large.

The system water-ethanol-polysulfone is a perfect example to demonstrate the presence of coupled transport. For pure water neither sorption nor permeation can be observed while in the presence of ethanol water is sorbed and trans-

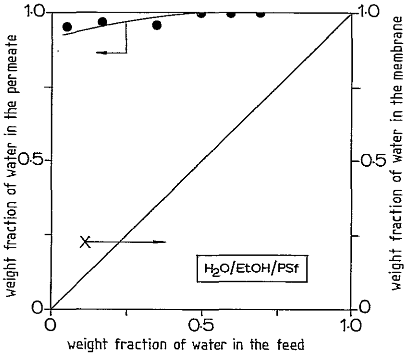

FIGURE 10. Experimental values for preferential sorption (one point x) and pervaporation for the system water-ethanol-polysulfone as a function of the weight fraction of water in the feed.

ported preferentially. In several models [3,17] it has been tried to predict selectivity and permeation rates from parameters obtained from single component experiments. The results presented here clearly demonstrate that it would be hardly possible to predict membrane characteristics for non-ideal mixtures like water-ethanol from single component experiments only. Coupling occurs in the thermodynamic part ('solution') as well as in the kinetic part ('diffusion') of the solution-diffusion mechanism.

Another interesting aspect which can be deduced from our experiments is that the assumption of ideal sorption behaviour cannot be used for non-ideal mixtures such as ethanol-water. This can be demonstrated clearly by the system water-ethanol-polysulfone (but also by the other two systems). Krewinghaus [18] assumed a linear relationship (ideal sorption) between the concentration of a component in the membrane and the concentration of that component outside the membrane according to eqb. (18)

$$c_i = x_i \, c_i^{o} \tag{18}$$

where c_i is the concentration of component i in the membrane, x_i is the mole fraction of component i in the liquid feed mixture and c_i^{o} is the solubility of the pure component in the membrane. Eqn. (18) cannot be used for the system water-ethanol-polysulfone because for pure water no sorption occurs in a polysulfone membrane while in the presence of ethanol water is sorbed preferentially. In general one can say that in cases where preferential sorption occurs eqn. (18) cannot be used.

CONCLUSIONS

Using Flory-Huggins thermodynamics, extended with concentration dependent interaction parameters, the agreement between theoretical and experimental values for the preferential sorption of low molecular weight components in polymeric membranes is reasonably well established. For the systems studied, preferential sorption of water from ethanol-water mixtures occurs and this can be ascribed to the large difference in molar volume between water and ethanol. Comparison of the preferential sorption values and the results for preferential permeation show that preferential sorption of water contributes to a large extent to selective water transport. From the results presented here it can be predicted that high selectivities for water from ethanol-water mixtures can be expected when the total amount of liquid inside the polymer is small (in this case the permeation rates will be low, however) and when the affinity between water and polymer is larger than that between ethanol and polymer.

In terms of the solution-diffusion model the conclusion is justified that the component that is sorbed preferentially will also permeate preferentially. This statement is in agreement with the observations of Aptel [5]. Furthermore it can be concluded that the assumption of ideal sorption cannot be used in general.

LIST OF SYMBOLS

a	activity
c	concentration inside the membrane
c^{o}	solubility of the pure component in the membrane
CR	composition ratio
g	concentration dependent interaction parameter
ΔG_{mix}	free energy of mixing (J mol^{-1})
ΔG^{E}	excess free energy of mixing (J mol^{-1})

ℓ	ratio of molar volumes (= $\frac{V_1}{V_2}$)
n	mole fraction in the ternary phase
P	pressure (Pascal)
R	gas constant (J mol^{-1} K^{-1})
T	temperature (K)
u	volume fraction confined to the nonsolvent part in the ternary phase
v	volume fraction in the binary phase
V	molar volume (cm^3 mol^{-1})
x	mole fraction in the binary phase
ε	coefficient of preferential sorption
χ	concentration independent binary interaction parameter
ϕ	volume fraction in the ternary system
μ	chemical potential (J mol^{-1})
Π	osmotic pressure (J cm^{-3})

Indices

1	water
2	ethanol
3	polymer
i	component i
m	membrane

REFERENCES

1 R.C. Binning, R.J. Lee, J.F. Jennings and E.C. Martin, *Ind. Eng. Chem.*, 53 (1961) 45.

2 D.R. Paul and J.D. Paciotti, *J. Pol. Sci. A-2*, 13 (1975) 1201.

3 C.H. Lee, *J. Appl. Pol. Sci.*, 19 (1975) 83.

4 M.H.V. Mulder and C.A. Smolders, *J. Membr. Sci.*, 17 (1984) 289; chapter 5 of this thesis.

5 P. Aptel, J. Cuny, J. Jozefowicz, J. Neel and B. Chaufer,

Eur. Pol. J., 14 (1978) 595.

6 P. Flory, *Principles of polymer chemistry*, Cornell University Press, Ithaca, New York, 1953.

7 A. Zivný and J. Pouchlý, *J. Pol. Sci. A-2*, 10 (1972) 1467.

8 J. Pouchlý and A. Zivný, *Makromol. Chem.*, 183 (1982) 3019.

9 R.L. Scott, *J. Chem. Phys.*, 17 (1949) 268.

10 W.R. Krigbaum and D.K. Carpenter, *J. Pol. Sci.*, 14 (1954) 241.

11 F.W. Altena and C.A. Smolders, *Macromolecules* 15 (1982) 1491.

12 T.M. Aminabhavi and P. Munk, *Macromolecules*, 12 (1979) 607.

13 S. Westmeier, *Chem. Techn.*, 28 (1976) 350.

14 M.H.V. Mulder, F. Kruitz and C.A. Smolders, *J. Membr. Sci.*, 11 (1982) 349.

15 F. Patat and G. Träxler, *Makromol. Chem.*, 33 (1959) 113.

16 A.R. Berens and H.B. Hopfenberg, Vapor sorption methods in studies of the glassy state: part 1, sorption isotherms and diffusivities, 10th Europhysics Conference on Macromolecular Physics. Noordwijkerhout 1980, p. 72.

17 F.W. Greenlaw, R.A. Shelden and E.V. Thompson, *J. Membr. Sci.*, 2 (1977) 333.

18 A.B. Krewinghaus, *Ph.D. thesis*, Massachusetts Institute of Technology, April 1966.

SUMMARY

In this thesis two aspects of the pervaporation process have been described: preparation of pervaporation membranes and considerations on the transport model.
The transport mechanism of pervaporation is a solution-diffusion mechanism. This mechanism runs like a thread through this thesis: the development of pervaporation membranes is directly related to the transport model.

When different molecules simultaneously diffuse through a (homogeneous) membrane this will not occur by entirely separate pathways because there will be an interaction with the membrane material and mutually between the diffusing molecules. Furthermore, the flow of component A may be enhanced or decreased by the flows of the other components. Because of these coupling phenomena transport descriptions of mixtures are often difficult to establish.

In order to prepare proper pervaporation membranes the solution-diffusion model has to be one's guide. Till now little attention has been paid to the solubility part of this model. A rather simple model which can be used to predict polymer-(non)solvent compatibility is the solubility parameter concept. This theory can only be applied to hydrophobic or weakly polar components. Chapter 2 gives a short evaluation of this theory applied to the separation of isomeric xylenes through cellulose ester membranes. The transport behaviour of this mixture can neither be predicted nor described by this solubility parameter concept. In fact, this is not so surprising because in this theory only properties of the pure components are taken into account i.e. binary or ternary effects are not being considered. As far as permeability of one component is concerned this theory can be used in a qualitative manner to select proper polymeric materials.

Most of the work described in this thesis has been performed with ethanol/water mixtures. Chapter 3 gives a ge-

neral description of ethanol/water separation by pervaporation. Different membrane structures can be used: homogeneous, aymmetric and composite. Although the different membranes give good performances the most promising membranes are the asymmetric membranes. The development of asymmetric pervaporation membranes is described more in detail in Chapter 4. In order to obtain highly selective asymmetric pervaporation membranes different factors are important: polymer concentration, ratio of solvent outflow and nonsolvent inflow during precipitation, location of the binodal demixing gap and location of the gel region. Asymmetric pervaporation membranes prepared from various polymers have in general better characteristics (higher permeation rates while selectivities remain the same or become slightly less) than the homogeneous membranes prepared from the same polymer.

In Chapter 5 a solution-diffusion model is described where second-order coupling effects are taken into account but cross-term diffusion coefficients are neglected in order to reduce the number of adjustable parameters. Because nonideal systems are considered (polymer/penetrant) activities should be used instead of concentrations. In Chapter 6 experimental concentration profiles of the system water/ethanol/cellulose acetate are given and these results are discussed in terms of the model described in Chapter 5. The results clearly demonstrate that in strongly interacting systems such as the system we studied cross-term diffusion coefficients have to be taken into account. This means that the flow of component A may be influenced strongly by the flow of component B. For the system water/ethanol/cellulose acetate the flow of ethanol is almost completely determined by the flow of water. Therefore, the model description given in Chapter 5 was extended to include these coupling effects. In the case where coupling effects are small the model description given in Chapter 5 can be used but in the case where medium or strong coupling effects occur the model should be extended as described in Chapter 6.

Another point which can be deduced from the experimental concentration profiles is the occurrence of sorption resistances i.e. equality of the chemical potential at the feed/ membrane interface during steady-state permeation does not exist a priori. In the case of ethanol/cellulose acetate and water/ethanol/cellulose acetate an activity drop at the interface can be observed while in the case of water/cellulose acetate there is no activity drop.

In my opinion the most important chapter of this thesis is Chapter 7. In this chapter two points are clearly stressed: *i*) the occurence of preferential sorption and *ii*) the observation that preferential sorption leads to preferential permeability. Although both statements are qualitative only it clearly indicates the importance of the choice of the polymeric material towards a certain liquid mixture. When a polymeric material is selected membrane performance can be further optimized as described in Chapter 4. Another point which is clearly demonstrated in Chapter 7 is that ideal sorption behaviour cannot be assumed at forehand or in general.

SAMENVATTING

In dit proefschrift worden twee aspekten van het pervaporatieproces beschreven: bereiding van pervaporatiemembranen en beschrijving van transport door deze membranen.

De transportbeschrijving van het pervaporatieproces loopt als een draad door dit proefschrift omdat ook de ontwikkeling van nieuwe membranen direkt is gekoppeld aan het transport mechanisme.

Wanneer verschillende komponenten door een membraan diffunderen dan zal dit niet onafhankelijk van elkaar gebeuren maar gekoppeld d.w.z. de diffunderende komponenten beinvloeden elkaar onderling terwijl ook interakties van de komponenten met het membraan(materiaal) een rol spelen. De aard van de koppeling wordt bepaald door keus van het te scheiden mengsel en het daarvoor gebruikte membraan. Door het optreden van koppeling is de beschrijving van het transport i.h.a. moeilijk.

Het ontwikkelen van geschikte pervaporatiemembranen dient te geschieden aan de hand van het oplos-diffusie model. Tot nu toe is in de literatuur weinig aandacht besteed aan het 'oplos'-gedeelte van dit model.
De oplosbaarheidsparameter theorie is een redelijk eenvoudige theorie die kan worden gebruikt voor het voorspellen van polymeer-(niet)oplosmiddel kompatibiliteit. Deze theorie kan echter alleen worden toegepast op hydrofobe of zwak polaire stoffen. Hoofdstuk 2 geeft een evaluatie van deze theorie toegepast op de scheiding van xyleen isomeren door cellulose ester membranen. Het transportgedrag van dit mengsel kan noch voorspeld noch beschreven worden door dit oplosbaarheidsparameter koncept. Dit is in feite niet zo verwonderlijk omdat bij deze theorie alleen de eigenschappen van de zuivere stof in beschouwing worden genomen d.w.z. effekten die optreden t.g.v. menging worden niet verdiskonteerd. De theorie kan wel gebruikt worden om de permeabiliteit van de zuivere stof te beschrijven op een kwalitatie-

ve wijze, d.w.z. voor zover het de permeatie van één komponent betreft kan een polymeer materiaal geselekteerd worden.

Het grootste gedeelte van het werk beschreven in deze dissertatie betreft onderzoek aan ethanol/water mengsels. Hoofdstuk 3 geeft een algemeen overzicht van de scheiding van ethanol/water mengsels d.m.v. pervaporatie. Hoewel de verschillende typen membranen (homogene, asymmetrische en komposiet of samengestelde) goede scheidingseigenschappen bezitten zijn asymmetrische membranen het meest belovend. In hoofdstuk 4 wordt de ontwikkeling van asymmetrische pervaporatiemembranen meer gedetailleerd beschreven. Verschillende faktoren zijn van belang voor het verkrijgen van asymmetrische pervaporatiemembranen met een hoog scheidend vermogen: polymeerkoncentratie, verhouding van uitstroom van oplosmiddel en instroom van niet-oplosmiddel, ligging van de binodaal en ligging van het gelgebied. De ontwikkelde asymmetrische membranen bezitten betere eigenschappen dan de overeenkomstige homogene membranen (hogere fluxen bij gelijkblijvende of enigszins verminderde selektiviteit).

In hoofdstuk 5 wordt een oplos-diffusie model beschreven waarbij tweede-orde koppelingseffekten zijn beschouwd maar waarbij kruis-diffusie koefficienten zijn verwaarloosd om het aantal onbekende parameters te verminderen.

In hoofdstuk 6 worden experimentele koncentratieprofielen van het systeem water/ethanol/cellulose acetaat gegeven en deze resultaten worden bediskusseerd aan de hand van het model beschreven in hoofdstuk 5. De resultaten tonen duidelijk aan dat het niet toegestaan is om kruis-diffusie koefficienten te verwaarlozen in het geval van mengsels zoals ethanol/water. Dit betekent dat de modelbeschrijving moet worden aangepast. In het geval van te verwaarlozen of geringe koppelingseffekten kan de modelbeschrijving van hoofdstuk 5 wel worden gebruikt.

Een ander interessant punt uit hoofdstuk 6 is dat de aanwezigheid van sorptie weerstanden aan het grensvlak voedding/membraan experimenteel is aangetoond. Dit betekent dat de chemische potentialen van een komponent in de beide fasen van het grensvlak niet gelijk zijn, terwijl dit veelal in de literatuur wordt aangenomen (zie ook hoofdstuk 5).

Hoofdstuk 7 is,mijn inziens, het meest belangrijke hoofdstuk van deze dissertatie. In dit hoofdstuk worden twee punten duidelijk benadrukt:*i*) de aanwezigheid van preferentiele sorptie en *ii*) de konstatering dat preferentiele sorptie leidt leidt tot preferentiele permeatie. Hoewel beide beweringen slechts kwalitatief zijn wordt duidelijk het belang van de keus van het polymeermateriaal aangetoond t.a.v. een bepaald vloeistofmengsel. Wanneer eenmaal een materiaal is geselekteerd kunnen de membraaneigenschappen verder geoptimaliseerd worden zoals in hoofdstuk 4 staat beschreven. Een ander belangrijk punt dat duidelijk in hoofdstuk 7 wordt aangettond is dat ideale sorptie op voorhand of in het algemeen niet plaats vindt.

SAMENVATTING VOOR DE LEEK

Deze samenvatting is bedoeld voor mensen die graag willen weten waarmee ik me heb beziggehouden zonder dat ze worden overladen met vaktermen.

In de afgelopen 4 jaar heb ik vooral gewerkt aan de scheiding van ethanol (in de volksmond alkohol)/water mengsels.

Waarom wil je ethanol en water van elkaar scheiden terwijl erg veel mensen het juist in gemengde toestand (al dan niet met geur- en smaakstoffen en toevoegingen zoals sulfiet) prettig vinden?
Voor het antwoord op deze vraag moeten we even terug naar 1973, het jaar van de zogenaamde energiekrisis. 1973 is in wezen het jaar van de doorbraak geweest m.b.t. onderzoek naar alternatieve (hernieuwbare) energiebronnen zoals zonneenergie, windenergie, getijdenenrgie etc..
Zonneenergie kan behalve direkt ook indirekt benut worden via de in de plant opgeslagen energie. Deze energie kan weer worden teruggewonnen via een gistingsproces waarbij bijvoorbeeld ethanol of methaan wordt gevormd. Afhankelijk van het soort gistingsproces kunnen verschillende soorten alkoholen worden gevormd (methanol, ethanol, butanol etc.). Deze alkoholen kunnen in zuivere vorm worden gebruikt als als vloeibare brandstof, een alternatief voor olie en gas, alleen met het verschil van een bijna onuitputtelijke voorraad. Wanneer alkohol als brandstof wordt gebruikt mag het, afhankelijk van de toepassing, maar weinig of geen water bevatten. Na gisting wordt globaal een alkohol percentage van ongeveer 10% verkregen d.w.z. het mengsel bevat nog 90% water (en verder nog andere stoffen) dat moet worden verwijderd.

De meest bekende manier om ethanol/water mengsels van elkaar te scheiden is d.m.v. destillatie. Het nadeel van deze methode is dat veel energie nodig is om deze scheiding uit te voeren vooral wanneer nog maar weinig water in het mengsel aanwezig is. De afgelopen jaren is er op tal van plaatsen in de wereld (USA, Japan, Rusland) onderzoek gepleegd naar de mogelijke toepassing van membraanfiltratie voor het scheiden van ethanol/water mengsels.

Membraanfiltratie is een scheidingstechniek waarbij mengsels worden gescheiden door een membraan, d.w.z. in het geval van ethanol/water zal een van de twee stoffen (bijv. water) beter door het membraan gaan dan de andere komponent (ethanol). De door mij onderzochte membranen worden gemaakt van plastiks, d.w.z. het membraan is niets anders dan een dun stukje plastik. Membranen kunnen ook gemaakt worden van een ander soort materiaal zoals glas of papier (Denk aan koffiefilters, waarbij de gemalen koffie wordt tegengehouden terwijl water met de geur- en smaakstoffen door het filter (membraan) gaan).
De bekendste toepassingen van membraanfiltratie is bij de nierdialyse en het ontzouten van zeewater voor de bereiding van drinkwater.

Ik heb me de afgelopen 4 jaar vooral beziggehouden met de vraag hoe het nu komt dat water van ethanol kan worden gescheiden door een membraan. Wanneer water en ethanol zich door het membraan verplaatsen dan beinvloeden ze elkaar terwijl ook het type plastik waar het membraan van gemaakt is erg belangrijk is. Het blijkt namelijk dat de mate van scheiding sterk afhangt van de keus van het plastikmateriaal. Door nu uit te zoeken welke faktoren belangrijk zijn om tot een goede scheiding te komen wordt het zoeken naar ander (nieuw) plastik iets eenvoudiger.

Wanneer eenmaal een bepaald type plastik is uitgekozen dan kan hiervan een membraan van gemaakt worden. Dit kan op verschillende manieren gebeuren waardoor membranen worden verkregen met verschillende eigenschappen. Op deze manier is het dus mogelijk om de scheiding verder te verbeteren.

Momenteel wordt membraanfiltratie voor ethanol/water scheiding nog nauwelijks toegepast maar de vooruitzichten zijn goed. Uit onderzoek, uitgevoerd op de TH Twente en in W-Duitsland, blijkt dat het ekonomisch aantrekkelijk is om membraanfiltratie toe te passen i.p.v. destillatie wanneer weinig water (minder dan 25%) moet worden verwijderd uit een ethanol/water mengsel.

LIST OF PUBLICATIONS

- Non-electrolyte permeability as a tool for studying membrane fluidity
  E.J.J. van Zoelen, C. Henriques de Jesus, E. de Jonge,
  M.H.V. Mulder, M.C. Blok and J. de Gier
  Biochimic et Biophysic Acta, 511 (1978) 335
- Polyelectrolytes obtained by reaction of β-lactam-N-sulfonylchloride groups with aqueous ammonia
  P.M. van der Velden, M.H.V. Mulder, L. van der Does and
  C.A. Smolders
  J. Pol. Sci. Pol. Letters Ed., 14 (1976) 5
- A survey of structure characterization for ultrafiltration
  C.A. Smolders, M.H.V. Mulder and P.M. van der Velden
  Desalination, 19 (1976) 481
- Phase separation phenomena during the formation of asymmetric membranes
  D.M. Koenhen, M.H.V. Mulder and C.A. Smolders
  J. Appl. Pol. Sci., 21 (1977) 199
- Membrane filtration for the ethanol production (in dutch)
  M.H.V. Mulder, C.A. Smolders and D. Bargeman
  PT-Procestechniek, 36 (9181) 604
- Separation of isomeric xylenes by pervaporation through cellulosic ester membranes
  M.H.V. Mulder, F. Kruitz and C.A. Smolders
  Journal of Membr. Sci., 11 (1982) 349
- Formation, structure and applications of membranes
  Part I (in dutch)
  M.H.V. Mulder and C.A. Smolders
  PT-Procestechniek, 37 (1982) 66, nr. 4
- Formation, structure and applications of membranes
  Part II (in dutch)
  M.H.V. Mulder and C.A. Smolders
  PT-Procestechniek, 38 (1982) 25, nr. 5

- Separation of ethanol/water by pervaporation
  M.H.V. Mulder, J. Oude Hendrikman, H. Hegeman and C.A. Smolders
  Journal of Membr. Sci., 16 (1983) 269
- The application of membranes in biotechnology (in dutch)
  M.H.V. Mulder, C.A. Smolders and D. Bargeman
  PT-Procestechniek, 38 (1983) 36, nr. 2
- On the mechanism of ethanol/water separation by pervaporation. I. Calculations of concentration profiles
  M.H.V. Mulder and C.A. Smolders
  Journal of Membr. Sci., 17 (1984) 289
- On the mechanism of ethanol/water separation by pervaporation. II. Experimental concentration profiles
  M.H.V. Mulder, T. Franken and C.A. Smolders
  Submitted to Journal of Membr. Sci.
- Preferential sorption versus preferential permeability
  M.H.V. Mulder, T. Franken and C.A. Smolders
  Submitted to Journal of Membr. Sci.
- A rationale for the preparation of asymmetric pervaporation membranes
  M.H.V. Mulder, J. Oude Hendrikman, J.G. Wijmans and C.A. Smolders
  Submitted to J. Appl. Pol. Sci.
- Separation of isomeric xylenes. A fundamental approach
  M.H.V. Mulder, T. Franken and C.A. Smolders
  to be published

LEVENSLOOP

Marcel Mulder werd geboren op 6 april 1951 te Enschede.
In 1968 werd het HBS-B diploma behaald aan het Jacobus College te Enschede. In datzelfde jaar begon hij met de studie Chemie aan de Hogere Technische School te Hengelo. In 1972 behaalde hij zijn ingenieursdiploma (Ing.) waarna hij zijn militaire dienstplicht vervulde. In maart 1974 trad hij in dienst van Wafilin. B.V. te Hardenberg als onderzoeksassistent waarbij hij gestationeerd werd op de Technische Hogeschool Twente.
In 1976 begon hij met de studie Scheikunde aan de Rijksuniversiteit van Utrecht waar hij in 1977 zijn kandidaatsexamen behaalde. In 1979 werd het doktoraalexamen behaald met als hoofdvak Biochemie en als bijvakken Klinische Chemie en Membraantechnologie. Vervolgens trad hij in dienst als wetenschappelijk assistent bij de Werkgroep Membraanfiltratie van de Technische Hogeschool Twente. In de periode tot 1 december 1983 is onderzoek verricht dat in dit proefschrift beschreven is.